

A631712

FACILITY FORM 808

N66 29523

(ACCESSION NUMBER)

(THRU)

151

(PAGES)

1

(CODE)

CR-75869

(NASA CR OR TMX OR AD NUMBER)

23

(CATEGORY)

GPO PRICE \$ _____

CFSTI PRICE(S) \$ _____

Hard copy (HC) 5.00

Microfiche (MF) 1.00

FF 653 July 65

Coordinated
Science
Laboratory



UNIVERSITY OF ILLINOIS - URBANA, ILLINOIS

Reproduction Document
307

PROGRESS REPORT
FOR
DEC., 1965, JAN. & FEB., 1966

April 1, 1966

The research reported in this document was made possible through support extended the Coordinated Science Laboratory, University of Illinois, by the Joint Services Electronics Program (U. S. Army Electronics Laboratories and U. S. Army Research Office, Office of Naval Research, and the Air Force Office of Scientific Research) under Contract Number DA 28 043 AMC 00073(E).

Portions of this work were also supported by

National Aeronautics and Space Administration

— Research Grants NsG-443, NsG-504 —

National Science Foundation

Grant NSF GK-36
Grant NSF GK-690
GRANT NSF GE-7809

Advanced Research Projects Agency

Through Office of Naval Research
Contract Nonr-3985(08)

Air Force Office of Scientific Research

Grant AFOSR 931.65.

Office of Naval Research

Contract
N00014-66-C0010-A01

U. S. Office of Education

Contract OE-6-10-184

as acknowledged in footnotes in the text.

Reproduction in whole or in part is permitted for
any purpose of the United States Government.

DDC Availability Notice: Qualified requesters may obtain
copies of this report from DDC. Release to OTS is authorized.

COORDINATED SCIENCE LABORATORY

SUMMARY OF

PROGRESS REPORT FOR DECEMBER 1965, JANUARY, FEBRUARY, 1966

1. Space Sciences

Studies of mechanical damping in possible gyro materials are reported along with studies of micrometeorite influence and the optimal choice of gyro diameter.

2. Surface Physics

Measurements of the scattering of electrons from the (100) surface of tungsten are reported. These measurements are interpreted in terms of the excitation of the vibrational states of surface atoms and in terms of the band structure. The experiments for the measurement of the angular distribution of particles scattered from surfaces and for the study of the adsorption-desorption kinetics of gases at surfaces are continuing. The status of these experiments is given.

3. Computer

Operation statistics, new facilities for bubble-chamber processing, and new display equipment are reported.

4. Control Systems

Several results were obtained in the continuing projects on the sensitivity problem, stability of nonlinear systems, optimization of systems with fixed control structure, and computer-oriented formulation of the optimal control problem. Bounds were obtained for sensitivity functions. Optimum regulator systems were found to be relatively insensitive. Some extensions of Popov's criterion were derived.

5. PLATO

Two "PLATO" university courses for credit are being given the second semester (LIB SCI 195 and EE 322). Three courses were completed by students during the fall term. Programming developments include an inquiry facility added to the new PLATO tutorial logic so that two different teaching methods for the electrical engineering course can be tried, a new logic for ARITHDRILL, a generalized program for the paired associate learning study, a program for a keyset design experiment, the first test program for the production of animated films for a language-free test of interpersonal norms, a general "messaging" program for use with group-interaction studies; and some initial SIRA routines for processing "dope" tapes (student response records). The twenty student-station circuitry-modernizing is nearing completion, a feasibility study of an audio feature for PLATO is being made, an investigation of the means for turning on and off the plasma display tube is underway as well as the construction of a new portable transistorized generator.

6. Vacuum Instrumentation

Final data for the pumping speeds of small diode and triode getter-ion pumps are given. Additional work on the conversion of O_2 to CO in vacuum systems has shown that the partial pressure of CO may be quite small in properly processed systems. The development of the Schuemann suppressor gauge is reviewed to the present, and a program of additional work intended to improve it still further is proposed.

7. Plasma Physics

Two methods of testing the accuracy of approximate solutions of the Boltzmann equation for a shock wave have been used to examine two different shock solutions. Enhanced diffusion resulting from the beam-plasma instability has been explored as a function of beam and plasma parameters. Experimental evidence has been obtained for the collisionless damping of Tonks-Dattner modes.

8. Superconductivity Studies

Progress is reported in studies of anisotropy of the energy gap in superconducting niobium and the superconducting parametric amplifier. The support of other activities of this group has been transferred to the Materials Research Laboratory.

9. High-Voltage Breakdown

Studies of the phenomenon of high-voltage breakdown are reviewed, and the theory of the melting of electrode projections is discussed. Predicted breakdown fields to produce melting are compared with experimental observations.

10. Thin Films

The state of the equipment to be used for size-effect measurements and for Hall mobility measurements in thin films is discussed.

11. Information Science

Further progress has been made in all three areas of algebraic coding theory under investigation. A new investigation is initiated in digital addressing.

12. Switching Systems

Further progress is reported on computer diagnosis studies, modular decompositions of sequential machines, the propagation of errors in finite-memory encoding/decoding schemes, and studies of quasi-linear machines. Progress is also reported on the problem of obtaining a realizable state model from an immittance matrix by node insertion. The study of time-shared computer systems has been suspended indefinitely. A new investigation on the generation of diagnostic tests for combinational logic nets has been started.

13. Networks and Communication Nets

In the study of nonlinear systems, new bounds on the solution trajectories for the Lienard equation have been found, and a varactor diode circuit has been studied with respect to perturbational stability to obtain improved bounds. In graph-theoretic studies, new results are reported on the properties of feedback arc sets, system reliability, system stability for time-varying components, multistage communication nets, and the realizability of switching functions.

COORDINATED SCIENCE LABORATORY PERSONNEL

Faculty, Research Associates, and Research Engineers

Compton, W. Dale,	Hohn, F.	Prothe, W. C.
Director	Huggins, R.	Asst. to Director
Alpert, D.	Ichikawa, Y.	Raether, M.
Anderson, R.	Kasami, T.	Ray, J.
Ash, R.	Killian, T. J.	Resh, J.
Barrows, J.	Kirkwood, B. D.	Satterthwaite, C. B.
Bitzer, D. L.	Knoebel, H. W.	Schuemann, W. C.
Böhmer, H.	Krone, H. V.	Skaperdas, D.
Brown, R. M.	Lee, D. A.	Slottow, H. G.
Chien, R.	Lyman, E. M.	Sobral, M.
Cooper, D. H.	Lyman, E. R.	Stake, R.
Cruz, J. B., Jr.	Mayeda, W.	Steinrisser, F.
Easley, J. A., Jr.	Metze, G.	Stifle, J.
Fenves, S.	Montague, W. E.	Trick, T.
Golden, W.	Peacock, R. N.	Trogdon, R.
Gooch, J.	Perkins, W.	Van Valkenburg, M. E.
Hastings, J. T.	Preparata, F.	Voth, B.
Hicks, B.	Propst, F. M.	Wax, N.
		Yen, S.

Research Assistants

Arora, B.	Gaddess, T.	Minning, L.
Agashe, S.	Gutman, D.	Moore, B. K.
Aubuchon, K.	Hartmann, C.	Morrison, H.
Bahl, L.	Hosken, R.	Murata, T.
Bleha, W.	Hsu, H. T.	Myers, J. L., Jr.
Bouknight, J.	Hsu, J.	Nishijima, M.
Bridges, C.	Hyatt, W.	Piper, T.
Brown, K.	Jacobs, J. T.	Reddy, D.
Carlson, J.	Jenks, R.	Rust, R. D.
Carr, W.	Kamae, T.	Schneider, R.
Chang, J.	Karr, G. R.	Schoenberger, M.
Chang, S. C.	Kraatz, J.	Secrest, M.
Chow, D.	Lie, T.	Singer, S.
Cooper, T.	Lum, V.	Smith, M.
Craford, M.	Marlett, R.	Tibbetts, G.
Crockett, E. D.	Martens, G.	Toepke, I.
Cummings, J.	Marzullo, E.	Toida, S.
Davies, M.	Mehta, N.	Wearing, A.
duPreez, R. J.	Mendel, C.	Willson, R. H.
Fillman, L.	Metze, V.	

Fellows

Herner, J. P.	Stumpff, G.	Werner, R.
Hoyt, R.	Tracey, R.	Powell, T.

Secretaries

Rudicil, J.
Schmidt, R.

Typists and Stenos

Butterworth, T.
Carrera, M. J.
Dewar, V.
Hanoka, N.
Harris, M.
Keel, D.
Lane, R.
McDonald, R.
Shaw, C.

Chief Clerk

Drews, C. E.

Accounting Clerk

Potter, R. E.

Draftsmen

Conway, E.
MacFarlane, R. F.

Res. Lab. Shop Supr.

Bandy, L. E.

Instrument Makers

Beaulin, W. E.
Bouck, G.
Merritt, K. E.
Zackery, R. L.

Laboratory Mechanics

Bales, R. B.
Burr, J. G.

Storekeepers

Jordan, F.
Lofton, C.
McElwain, W.

Glassblower

Lawrence, W.

Photographer

Fairchild, J.

Student Assistants

Arnold, C.
Babirak, M.
Bernhard, W.
Bollenbacher, G.
Borris, J.
Bullard, C.
Corcoran, J. P.
Eickert, D.
Fancher, D.

Groene, P.
Hodges, M.
Hughes, J.
Nanninga, J.
O'Meara, T.
Pinsky, H.
Ries, R.
Roberts, D.
Rundgren, W.

Electronics Engr. Asst.

Carter, E. N.
Gardner, O. E.
Hedges, L.
Neff, E. H.
Vassos, N.

Electronics Technicians

Casale, T. C.
Coad, D. E.
Crawford, G.
Deschene, D. R.
Holy, F. O.
Johnson, M.
Jordan, H.
Knoke, J. H.
Merrifield, F.
Roberts, G. R.
Schmidt, W.
Streff, L. W.
Susedik, A. J.
Turpin, F. G.

Phys. Sci. Staff Asst.

Thrasher, W.

Samson, C.
Smith, S.
Steinberg, L.
Stozek, R.
Sutton, C.
Trombi, P.
Walker, M.
Walsh, F.
Williams, R.
Zapatero, G.

PUBLICATIONS AND REPORTS

1. Journal Articles Published or Accepted

J. T. Barrows, "Extension of Fuessner's Method to Active Networks," IEEE Trans. on Circuit Theory (to appear).

L. O. Chua and R. A. Rohrer, "On the Dynamic Equations of a Class of Nonlinear RLC Networks," IEEE Trans. on Circuit Theory, CT-12, pp. 475-489 (December, 1965).

J. B. Cruz, Jr., and W. R. Perkins, "Conditions for Signal and Parameter Invariance in Dynamical Systems," IEEE Trans. on Automatic Control, AC-11 (to appear).

Y. Ichikawa, "Dielectric Properties of a Weakly Turbulent Plasma," Physics of Fluids, 9, 111 (1966).

W. Mayeda, "Application of Linear Graph Theory to Communication Nets," Progress in Radio Science, 1960-63, Vol. VI (Radio Waves and Circuits), F. L. H. M. Stumpers, Editor, pp. 67-70 (Elsevier Publishing Company, Amsterdam, 1966).

J. A. Resh, "On the Synthesis of Oriented Communication Nets," IEEE Trans. on Circuit Theory, CT-12, pp. 540-546 (December, 1965).

2. Meeting Papers

J. B. Cruz, Jr. and W. R. Perkins, "On Invariance and Sensitivity," 1966 IEEE International Convention, New York, March, 1966.

J. B. Cruz, Jr. and W. R. Perkins, "Criteria for System Sensitivity to Parameter Variations," Third Congress of the International Federation on Automatic Control, London, June, 1966.

S. C. Lee, "On Multiparameter Sensitivity," Proceedings Allerton Conference on Circuit and System Theory, pp. 407-420, October, 1965.

T. Murata, "Analysis of Lossy Communication Nets by Modified Incidence Matrices," Proceedings Allerton Conference on Circuit and System Theory, pp. 751-761, October, 1965.

K. Onaga, "Stochastic Flow and Efficient Transmission through Communication Nets," Proceedings Allerton Conference on Circuit and System Theory, pp. 762-771, October, 1965.

T. N. Trick and D. R. Anderson, "Lower Bounds on the Thresholds of Subharmonic Oscillations," Proceedings Allerton Conference on Circuit and System Theory, pp. 524-535, October, 1965.

3. Technical Reports

- R-136 REVISED REPORT. Manual for the CSX-1 Computer. R. M. Brown, R. D. Jenks, J. Stifle, R. L. Trogon (December, 1965).
- R-260 REPLAB: A Lesson in Scientific Inquiry Using the PLATO System. D. L. Bitzer, E. R. Lyman, J. R. Suchman (December, 1965).
- R-270 Set of Cut Sets and Optimum Flow. W. Mayeda and M. E. Van Valkenburg (November, 1965).
- R-271 Ion Oscillations in a Weakly Turbulent Plasma. Yoshi H. Ichikawa (November, 1965).
- R-272 Elementary Complete Tree Transformation. Wataru Mayeda (December, 1965).
- R-273 High Resolution Radio Frequency Measurements of Faraday Rotation and Differential Absorption with Rocket Probes. H. Knoebel, D. Skaperdas, J. Gooch, B. Kirkwood, H. Krone; ed. by D. Skaperdas (December, 1965).
- R-274 Effects of Micrometeoroid Cratering on the Direction of the Axis of Maximum Moment of Inertia. H. O. Barthel (February, 1966).
- R-275 Aerodynamic Torque on a Spinning Spherical Satellite. Gerald R. Karr (January, 1966).
- R-276 Thermodynamic Properties of an Electron Plasma. T. J. Lie and Y. H. Ichikawa (February, 1966).
- R-277 A New Method for Constructing Multiple Error Correcting Linear Residue Codes. John T. Barrows, Jr. (January, 1966).
- R-278 System Optimization with Fixed Control Structure. M. Schoenberger (January, 1966).
- R-279 Necessary and Sufficient Conditions for Realizability of Given Switching Functions. Shunichi Toida (January, 1966).
- R-280 Calculations Concerning Electrical Breakdown Induced by the Melting of Microscopic Projections. D. A. Lee (January, 1966).

TABLE OF CONTENTS

	Page
1. Space Sciences	1
1.1 Research in Gyro Materials	1
1.2 Influence of Meteoroids	4
1.3 Gyro Diameter Optimization	9
2. Surface Physics	15
2.1 High-Resolution Electron Spectrometry of Surfaces . . .	15
2.1.1 Discrete Loss Mechanisms	15
2.1.2 Energy Distributions and Inelastic Scattering Probabilities	17
2.2 Angular Distribution of Particles Scattered from Surfaces	24
2.3 Adsorption-Desorption of Gases at Metal Surfaces . . .	31
3. Computer	32
3.1 Introduction	32
3.2 CSX-1 Computer	32
3.2.1 Operations	32
3.3 CDC 1604 Computer	32
3.3.1 Operations	32
3.3.2 Computer Display	33
3.3.3 Analog to Digital Converter	34
4. Control Systems	36
4.1 Introduction	36
4.2 Sensitivity of Dynamical Systems	37
4.2.1 Bounds on Norms of Sensitivity Functions . . .	37
4.2.2 Synthesizing Comparatively Insensitive Linear Systems	38
4.2.3 Sensitivity Considerations for Nonlinear Systems	39
4.2.4 Sensitivity Analysis of Dynamic Systems . . .	39
4.2.5 Sensitivity Considerations in the Synthesis of Doubly-Terminated Coupling Networks	41

	Page
4.2.6 Linear Regulators with Plant Parameter Perturbation	41
4.2.7 Sensitivity of Optimal Control Systems	42
4.3 System Optimization with Fixed Control Structure	43
4.4 Stability of Nonlinear Systems	44
4.5 Computer-Oriented Formulation and Solution of the Optimal Control Problem: Characterization of Linear, Time-Invariant Differential Systems.	46
5. PLATO	48
5.1 Introduction	48
5.2 PLATO III System Equipment	50
5.3 Plasma-Discharge Display-Tube Research	51
5.4 PLATO Learning and Teaching Research	55
5.4.1 University Courses	55
5.4.1.1 Electrical Engineering 322-- Circuit Analysis.	55
5.4.1.2 FORTRAN Programming for Business Students.	57
5.4.1.3 Library Science 195	58
5.4.2 Mathematics Instructional Projects	58
5.4.2.1 ARITHDRILL.	58
5.4.2.2 PROOF	59
5.4.3 Behavioral Science Projects.	59
5.4.3.1 Retention of Conceptual Materials Research.	59
5.4.3.2 Man-Computer Interface Study.	60
5.4.3.3 A Language-Free Test of Inter- personal Norms.	60
5.4.3.4 Interaction Studies Group	61
5.4.4 Project SIRA (System for Instructional Response Analysis)	61
5.5 The CATO Manual.	62
5.6 PLATO Seminars and Demonstrations.	63

	Page
6. Vacuum Instrumentation.	65
6.1 Pumping Speed of Getter-Ion Pumps.	65
6.2 CO Production under O ₂ Admission	66
6.3 Resumption of Work on the Suppressor Ionization Gauge.	68
6.4 Proposed Work on the Suppressor Gauge.	69
7. Plasma Physics.	71
7.1 Boltzmann Equation	71
7.2 Beam-Plasma Interaction.	72
7.3 Landau Damping in an Inhomogeneous Plasma.	79
8. Superconductivity Studies	85
8.1 Introduction	85
8.2 Superconducting Parametric Amplifier (Picovoltmeter) .	85
8.3 Superconductive Tunneling in High-Purity Single- Crystal Niobium.	86
9. High Voltage Breakdown.	87
9.1 Review	87
9.2 Calculations Concerning Electrical Breakdown	88
10. Thin Films.	94
10.1 Size Effects	94
10.2 Cryopump Tests	95
10.3 Hall-Effect System	96
11. Information Science	97
11.1 Introduction	97
11.2 Algebraic Theory of Bose-Chaudhuri-Hocquenghem Codes .	97
11.3 Coding Methods for Information Retrieval	99
11.4 Coding for Compound Channels	100
11.5 Linear Residue Codes	102
11.6 Coding for the Time-Discrete Gaussian Channel.	105
11.7 Digital Addressing	105

	Page
12. Switching Systems	106
12.1 Computer Compiler.	106
12.2 Diagnosis of Computers	107
12.3 Diagnosis of Combinational Logic Nets.	107
12.4 Synthesis of Sequential Networks	108
12.5 Analysis of Convolutional Transformations of Binary Sequences	108
12.6 Quasi-Linear Sequential Machines	110
12.7 Algebraic Network Synthesis.	110
12.8 Computer System Evaluation	111
13. Network and Communication Nets.	112
13.1 Some Periodic Solutions of the Lienard Equation.	112
13.2 Stability of Nonlinear Networks.	112
13.3 On a Minimum Feedback Arc Set.	115
13.3.1 Partition Not Affecting the Minimumness.	115
13.3.2 Topological Properties	116
13.3.3 Bounds on the Order of a Minimum Feedback Arc Set.	116
13.4 Linear Graphs in the Study of Reliability.	117
13.5 A Generating Function for R_{ij}	118
13.6 Multistage Communication	119
13.7 The State Axioms in System Theory.	120
13.8 Topological Method for Stability Analysis of Linear Time-Varying Networks.	121
13.9 Realizable Switching Conditions.	121
13.10 Flows in Communication Nets.	123
13.11 Computer Generation of Complete Trees.	124

1. SPACE SCIENCES

H. W. Knoebel	J. D. Gooch	E. Marzullo
D. O. Skaperdas	G. R. Karr	H. C. Morrison
J. R. Ray	B. D. Kirkwood	J. L. Myers, Jr.
D. H. Cooper	H. V. Krone	N. Mehta

1.1 Research in Gyro Materials[†]

Considerations of torques due to 1) a fixed charge on a sphere in an electric field, 2) induced currents in a conductive sphere rotating in a magnetic field, and 3) induced currents in a conductive sphere rotating in an electric field have established a range of material electrical resistivity of $10^3 < \rho_e < 10^{10}$ ohm cm. By using a passive temperature stabilization technique of controlling the solar absorptivity α to thermal emissivity ϵ of multilayer coatings on the satellite gyro,^{1,2} a desired operating temperature range between the approximate temperature limits -80°C to 100°C can be engineered.. Since the operating temperature has not yet been established, a search for materials which have acceptable electrical resistivity within the above temperature limits has been instituted. The materials germanium, silicon, and titanium dioxide, when properly doped, and a sodium silicate

[†]Portions of this work were supported by the National Aeronautics and Space Administration under Grant NASA Nsg 443.

¹Hass, G., Drummeter, L., and Schach, M., "Temperature Stabilization of Highly Reflecting Satellites," Journ. Opt. Soc. Am. 49, (September 1959) pp. 918-924.

²Symposium on Thermal Radiation of Solids, ed. by S. Katzoff (March 4-6, 1964). NASA, Sp-55.

glass³ composed of 60% SiO₂, 30% Na₂O, and 10% CaO are among a number which appear to satisfy the electrical resistivity requirements.

In addition these materials must satisfy other properties, one of the most important being high mechanical damping. After launch and gyro spin-up and after any micrometeorite cratering the gyro angular momentum vector, instantaneous spin vector, and symmetry axis vector will not in general be aligned. The inherent damping, in which elastic vibrations due to gyroscopic action cause energy dissipation and consequent realignment of these vectors, will be used. The time required for the gyro symmetry axis vector to align itself from an angle θ_i to θ_f with respect to the angular momentum axis is given by

$$T = (2\pi C \omega_o / \gamma W) \ln(\theta_i / \theta_f)$$

where C is the gyro polar moment of inertia, ω_o is the gyro spin frequency, γ is the damping factor defined by the fraction of the elastic energy dissipated to the amount of energy stored per cycle and W is the total elastic strain energy of the gyro.

The more familiar and common term Q will be used to replace the damping factor γ by the relation $Q = 2\pi/\gamma$. For conditions of this experiment, a 12-inch diameter gyro rotating at 250Hz, approximate calculations of W indicate that for damping times T of about half a day, with $\theta_i \approx 5^\circ$ and $\theta_f = 0.1$ arc second, a value of $1/Q$ larger than about 10^{-3} is required. More exact calculations of W are now being undertaken.

³Goldsmith, A., Waterman, T. E., Hirschorn, H. J., Handbook of Thermophysical Properties of Solid Materials, Vol. II: Ceramics (The MacMillan Co., New York, 1961), VII-C-1-b.

Among the more promising high damping factor materials are the glasses. Among other things, $1/Q$ is a function of the elastic vibrating frequency which, for the gyro, is given by $[(A-C)/A]\omega_0 \cos\theta$. Present gyro parameters indicate a frequency of about 1 to 3 Hz. Glass has a maximum value for $1/Q$ of 4.3×10^{-3} in this range of frequencies.^{4,5}

In order to check this result a four foot torsional pendulum consisting of a fine strand of Pyrex glass was constructed within a vacuum chamber and the logarithmic decrement $\delta = \pi/Q$ was measured. The natural frequency of the pendulum was about 0.3 Hz, at which a measured value of .0043 for $1/Q$ was obtained, as compared with a value of .004 at the same frequency from reference 5. Hence, it appears that a glass gyro rotor can satisfy the damping requirement and possibly the resistivity requirement. The latter will be checked by measuring a sample of the glass.

Preparations are being made to spin simulated glass rotors in a motor-driven test fixture in order to discover any problems associated with the use of glass under severe centrifugal stress. Adequate protection will be provided to absorb the energy in case of structural failure.

⁴Zener, C., Elasticity and Anelasticity of Metals, (University of Chicago Press, 1948), p. 55.

⁵Bennewitz, K., and Rötger, H., "Über die Innere Reibung fester Körper; Absorptionsfrequenz von Metallen in akustischen Gebiet," Phys. Zeitschr., 37, 578 (1936).

1.2 Influence of Meteoroids[†]

The degree to which the relativity satellite of the Coordinated Science Laboratory is immune to the momentum transfer of impacting meteoroids depends upon the model of the meteoroid flux. The best known, and also the most conservative, model of the meteoroid environment was developed by Whipple in 1957. This model can be represented by

$$\Phi_1 = 1.3 \times 10^{-12} m^{-1},$$

where Φ is the flux per meter² sec of particles with mass m grams and greater.⁶ A 1961 evaluation of rocket and satellite data obtained

$$\Phi_2 = 10^{-17.0} m^{-1.70},$$

applicable between masses of 10^{-10} to 10^{-6} gm.⁶ However, observations of meteors simulated by shaped charge firings indicated that Whipple's 1957 estimate should be revised by an order of magnitude to give⁶

$$\Phi_3 = 1.3 \times 10^{-13} m^{-1}.$$

These are three meteoroid models currently used, all subject to revision as more is learned of the space environment.

The number of particles hitting a given satellite in a given amount of time can be calculated, using the flux expression, to be

[†]Portions of this work were supported by the National Aeronautics and Space Administration under Grant NASA NsG 443.

⁶Orbital Flight Handbook, NASA Sp-33, Part 1, pp. II46-II47.

$$N = \Phi AT ,$$

where A is the area exposed to meteoroids and T is the time of exposure. Assume, for calculation purposes, a possible CSL gyro satellite to be a solid, nearly spherical body of density 2.2 gm/cm^3 , having a radius of 15 cm, spinning at 250 Hz and monitored for one year. A plot of the number of meteoroids striking the satellite versus the meteoroid mass is given in Fig. 1.1 using the above satellite radius and the three different flux estimates. Figure 1.1 reveals that large numbers of small meteoroids will hit the satellite while few meteoroids heavier than 10^{-5} grams are to be expected within a year's time.

The effect of a meteoroid hit will depend upon the momentum of the impinging particle. Visual observations of meteor showers indicate that large meteoroids have approximate velocities of 28 km/sec while smaller particles have a velocity of about 15 km/sec. The velocity distribution tabulated in Table 35 of Ref. 6 is used for calculations in this analysis. A conservative approach to the momentum exchange analysis is to assume that the momentum vector of all impinging particles is perpendicular to the spin axis and passes through the spin axis. The impulsive angular displacement, δ , caused by one meteoroid hit would then be

$$\delta = mvr/C\Omega ,$$

where C is the moment of inertia, Ω is the spin rate, and mvr is the momentum of the meteoroid acting at a distance r from the center of mass of the satellite. For a conservative calculation let r be the radius

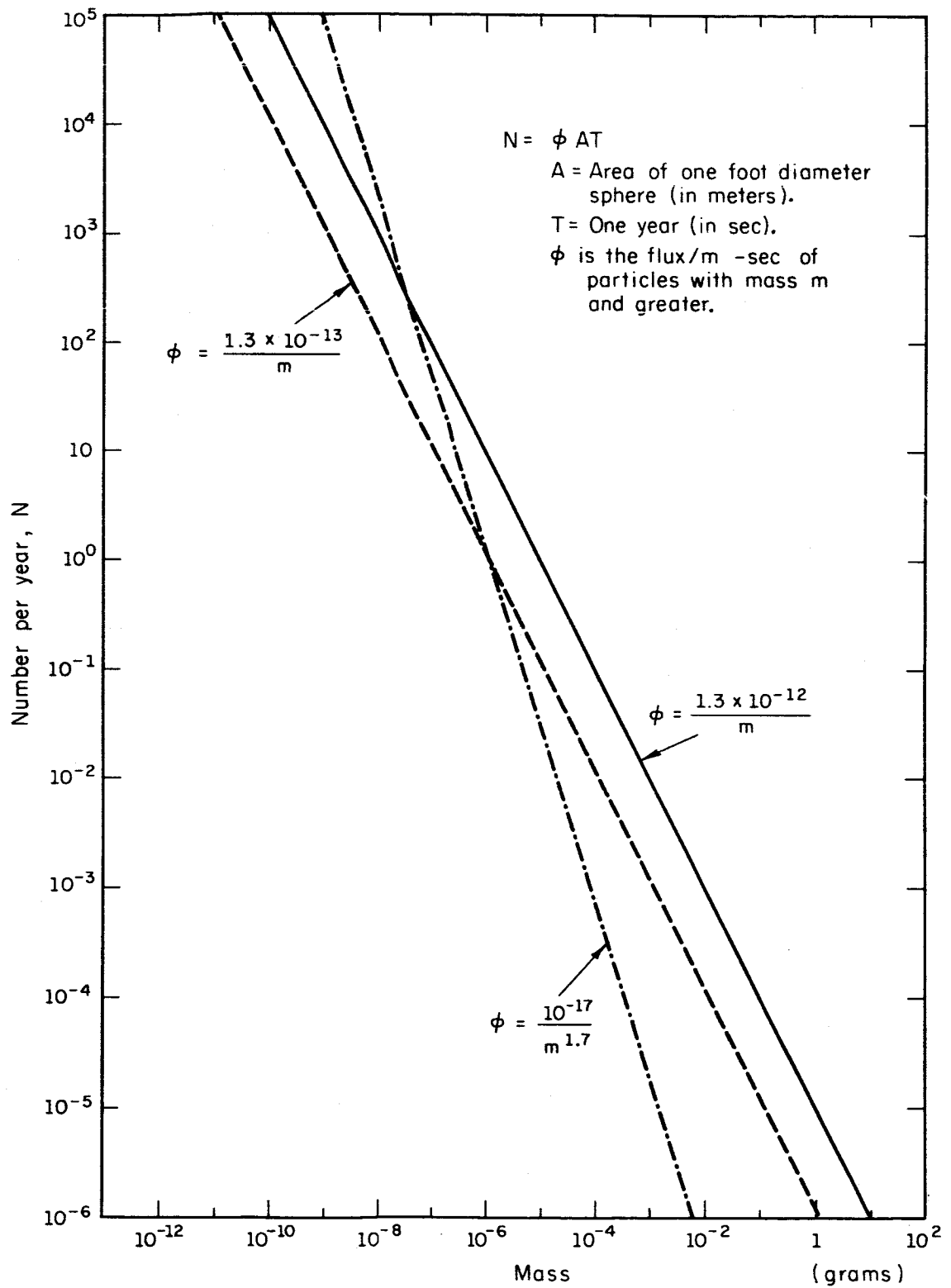


Fig. 1.1. Number of Meteoroids Striking Proposed Gyro per Year versus the Meteoroid Mass for Three Flux Models.

of the satellite, R . The moment of inertia of the spherical gyro is

$$C = 8\rho_s R^5/15$$

where ρ_s is the density, and the impulsive angular deviation due to one meteoroid hit becomes

$$\delta = \frac{15}{8\pi} \frac{mv}{\rho_s R^4 \Omega}.$$

A large satellite then would be less affected by meteoroid hits than a smaller one. However, a larger satellite is hit by a greater number of particles. This can be taken into consideration by assuming a mean square deviation of events along the spin axis and writing an expression for the net angular deviation, σ , of N hits,

$$\sigma = \delta\sqrt{N}.$$

This function is plotted versus meteoroid mass in Fig. 1.2 using the conservative 1957 Whipple estimate of meteoroid flux. Since the surface area of a sphere is $2\pi R^2$, σ is inversely proportional to the radius cubed.

Figure 1.2 indicates that the larger meteoroids will be detrimental to the relativity experiment which requires spurious deviations of less than 1 sec of arc per year. However, the probability of being hit by the larger meteoroids is of course less than for the smaller particles. Assuming a Poisson distribution of events, the probability of no impact, $P(0)$, within a year by a meteoroid of a given mass is given by

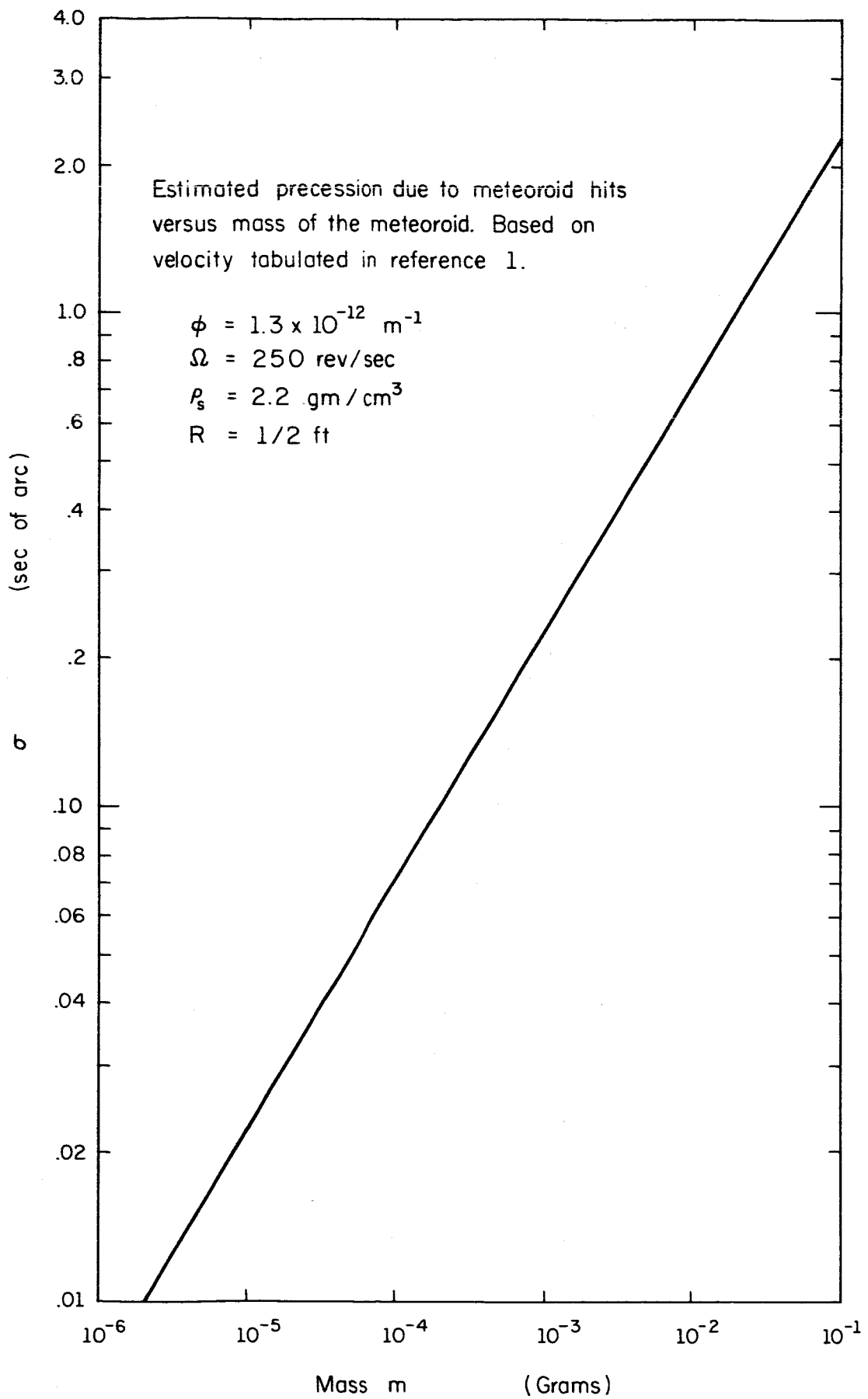


Fig. 1.2. Net Angular Deviation of Gyro Spin Axis versus Meteoroid Mass.

$$P(0) = e^{-N}$$

where $N = \phi AT$. Therefore, for a meteoroid of a given mass, the maximum impulsive precession due to its impact and the probability of it not hitting the satellite can be calculated. A plot of $P(0)$ versus δ using the three meteoroid flux models is given in Fig. 1.3. This plot can be interpreted to give the probability of success of the experiment with reference to meteoroids if a maximum δ to be tolerated is defined. For the CSL relativity experiment this maximum δ would be 1 sec of arc in a year which would correspond to better than 97% chance of success using the most conservative flux estimate. The effect of meteor showers in which the flux rate may increase by two or three orders of magnitude is being investigated.

1.3 Gyro Diameter Optimization[†]

The previous report analyzed the gyro torque due to gravity gradient for a non-regressing orbit. The present report extends this analysis for a regressing orbit due to the earth's oblateness. Furthermore, the effects of centrifugal deformation and the statistics of micrometeorite cratering along with the effects of gravity gradient give rise to an optimum gyro diameter, as shown by the following discussion.

[†]Portions of this work were supported by the National Aeronautics and Space Administration under Grant NASA Nsg 443.

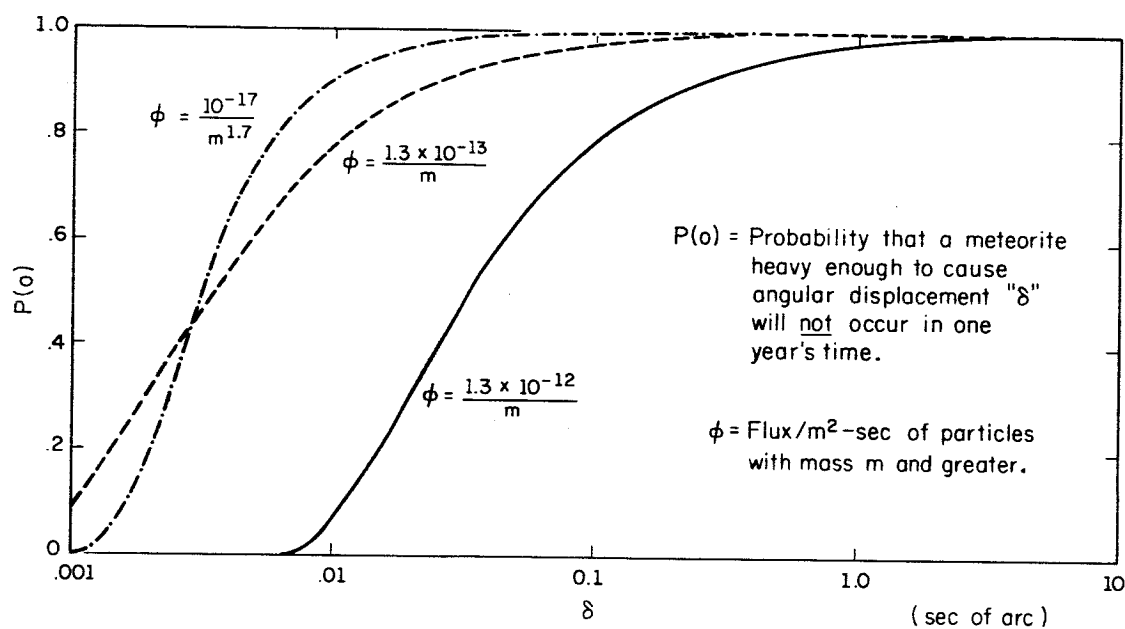


Fig. 1.3. Probability of No Meteoroid Impact with the Proposed Gyro in One Year versus the Impulsive Angular Deviation due to One Impact, for Three Flux Models.

The spin axis deviation due to gravity gradient for a gyro orbiting in a regressing, elliptic orbit is

$$\dot{\varphi} = -2\Lambda [\sin i \cot \epsilon \cos(\Omega - \varphi) - \cos i] \cos \theta, \quad (1)$$

$$\dot{\epsilon} = -2\Lambda \sin i \sin(\Omega - \varphi) \cos \theta, \quad (2)$$

in which

i is the orbital inclination,

Ω is the right ascension of the orbit,

ϵ is the inclination of the gyro equatorial plane,

φ is the right ascension of the gyro,

θ is the angle between the gyro spin axis and the orbital plane,

and

$$\Lambda = (3GM/4a^3 \omega_s) [(1+3e^2/4)/(1-e^2)^3] (C-A)/C \quad (3)$$

in which

G is the universal gravitational constant,

M is the mass of the earth,

a is the semi-major axis of the orbital ellipse,

e is the eccentricity of the ellipse,

ω_s is the gyro angular velocity,

C is the gyro polar moment of inertia,

A is the gyro transverse moment of inertia.

Because of centrifugal deformation the gyro moment of inertia ratio

$(C-A)/C$ can be written as the sum of two components--a static or manufactured component $[(C-A)/C]_s$ and a component due to centrifugal

deformation, so that

$$(C-A)/A = [(C-A)/C]_s + F(\sigma) \rho r^2 \omega_s^2 / E \quad (4)$$

in which

$F(\sigma)$ is a function of the Poisson ratio,

ρ is the gyro density,

E is the modulus of elasticity,

r is the gyro radius.

A plot of Λ versus r for various peripheral velocities $v = \omega_s r$ from Eq. (3) is shown in Fig. 1.4. Orbital eccentricities smaller than 0.1 are used, in which case the error in Λ is less than 4 per cent. From a family of such plots, it is found that the values of r and v which produce the minimum value of Λ also cause the centrifugal deformation inertia ratio component to equal the static value component. It is also seen from Fig. 1.4 that the curve of Λ vs r has a broad minimum which includes the reasonable gyro radius of 15 cm. From Eqs. (3), (4), and Fig. 1.4, it can be shown that for minimum Λ , and hence minimum precession, the peripheral velocity v should be as large as possible and the static inertia ratio be as small as possible. For most materials the yield point is reached when the peripheral velocity is about 300 meters/sec.

The data readout system requires a finite $[(C-A)/A]_s$. This is seen from Fig. 1.1 of the previous progress report, in which the number of hits per year, each of which could cause an angular disturbance of 0.6 arc sec, is plotted versus $(C-A)/C$. For this plot, the meteoroid flux model of Eq. (2) was used. If such disturbances occur at a rate less

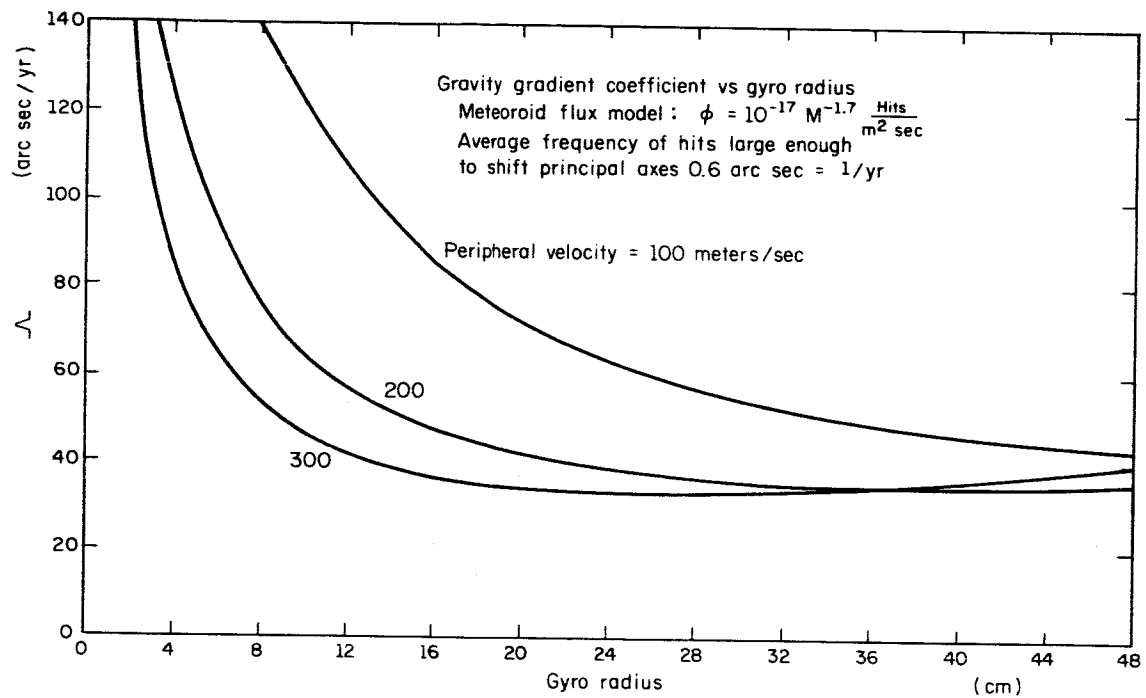


Fig. 1.4. Λ versus Gyro Diameter r for Various Peripheral Velocities.

than once per month, and for a spin-axis damping time of less than one day, the effect of the disturbance can be readily removed from gyro spin-axis orientation data. Assuming the meteorite flux has a Poisson distribution, then, if angular disturbances of one-tenth the relativity effect occur once per year, the probability of having one month of undisturbed data is 0.92; and, from Fig. 1.1 of the previous progress report, the required $(C-A)/C$ ratio is 0.01. The curves for this figure are for a 15 cm radius solid. For a fused silica gyro of 15 cm radius and a peripheral velocity of 300 meter/sec, Λ is about 40 arc sec per year.

From Eqs. (1) and (2), the theoretically determined minimum value of Λ and the requirement that the spurious gyro drift be one order of magnitude less than the general relativity precession, the requirements are obtained that the gyro spin axis must lie in the plane of either a polar orbit or the earth's equatorial plane for a nearly equatorial orbit to better than 0.44 degrees.

2. SURFACE PHYSICS

F. Propst
F. Steinrisser

T. Cooper
M. Nishijima

T. Piper
G. Tibbetts

2.1 High-Resolution Electron Spectrometry of Surfaces

A substantial number of measurements have been made with the high-resolution electron spectrometer described in previous progress reports. The measurements which have been made with this instrument to date have been on the (100) surface of a tungsten single-crystal ribbon. Measurements have been made of the energy distribution of secondary electrons for primary energies between 1 and 45 eV; the number of electrons produced with 1.0, 1.5, 2.0, 2.5, and 3.0 eV energy less than the primary energy as a function of primary energy; and the elastic reflection coefficient for primary energies between 0 and 100 eV. These measurements have been made for the target cleaned by flashing to 2300⁰K and with N₂, H₂, and CO adsorbed on the surface. The results indicate that several of the processes discussed in previous progress reports have been observed.

2.1.1 Discrete Loss Mechanisms. Figure 2.1 shows a logarithmic plot of the energy distribution of scattered electrons from the tungsten surface. These results were obtained after system bakeout and before any further processing of the target. The region of the distribution shown is in the "valley" just below the very strong elastic peak (the elastic peak is not shown). The peaks in the distribution are due to excitation of discrete states in the surface. They are separated by approximately 400 meV, the separation becoming somewhat less between the peaks of lower intensity. It is very likely that this structure represents

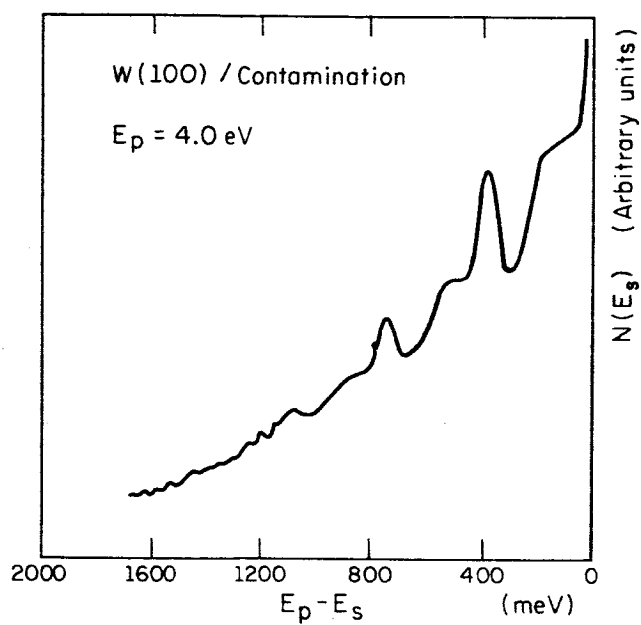


Fig. 2.1. Energy Distribution of Secondary Electrons from a Contaminated Tungsten (100) Surface, Showing the Existence of Low Energy Discrete Losses.

the excitation of the vibrational states of gas adsorbed on the surface. The structure disappears after flashing the target. Efforts to observe the structure with N_2 , H_2 , and CO adsorbed on the surface have not been successful. It is possible that the system which exhibits the structure of Fig. 2.1 is the hydrogen-nitrogen bond on tungsten. The value of 395 meV observed for the surface loss is close to the N-H stretching bond in a number of systems. Figure 2.2 shows the same type of structure which resulted from exposing the clean target to the outgassing products of a gauge which had been exposed to O_2 . The structure is very similar to that in Fig. 2.1, and again it seems likely that N-H or C-H is the source. Various vapors will be introduced directly into the system to check this hypothesis.

These results, although by no means complete, open the possibility of a technique for the analysis of surface contaminants and structure similar to the technique of infrared spectroscopy.

2.1.2 Energy Distributions and Inelastic Scattering Probabilities.

Figures 2.3 and 2.4 show the energy distributions for secondary electrons from clean tungsten for the primary energies indicated. There are two interesting features in these curves. First, there is a peak at approximately 1 eV below the elastic peak. This is very likely due to a peak in the density of states in the band structure of the solid at 1 eV above or below the Fermi level. The calculation of the band structure of tungsten by Mattheiss¹ indicates a peak at this energy below the Fermi

¹L. F. Mattheiss, "Fermi Surface in Tungsten," Phys. Rev. 139, A1893 (1965).

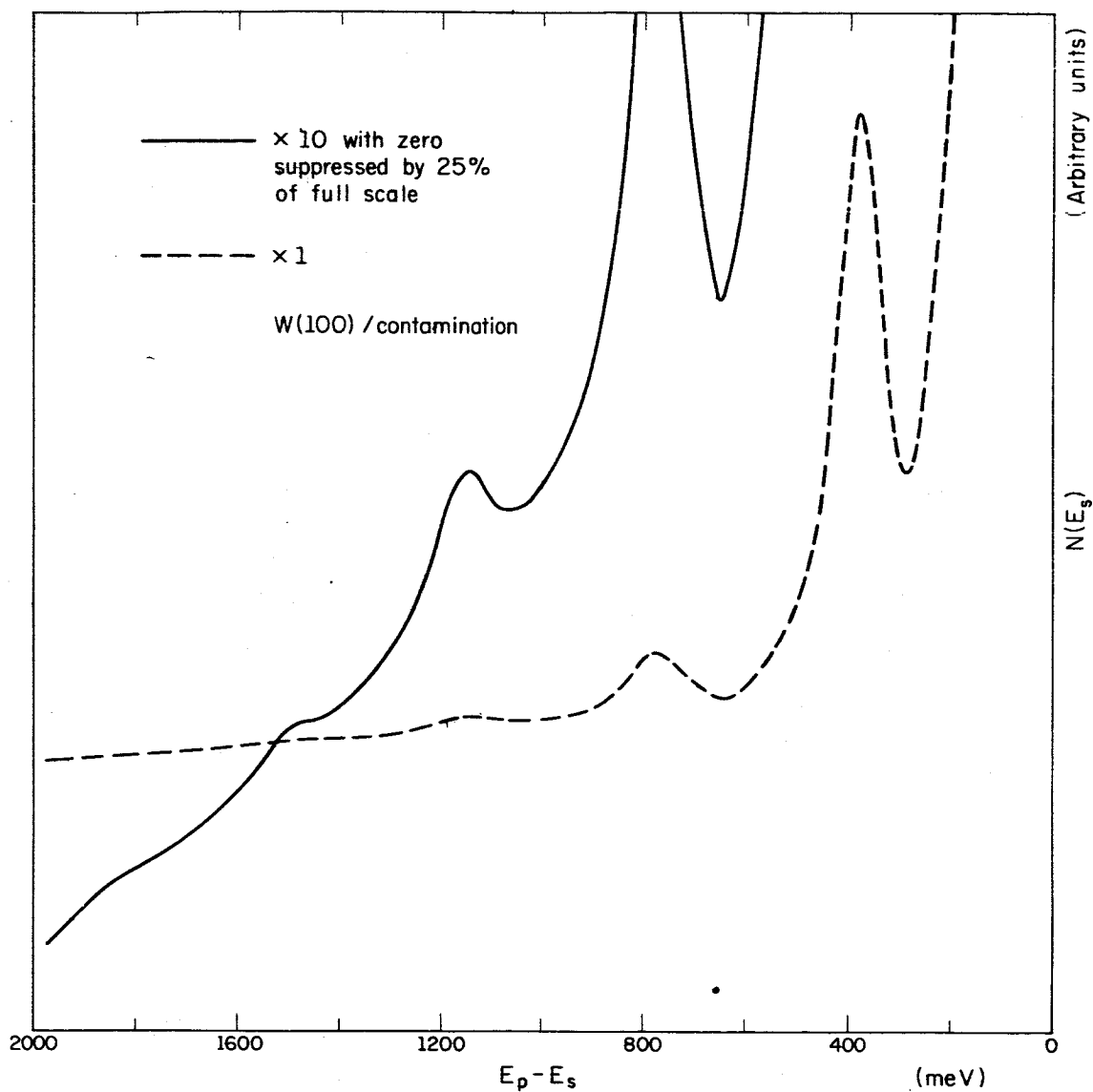


Fig. 2.2. Energy Distribution of Secondary Electrons from a Tungsten (100) Surface after Exposing the Surface to Nitrogen and the Reaction Products of the Nitrogen with an Operating Hot Cathode Ionization Gauge.

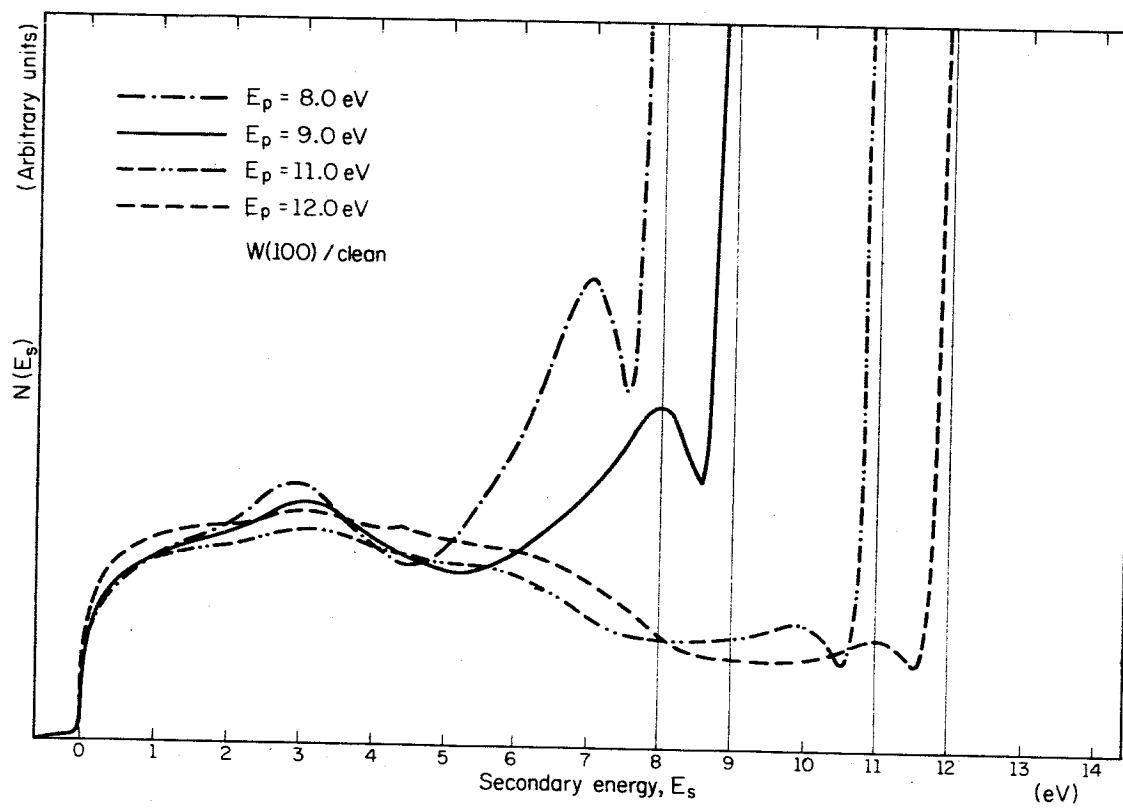


Fig. 2.3. Energy Distribution of Secondary Electrons from a Clean Tungsten (100) Surface.

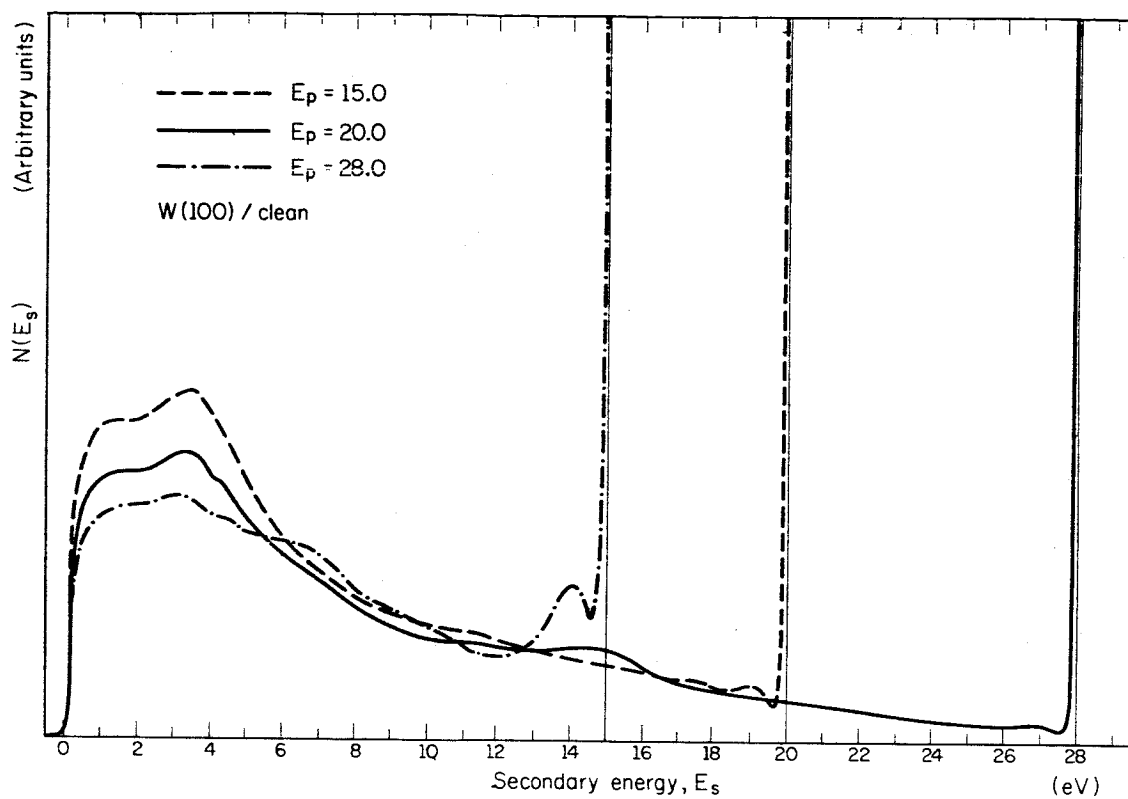


Fig. 2.4. Energy Distribution of Secondary Electrons from a Clean Tungsten (100) Surface.

level. In addition, there is structure in the low energy region of these distributions. In particular, there are small peaks at approximately 1 eV and 2.7 eV. These would indicate peaks in the density of states at these energies relative to the vacuum level.

Figure 2.5 shows the number of electrons leaving the target with 0.0, 1.0, 2.0, and 2.5 eV energy less than the primary energy, plotted as a function of the primary energy. Figure 2.6 shows the same data, plotted as a function of the energy of the electrons leaving the target. We note two things.

First, in Fig. 2.5, there is a peak in each of the curves at 4 eV primary energy. (In the curves shown the electrons leave the target with 4.0, 3.0, 2.0, and 1.5 eV kinetic energy when the primary energy is 4 eV.) In Fig. 2.6, there is a peak in the number of electrons leaving the target with 1.0, 2.7, 4.0, and 6.0 eV kinetic energy regardless of the primary energy. The first of these results indicates that there is a high probability of elastic scattering of 4 eV primary electrons, followed by inelastic scattering to give the structure at 4 eV (Fig. 2.5). The structure in Fig. 2.6, being fixed with respect to the kinetic energy of the electrons leaving the target, is indicative of structure in the density of states of the metal. The first two of the peaks (1.0 and 2.7 eV) of Fig. 2.6 correspond to the weak structure at the same energy in the energy distribution of secondary electrons (Figs. 2.3 and 2.4).

The peaks at approximately 1.0, 2.7, and 4.0 eV are in reasonably good agreement with the energies of the H_{25} , N_3 , and H_{15} symmetry points of the tungsten band structure as calculated by Mattheiss.¹

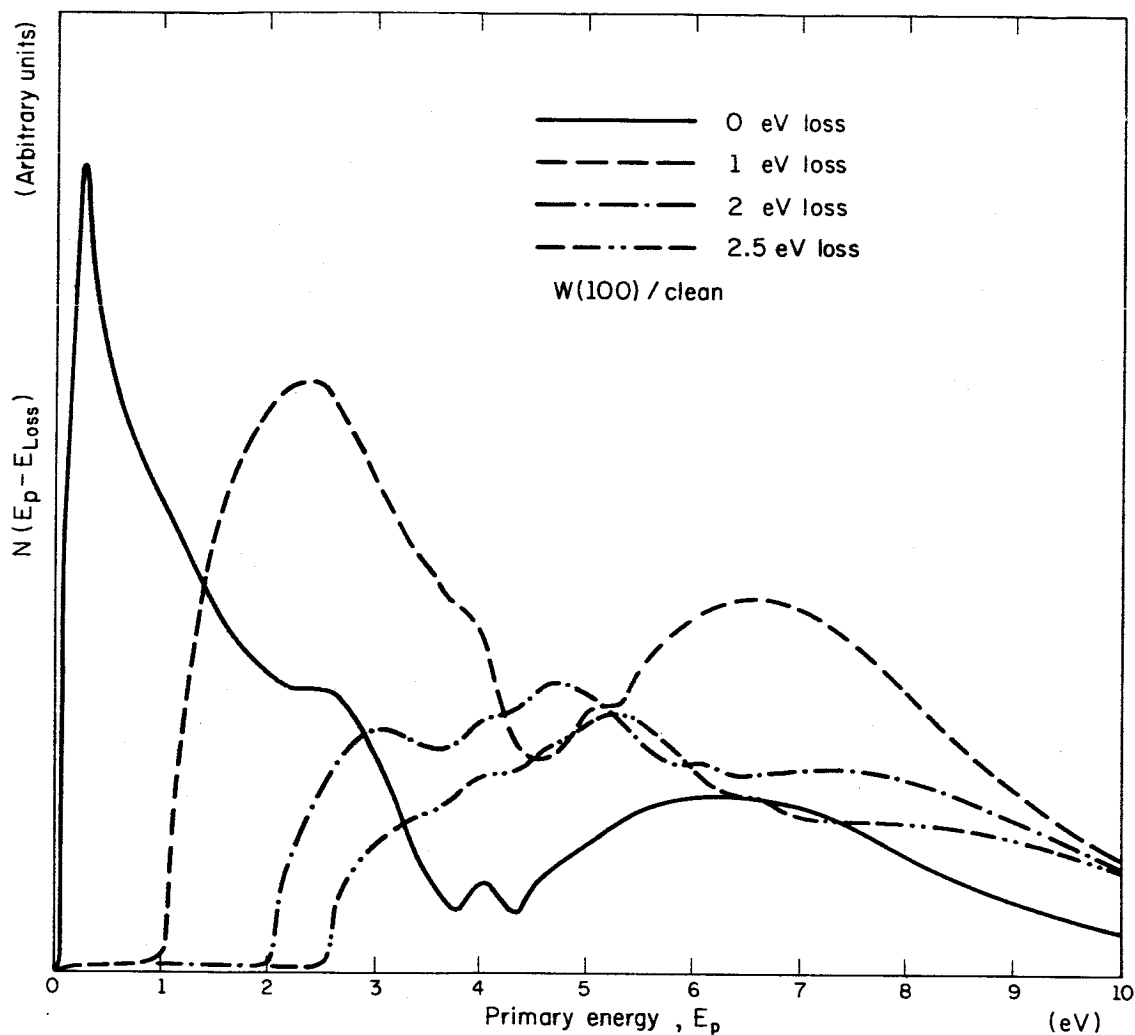


Fig. 2.5. Plot of the Number of Electrons Produced with 0.0, 1.0, 2.0, and 2.5 eV Kinetic Energy Less than the Primary Kinetic Energy Plotted as a Function of the Primary Energy. The data shown are for the clean tungsten (100) surface.

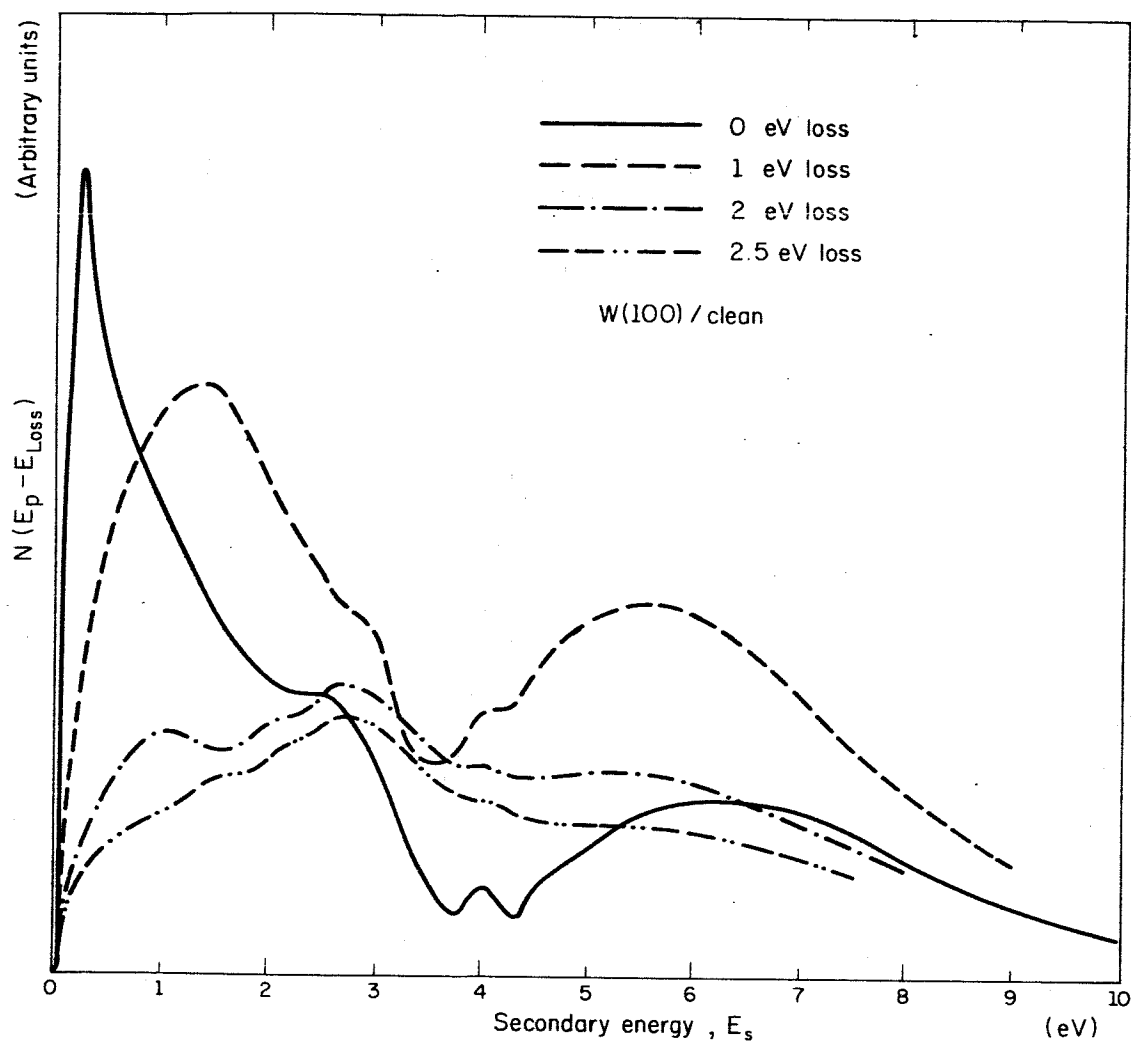


Fig. 2.6. Data of Fig. 2.5 Plotted as a Function of the Energy of the Electrons Leaving the Target.

In particular, Mattheiss gives the band structure calculated using two potentials, V_1 and V_2 . These potentials are identical with the exception that the exchange potential in V_1 is reduced by 30% in the case of V_2 . If one assumes a linear dependence of the energy separation of these symmetry points on the strength of the exchange potential, the energies for the H_{25} , N_3 , and H_{15} points are 1.4, 2.7, and 4.0 eV, respectively, when the exchange potential of V_1 is reduced by approximately 20%.

Figures 2.7 through 2.12 show the same type of results as above, but for the target exposed to N_2 and H_2 . The main feature illustrated is that the structure (although somewhat diminished) is qualitatively the same as for the clean surface. Again, we have the indication that the structure that is observed is due to the bulk properties.

In the studies of gas adsorption, the target exposure was approximately 10^{-3} Torr sec in each case. Flash-filament measurements indicate an extremely low sticking probability. In particular, there is probably very little N_2 adsorbed on the target for the curves of Figs. 2.7, 2.8, and 2.9, even after the very long exposure of the target.

2.2 Angular Distribution of Particles Scattered from Surfaces

New flanges have been constructed for the trap-to-baffle connector on the vacuum chamber for the angular-distribution measurement. The flanges were made from 3/4-inch thick stainless steel flat stock and hand lapped to an estimated 1/10-micron finish. Six 5/16 bolts are on a 4-1/2" bolt circle. Attempts to seal these flanges with platinum O rings have failed. It is not clear at this time exactly what the problem is.

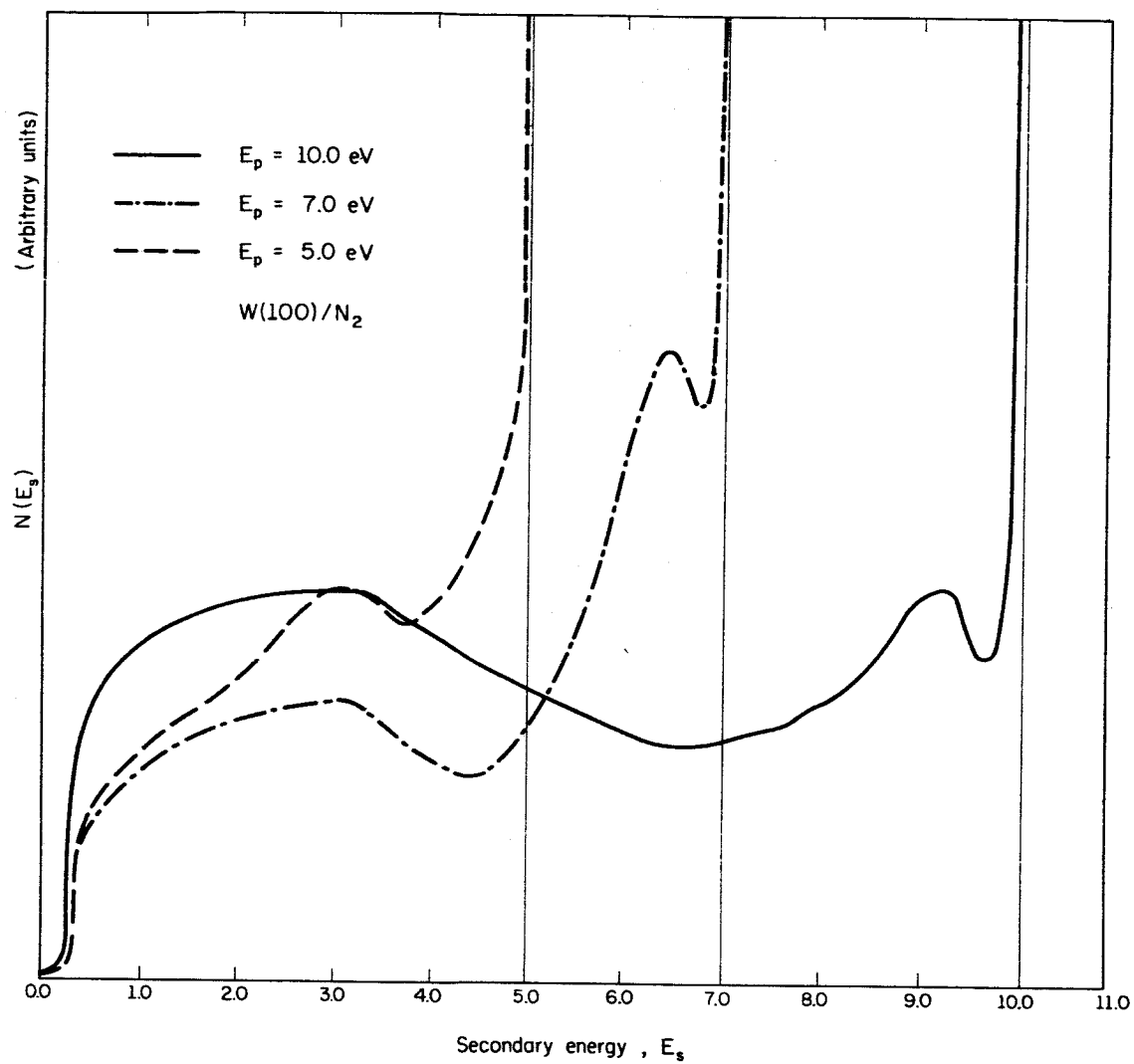


Fig. 2.7. The Energy Distribution of Secondary Electrons from the Tungsten (100) Surface after Exposure of the Surface to N_2 .

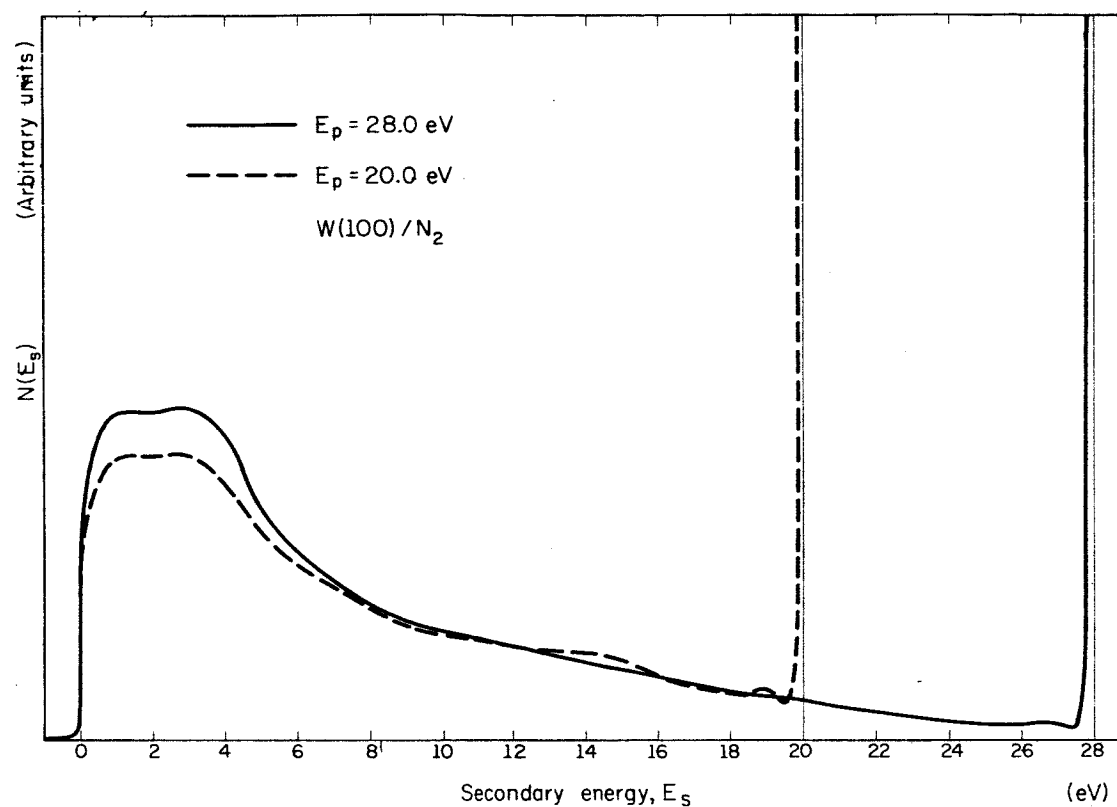


Fig. 2.8. The Energy Distribution of Secondary Electrons from the Tungsten (100) Surface after Exposure of the Surface to N_2 .

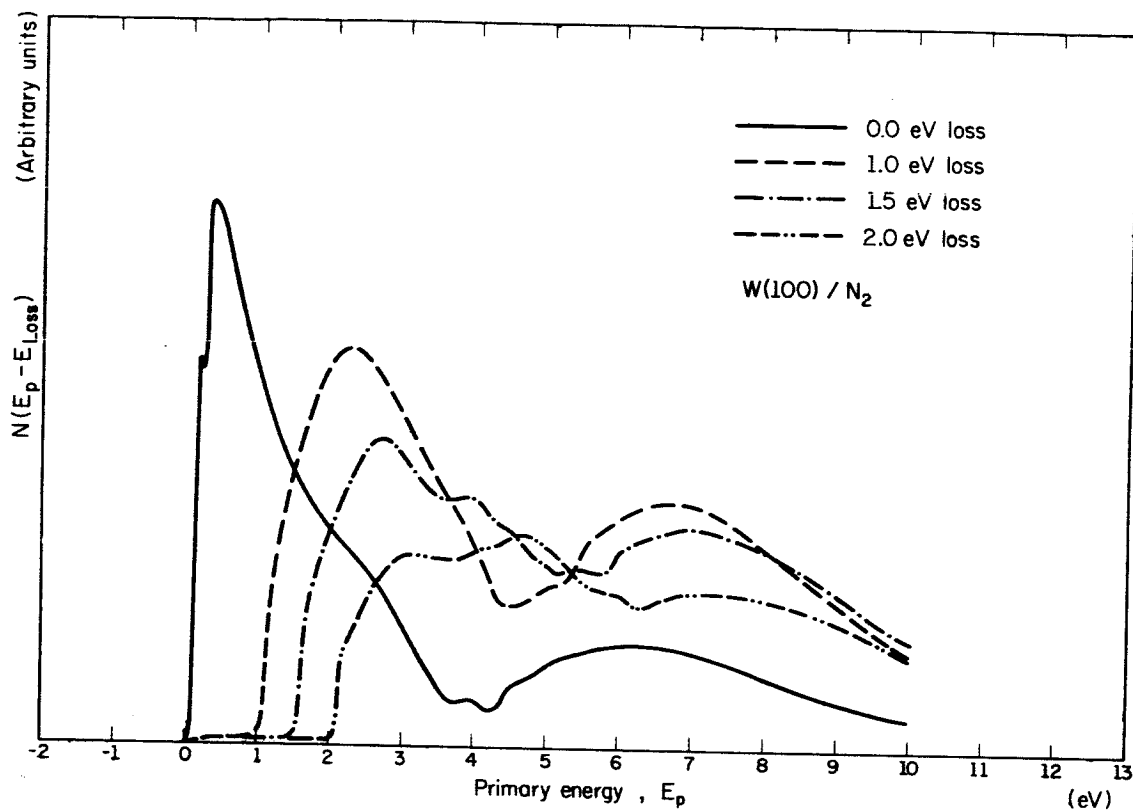


Fig. 2.9. Plot of the Number of Electrons Produced with 0.0, 1.0, 1.5, and 2.0 eV Kinetic Energy Less than the Primary Kinetic Energy Plotted as a Function of the Primary Energy. The data presented are for the (100) tungsten surface after exposing the surface to N_2 .

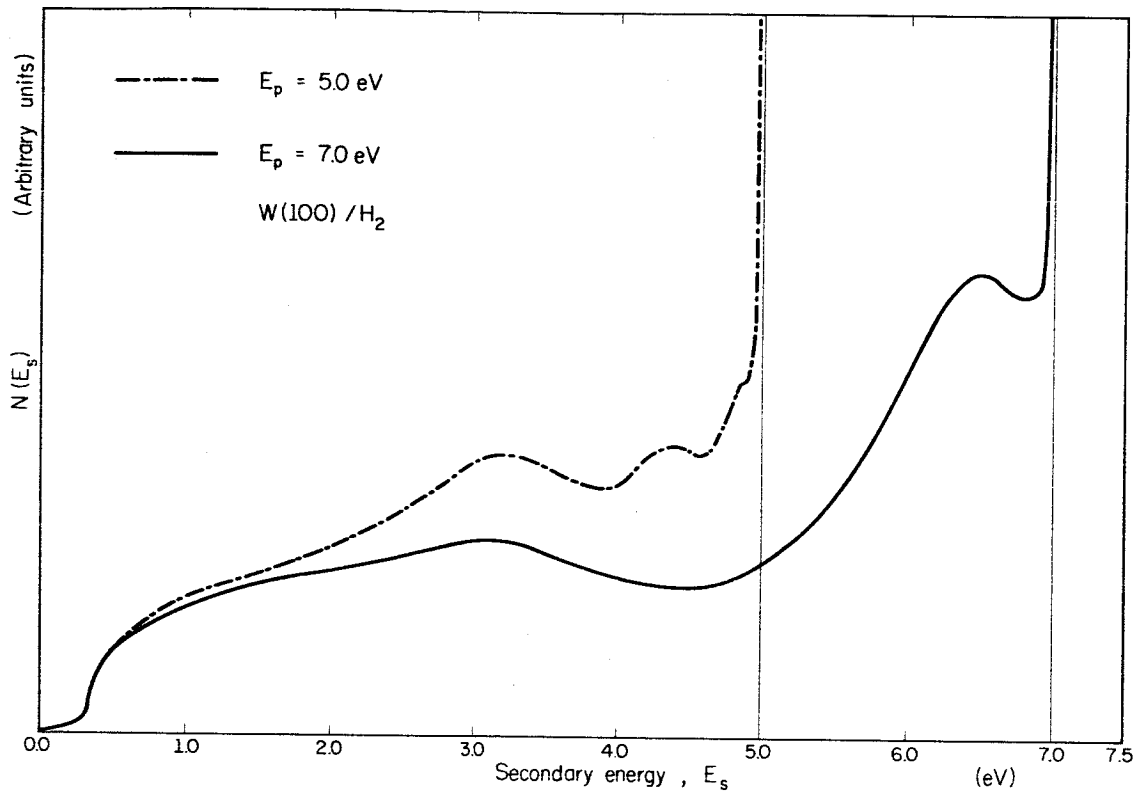


Fig. 2.10. The Energy Distribution of Secondary Electrons from the Tungsten (100) Surface after Exposure of the Surface to H_2 .

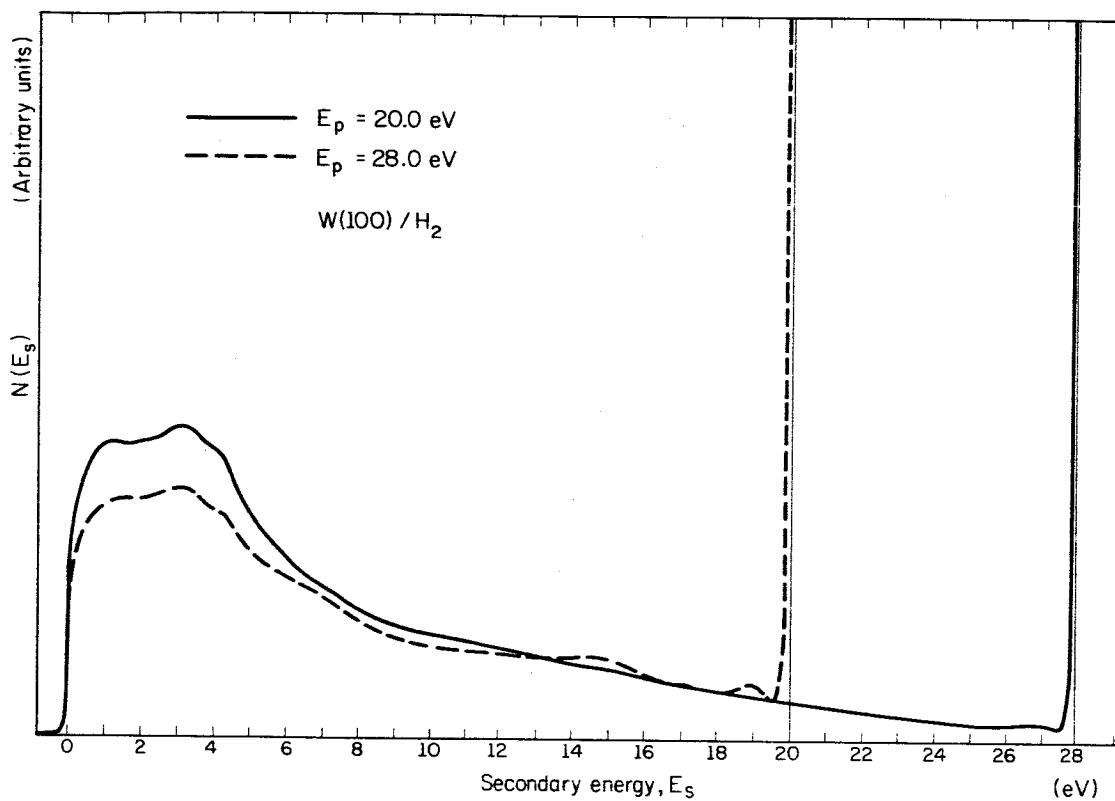


Fig. 2.11. The Energy Distribution of Secondary Electrons from the Tungsten (100) Surface after Exposure of the Surface to H_2 .

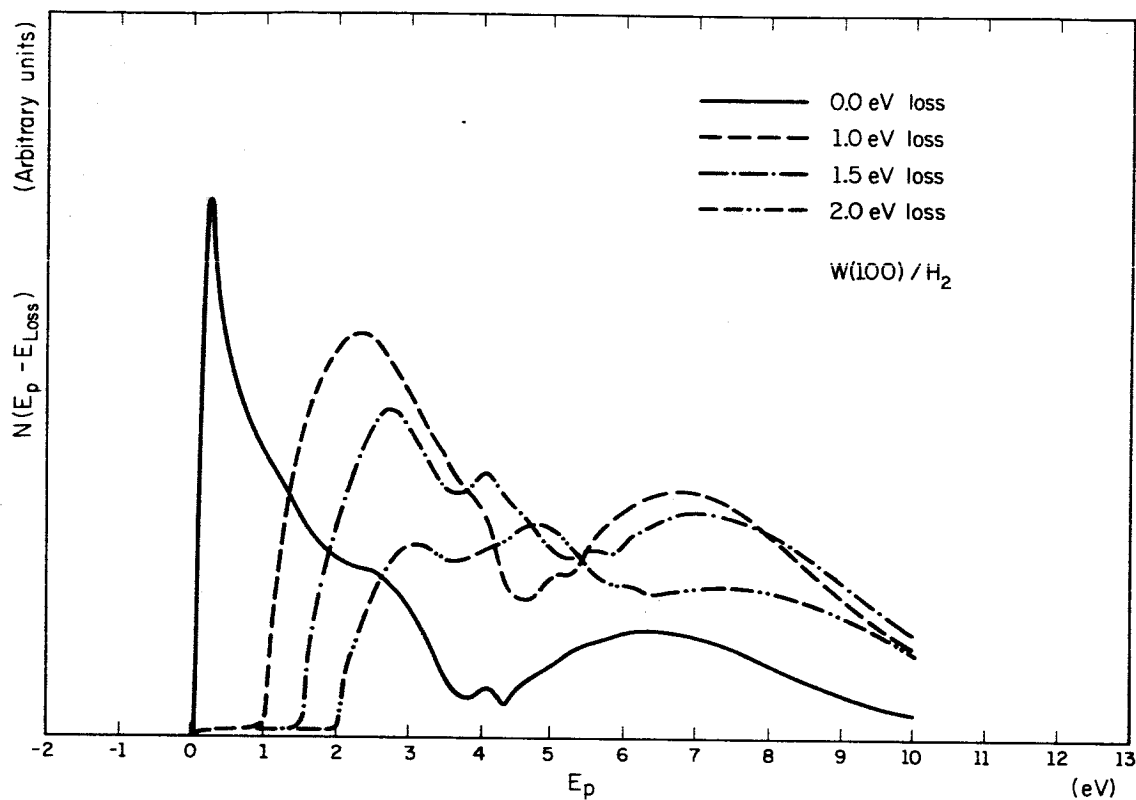


Fig. 2.12. Plot of the Number of Electrons Produced with 0.0, 1.0, 1.5, and 2.0 eV Kinetic Energy Less than the Primary Kinetic Energy Plotted as a Function of the Primary Energy. The data presented are for the (100) tungsten surface after exposing the surface to H₂.

Two possibilities are being considered:

- (1) There may be soft spots or some other flaw in the stainless steel. Evidence for this is that a platinum O ring has been sealed between surfaces of commercially supplied flanges.
- (2) The spacing between flange bolts may be too large to crush the O ring uniformly. This appears to be more unlikely since seals have been made with flanges with the same bolt circle and spacing. On the other hand, evidence for this is simply that no flange with this bolt circle and spacing has been very reliable.

The geometry of the new flanges may eliminate the problem of mercury amalgamation by keeping the O ring out of the vicinity of intense mercury contamination, thus allowing the use of a much softer pure aluminum O ring.

The experimental apparatus is near completion. Helmholtz coils have been designed and are being constructed. A magnetic shield has been designed, and an electron gun is being designed.

2.3 Adsorption-Desorption of Gases at Metal Surfaces

Continued and severe problems with the ultrahigh-vacuum feedthroughs stopped work on the desorption experiment at the beginning of this period. New apparatus to continue the experiment has been designed.

Electronic apparatus to quickly heat the target to a constant temperature has been constructed, but has not been tested because of the feedthrough leaks.

3. COMPUTER

H. G. Slottow
G. Crawford
L. Hedges

R. Jenks
J. Knoke
V. Metze

E. Neff
J. Stifle
R. Trogden
P. Trombi

3.1 Introduction

This group is responsible for the development and maintenance of the CSL computing facility.

3.2 CSX-1 Computer

3.2.1 Operations

Period: 1 December 1965 to 1 March 1966

Total Running Time: 2121.7 hours

Average per Day (7 day week): 23.57 hours

Operational Time: 99.97% 2121.2 hours

Scheduled Maintenance Time: 0% 0.0 hours

Emergency Maintenance Time: .03% 0.5 hours

Computer was off 17:1/4 hours for modification for addition of new memory section.

L. Hedges

3.3 CDC 1604 Computer

3.3.1 Operations

Period: December 1, 1965 to February 28, 1966

Total Running Time: 1237.40 hours

Average per Day (7 day week): 13.75 hours

Operational Time: 95.86% 1186.15 hours

Preventive Maintenance Time:	3.62%	44.83 hours
Engineering Time:	0.5%	6.42 hours
Emergency Maintenance Time:	0.00%	0.00 hours

E. Neff

3.3.2 Computer Display. During this quarter, construction was started on a CRT display to be installed as an on-line facility of the 1604 computer.

The display is a digitally operated device containing a 12" CRT with 2^{12} X and Y positions. Thus, a point may be displayed at any of more than 16×10^6 positions on the CRT.

The display may be operated in any of seven different modes. A brief description of each mode is summarized below.

- MODE 1. Plots points as they are transmitted to the display from the computer. Maximum plotting rate will be approximately 350,000 points/sec.
- MODE 2. Plots a graph using Y as the dependent variable. Computer transmits origin and size of X increment and thereafter transmits only Y coordinates.
- MODE 3. Same as MODE 2 with role of X and Y reversed.
- MODE 4. Plots a symbol as determined by the contents of a 48-bit "pattern word" specified by the computer.
- MODE 5. Plots a line between two points specified by the computer.
- MODE 6. Same as MODE 5 except the terminal point of one line is also interpreted as the origin point for the next line.

MODE 7. Character Mode. The computer transmits a BCD Code for each of the 64 characters and symbols available and the display generates the character. Four sizes of characters are available. Maximum character display rate will be approximately 125,000 characters/sec.

Provisions exist for the addition of up to nine additional modes of operation.

A typewriter will provide for control communication between the display and the computer. Additional communication will be provided by a light pen.

It is tentatively planned to include a five inch monitor scope and camera unit to permit photographic work.

J. Stifle
L. Hedges

3.3.3 Analog to Digital Converter. Construction of a new general-purpose analog to digital converter was started this quarter. This unit can be connected to either the 1604 or the CSX-1 computer, thereby providing either computer with an analog input channel.

The converter will perform 10 bit A to D conversions at a maximum rate of 50 KC with an accuracy of better than 0.1%. Minimum resolution is ± 1.5 mv.

Three modes of clock control are provided.

1. INTERNAL CLOCK--Four internal clock speeds are available--
5 KC, 10 KC, 20 KC, 50 KC.
2. EXTERNAL CLOCK--Any rate up to 50 KC may be used.
3. COMPUTER--Conversions are performed on command from computer.

The maximum analog input signal which can be converted is +12 volts. This unit is scheduled to be put into operation late in the coming quarter.

J. Stifle
L. Hedges

4. CONTROL SYSTEMS

J. B. Cruz, Jr.
W. R. Perkins
M. Sobral, Jr.
M. Schoenberger

S. D. Agashe
M. S. Davies
R. L. Gonzales
C. R. Hartmann

J. P. Herner
R. A. Hoyt
D. C. Reddy
R. Werner

4.1 Introduction

The analytical and computational aspects of analysis and design of control systems constitute the major effort of this group. Several projects are concerned with the sensitivity problem. The problem arises from the fact that almost all parameters involved in the mathematical description of dynamical systems are subject to variation and uncertainty. These parameter variations may be due to aging, inaccuracies of the assumed model, as well as environmental disturbances. Control systems must be designed to as to remain within acceptable performance limits in spite of these variations. Various methods of analysis and design which take these parameter variations into account are being developed.

One project of the group is the development of a design procedure for a system with a fixed control structure, which optimizes a given performance index. The structure is chosen for ease of implementation.

Another project is directed towards obtaining sufficient conditions for stability for a class of nonlinear systems. Several extensions of Popov's criterion have been obtained. Presently, a convenient graphical stability criterion for a system with several nonlinearities is being sought.

Since a computer is inevitably involved in synthesizing fairly complex control systems, a direct computer-oriented formulation of an

optimization problem is desirable. One project of this group is devoted to a study of the mathematical foundations for such a formulation.

4.2 Sensitivity of Dynamical Systems

4.2.1 Bounds on Norms of Sensitivity Functions.[†] Consider a linear time-invariant system described by

$$\dot{\underline{x}} = \underline{A}\underline{x}, \quad \underline{x}(t_0) = \underline{x}_0,$$

$$\underline{y} = \underline{C}\underline{x},$$

where \underline{x} is the state vector, \underline{y} is the output vector, and the time-invariant matrices \underline{A} and \underline{C} depend on some parameter vector $\underline{\alpha}$. The sensitivity of the output vector with respect to the i^{th} component of $\underline{\alpha}$ is defined as

$$\underline{w}^i(t, \underline{\alpha}) = \partial \underline{y}(t, \underline{\alpha}) / \partial \alpha_i.$$

Let $\|\underline{x}(t)\|$ denote norm of the vector $\underline{x}(t)$, considering t as a parameter. The following result has been obtained:

$$\|\underline{w}^i(t, \underline{\alpha})\| \leq \|\underline{C}\| \|\partial \underline{A} / \partial \alpha_i\| \|\underline{x}_0\| K_1^2 t e^{\sigma t}, \quad t \geq 0,$$

where σ is the maximum real part of an eigenvalue of \underline{A} , and K_1 is a finite positive constant which is a factor in the bound of $e^{\underline{A}t}$,

$$\|\underline{e}^{\underline{A}t}\| \leq K_1 e^{\sigma t}, \quad t \geq 0.$$

[†]Portions of this work were supported by the Air Force Office of Scientific Research under Grant No. AFOSR 931.65.

The bound is linearly proportional to $\|\underline{C}\|$, $\|\partial \underline{A} / \partial \alpha_i\|$, and $\|\underline{x}_0\|$. Furthermore, if the system is asymptotically stable, one has $\sigma < 0$ and the norm approaches zero as $t \rightarrow \infty$. The bound starts at zero for $t = 0$ and rises to a maximum at $t = -\frac{1}{\sigma}$.

The above result will appear in a paper "On Invariance and Sensitivity" to be presented at the 1966 IEEE International Convention.

J. B. Cruz, Jr.
W. R. Perkins

4.2.2 Synthesizing Comparatively Insensitive Linear Systems.[†]

Consider a linear time-invariant plant described by the state equations $\dot{\underline{x}} = \underline{A}\underline{x} + \underline{b}u$ and variations $\underline{A}' = \underline{A} + \underline{b}\underline{d}^T$. Then, performing the optimization of the linear regulator problem yields a feedback solution that satisfies the sensitivity requirement

$$[\underline{S}^*(s)\underline{Q}\underline{S}(s) - \underline{Q}]_{s=j\omega} < 0,$$

for all real ω and $\underline{Q} > 0$.

The above result suggests that the eigenvalues of the sensitivity matrix $\underline{S}(s)$ are related to those of the matrix $\underline{I} - \underline{F}\Phi p(s)\underline{B}$. Therefore work is being done on finding the above relationship in the hope that

$$[\underline{I} - \underline{F}\Phi p(j\omega)\underline{B}]^* [\underline{I} - \underline{F}\Phi p(j\omega)\underline{B}] - \underline{I} > 0$$

will imply

$$[\underline{S}^{-1}(j\omega)]^* \underline{S}^{-1}(j\omega) - \underline{I} > 0,$$

for all real ω .

J. P. Herner

[†]Portions of this work were supported by the Air Force Office of Scientific Research under Grant No. AFOSR 931.65.

4.2.3 Sensitivity Considerations for Nonlinear Systems.[†]

Investigations are being undertaken to formulate an approach for the analysis of nonlinear control system sensitivity. In particular, a proposed method of analysis has been developed for single variable systems with one nonlinear frequency-independent element. The proposed method involves a structural approach to the problem coupled with the use of a statistical describing function for the nonlinear element. This method leads to a statistical sensitivity index for the nonlinear system. The method also appears to lend itself to parameter optimization for minimum sensitivity when the form of the system is constrained.

R. L. Gonzales

4.2.4 Sensitivity Analysis of Dynamic Systems.[†] The dynamic behavior of (linear) systems is determined substantially by the eigenvalues of the system. Any changes planned or otherwise in the system parameters affect the eigenvalues of the system and hence the system response.

Of particular interest is the change in system performance--sensitivity of system performance--to small changes--perturbations--in system parameters that inevitably occur in the assembly and operation of a specified system.

[†]Portions of this work were supported by the Air Force Office of Scientific Research under Grant No. AFOSR 931.65.

It is found that a direct relationship exists between perturbations in system parameters and its eigenvalues.^{1,2} Specifically for the system

$$\dot{\underline{x}} = \underline{A}\underline{x} + \underline{f}$$

where \underline{f} is the control vector representing the effect of the forcing functions, a small change in any element of the \underline{A} matrix with respect to a small change in any eigenvalue of the system--Eigenvalue Sensitivity--can be fairly directly determined.

Similarly a relationship between perturbations in any element of the \underline{A} matrix and corresponding perturbations in the eigenvectors--Eigenvector Sensitivity--can be established.

It is hoped that, through a knowledge of the changes in eigenvalues and eigenvectors to system parameter variations, a design procedure may be evolved so as to minimize the variations on the specified performance criterion such as maximum overshoot, rise time, settling time.

Some interesting relationships were observed in the case of single-input single-output systems with unity feedback.

Investigation is continuing into the case of free, stationary, linear multivariable systems, where the performance indices are a particular class of time weighted functionals of the form

¹MacFarlane, A. G. J., Notes on the Use of Matrix Theory in the Analysis of Linear Feedback Circuits, 1963 Proc. Inst. Elect. Engrg., 110, 139.

²Laughton, M. A., Sensitivity in Dynamical System Analysis, 1964 Journal of Electronics and Control, 577, 591.

$$\int_0^{\infty} t^r \tilde{x}^T Q \tilde{x} dt \quad \text{where } Q \text{ is positive definite}$$

and the change in these performance indices with respect to changes in any element of the matrix \tilde{A} .

D. C. Reddy

4.2.5 Sensitivity Considerations in the Synthesis of Doubly-Terminated Coupling Networks.[†]

As it is well known, Darlington's synthesis method for doubly-terminated coupling networks does not have a unique solution in general.^{3,4} In this investigation, the sensitivity of the voltage transfer ratio with respect to load and source impedances is examined. In particular, the possibility of determining which network is best under the sensitivity viewpoint is the main goal of this research.

C. R. Hartmann
M. Sobral, Jr.

4.2.6 Linear Regulators with Plant Parameter Perturbation.[†]

Work is continuing on the problem of designing optimal linear regulators which are relatively insensitive to perturbations of plant parameters.

[†]Portions of this work were supported by the Air Force Office of Scientific Research under Grant No. AFOSR 931.65.

³M. Sobral, Jr., "Sensitivity Considerations in the Synthesis of Doubly-Terminated Coupling Networks," IEEE Trans. on Circuit Theory, CT-12, 272-74 (June, 1965).

⁴C. R. P. Hartmann, "Estudo da Sensibilidade da Funcao de Transferencia de Redes Passivas Com Relacao a Variacao da Resistencia Interna do Gerador," Master's Thesis, Instituto Tecnologico de Aeronautica, S. Jose dos Campos, S. Paulo, Brazil (1966).

Two criteria for the "best" design of optimal control systems with plant perturbations have been previously outlined.^{5,6} These two synthesis techniques have not been carried to the point of practical application, but instead have been theoretically outlined. At present, applications of these two techniques are being studied for two linear regulator problems. It should be noted here that computational methods for the two design criteria^{5,6} appear very similar.

The two regulator problems are first the infinite-time case with a quadratic performance index (this has a linear feedback solution) and a linear feedback approximation to the finite-time case with a quadratic performance index. Of course, the final solution to the problems outlined above will necessitate the use of computing machines.

R. Hoyt

4.2.7 Sensitivity of Optimal Control Systems. Sensitivity of automatic control system performance due to variation of certain parameters in the system is being studied. Interest is concentrated on the variation of the performance index of a system that has been designed to optimize the performance (with respect to the given performance index) when the parameters have their nominal values. Use of various sensitivity indices that are a measure of the change in the

⁵P. Dorato and A. Kestenbaum, "Application of Game Theory to the Sensitivity Design of Systems with Optimal Controller Structures," Proc. of the Third Annual Allerton Conference, 35-45 (1965).

⁶R. Rohrer and M. Sobral, Jr., "Sensitivity Considerations of Optimal System Design," IEEE Trans. on Automatic Control, AC-10, 43-48 (January, 1965).

performance index are being studied, and methods of minimizing these indices are being tried.

R. A. Werner

4.3 System Optimization with Fixed Control Structure[†]

During this quarter, the results of the past year were prepared for CSL Report R-278. The procedures which were developed during this period were applied to the problem of optimal submarine diving.

Consider a submarine which is to dive from the water's surface to a prescribed depth in a prescribed time. It is assumed that control of the submarine's stern plane angle is the only means of regulating its depth. Letting x_1 be the pitch angle, x_2 be the pitch rate, x_3 be the angle of the attack, x_4 be the depth error, and u be the stern plane angle, a set of linearized equations of motion are obtained

$$\dot{\underline{x}} = A\underline{x} + b\underline{u}.$$

Since it is desired for the trajectory to be as "low" as possible with bounded control, the performance index

$$J = \underline{x}(T)^T P \underline{x}(T) + \int_0^T (\underline{x}^T Q \underline{x} + u^2) dt$$

is chosen.

Rekasius has shown that the optimal control for this problem is

[†]Portions of this work were supported by the Air Force Office of Scientific Research under Grant No. AFOSR 931.65.

$$u^0 = c_0^T x + v(t) ,$$

where c_0 is a constant vector and v is a time-varying open loop control. Since the time-varying portion of the optimal control is difficult to implement in this problem, alternative control laws were suggested.

When the control was a constant times the depth error; $u_1 = Kx_4$, $K = 0$; the trajectory was within 20 per cent of the optimal at all times. The performance index associated with u_1 was about 10 per cent greater than the optimal.

Progressively more complex control structures were compared to these trajectories, and the control

$$u_2 = c_3x_3 + c_4x_4 + d, \quad \dot{c}_3 = \dot{c}_4 = \dot{d} = 0 ,$$

was found to be a good compromise between ease of implementation and optimal control. The trajectory was within 10 per cent of the optimal at all times, and the performance index associated with u_2 was about 5 per cent greater than the optimal.

M. Schoenberger

4.4 Stability of Nonlinear Systems[†]

Consider a nonlinear continuous system described by the equation

$$\dot{\sigma}(t) = u(t) - \int_0^t g(t-\tau)\varphi(\tau)d\tau .$$

[†]Portions of this work were supported by the Air Force Office of Scientific Research under Grant No. 931.65.

Here, σ , u , and φ are $m \times 1$ vectors and g is an $m \times m$ impulse response matrix. The i^{th} component of φ is related to the corresponding component of σ in a nonlinear manner: $\varphi_i(0) = 0$ with $0 < h_i \sigma_i^2 \leq \varphi_i \sigma_i \leq g_i \sigma_i^2 < k_i \sigma_i^2$. It has been shown that such a system is stable if $K^{-1} + \text{Re}[I + j\omega Q]G(j\omega)$ is a positive semi-definite matrix for all real ω and some diagonal constant matrix Q . This result, a generalization of that of V. M. Popov for systems with a single nonlinearity, has been derived using methods similar to those of Popov.

A convenient graphical method of testing the stability criterion exists for the case of a single nonlinearity, but no such means seem evident in the more general case. The matrix inequality given above is cumbersome to apply in practice and some way of simplifying it seems desirable. A result rather more general than the above has been derived which, it is hoped, will allow some simplification of the stability criterion when the actual configuration of the system being tested is taken into account.

It has also been shown that, with $Q = 0$, the stability criterion is equivalent to passivity conditions on an n -port network.

A similar stability criterion has been derived for systems involving time lag. Such systems may be described by equations of the form

$$\dot{x}(t) = Ax(t) + Bx(t-r) + L\varphi[\sigma(t-r)] ,$$

where the nonlinearity is constrained by inequalities similar to those given above.

M. S. Davies

4.5 Computer-Oriented Formulation and Solution of the Optimal Control Problem: Characterization of Linear, Time-Invariant Differential Systems†

Regarding the n -vector differential equation

$$\dot{\underline{x}} = A\underline{x}, \quad (1)$$

where A is a constant matrix, we ask the following question. How can we characterize P , the set of all solutions of (1) and a subset of the set $S[t_o, t_f]$ of vector-values functions, say, on an interval $[t_o, t_f]$, in an "intrinsic" fashion? (By an "intrinsic" characterization is meant characterization as a subset of a function space.) This question arises as follows.

It is well known that the corresponding matrix differential equation

$$\dot{\Phi} = A\Phi \quad (2)$$

has a solution corresponding to an initial value I_n (n -dimensional unit matrix), that $\Phi(t)$ is nonsingular for each t and that the general solution of (1) having initial value \underline{x}_o is given by

$$\underline{x}(t) = \Phi(t)\underline{x}_o. \quad (3)$$

From (3), (or even from (1)), we see that (i) P is a linear subspace of S ; (ii) each element of P is differentiable; and (iii) if the vector functions \underline{p}^i , $i = 1, \dots, n$, are solutions of (1) corresponding to initial values \underline{x}^i , $i = 1, \dots, n$, then the set $\{\underline{x}^i, i = 1, \dots, n\}$ forms

†Portions of this work were supported by the Air Force Office of Scientific Research under Grant No. AFOSR 931.65.

a basis of n -dimensional space R_n if for any t , the set $\{\underline{p}^i(t), i = 1, \dots, n\}$ is a basis of R_n if $\{\underline{p}^i, i = 1, 2, \dots, n\}$ is a basis of P .

Our question stems from the desire to know under what conditions does the converse theorem hold, i.e., under what conditions does a set $\{\underline{p}^i, i = 1, \dots, n\}$ of differentiable vector functions, such that for each t , $\{\underline{p}^i(t), i = 1, \dots, n\}$ is a basis of R_n , correspond to a matrix A . Attempts are being made to answer this question.

For a "computer-oriented" formulation, the condition of differentiability will have to be replaced by a finitistic condition such as piecewise linearity with a finite number of time-wise arbitrary corner points.

S. D. Agashe

5. PLATO

D. L. Bitzer	B. Hicks	H. W. Smoker, Jr.
J. H. Adams	P. Koo	B. Stake
B. M. Arora	J. M. Kraatz	M. Uretsky
M. Axeen	R. Johnson	B. Voth
J. A. Easley, Jr.	E. R. Lyman	J. Walker
L. Fillman	W. E. Montague	M. Walker
J. Gilpin	C. E. Osgood	A. Wearing
W. Golden	M. Secrest	C. E. Webber
H. Guetzkow	S. Singer	M. Wilkins
T. Hastings	T. L. Smith	R. Willson
		B. Wilson

5.1 Introduction[†]

The purpose of the PLATO project has been to develop an automatic computer-controlled teaching system of sufficient flexibility to permit experimental evaluation of a large variety of ideas in automatic instruction including simultaneous tutoring of a large number of students in a variety of subjects. The PLATO system differs from most teaching systems in that the power of a large digital computer is available to teach each student, since one such computer controls all student stations. The project work has fallen into three categories, no two of which are wholly separate from each other: (1) development of the tools for research; (2) provision of a prototype for multi-student teaching machines; (3) learning and teaching research. Under the first category has come the development of three successive versions of the PLATO equipment with PLATO IV, which includes an audio facility, now under construction. The

[†]Portions of this work were supported by the Advanced Research Projects Agency through the Office of Naval Research under Contract Nonr-3985(08).

twenty-student station classroom provides the prototype for multi-student teaching machines mentioned in the second category.

The learning and teaching research, the third area of PLATO research, has covered curriculum studies, college teaching, and behavioral science research. Cooperative work with the University of Illinois Committee on School Mathematics is now in its fourth year. Professor W. E. Montague of the Department of Psychology is a half-time member of the PLATO group and is directing two behavioral-science studies. Cooperative work with three university departments (electrical engineering, library science, and business administration) has resulted in three credit courses offered this semester. Other interactions of the PLATO group with various disciplines at the University have suggested experiments and studies in negotiation (Guetzkow), health education (Creswell), evaluation of teaching materials in many fields (The SIRA Project), language analysis (Myers), comparative psycholinguistics (Osgood), and many other areas. The demands on the PLATO staff and the computer facility have resulted in the gift of the use of a 1604 computer from the Control Data Corporation which will be installed in the spring of 1966, and which will be for the sole use of PLATO research.

The plasma display discharge-tube research, another important part of research in category one, is offering definite promise for the possibility of a less expensive PLATO display. Small display holes of approximately ten-thousandths of an inch in diameter have been constructed and tested. The light from these holes is sufficiently bright to be clearly visible in a lighted room. It has been shown that the display

spot can be turned on, erased, or read, to see if it is on or off, all within two microseconds. The light emitted from the hole occurs in bright pulses, each of which lasts less than twenty nanoseconds.

5.2 PLATO III System Equipment

During this quarter work continued in the development and construction of circuitry required for the realization of a 20-station teaching system.

Student-station circuitry constructed to date includes all that required for the full operation of 20 student stations. Construction of the remaining required to update 10 stations that have been in use over the past two years continues and is expected to be complete during the coming quarter. Due to slowness in processing of requisitions and the delivery of components requested, construction has been somewhat delayed. As a consequence, checkout has resulted in only 12 stations being fully operational. The checkout of the remaining station circuitry is expected to be complete by the end of the coming quarter.

Developmental circuitry required to update the present system or to provide new system facilities continues to be under study. Included are transistor deflection circuitry that will replace vacuum-type tubes operating in existing flying-spot scanner equipment, and audio-storage equipment to provide for random-access audio readout capability for all student stations in the PLATO system.

B. Voth

5.3 Plasma-Discharge Display-Tube Research

Development of the plasma display tube has been motivated by the need for a simple display that responds directly to the digital signals from the computer and that retains its images without the need for regeneration. The basic element in the display is a bistable gas discharge cell in which charge storage on insulating walls provides the memory. In the preceding progress report, we discussed the circuit properties of the cell. In this section, we discuss a technique for changing the state of a selected cell, and we describe a new transistorized generator for driving the display.

A cell in a "0" or "off" state does not respond to the sustaining signal, shown in Fig. 5.1A, whose amplitude is less than the firing voltage. However, when a bias is superimposed on the sustaining voltage, as in Fig. 5.1B, the cell eventually fires, and because of differential charging in the next few cycles, the firing points reach a symmetrical phase condition. If now the bias voltage is slowly reduced to zero, the firing times on the positive excursions are delayed slightly and the firing times on the negative excursions are advanced slightly. The greater slope on the negative half cycle results in an increased charge transfer during the discharge, and, when the bias voltage is 0, the cell is in a "1" or "on" state, and the firing points are symmetrical in phase.

When, as in Fig. 5.1C, the bias voltage is gradually increased on a cell that is "on," the positive firing points are advanced in time, the negative firings are retarded, and the differential charging

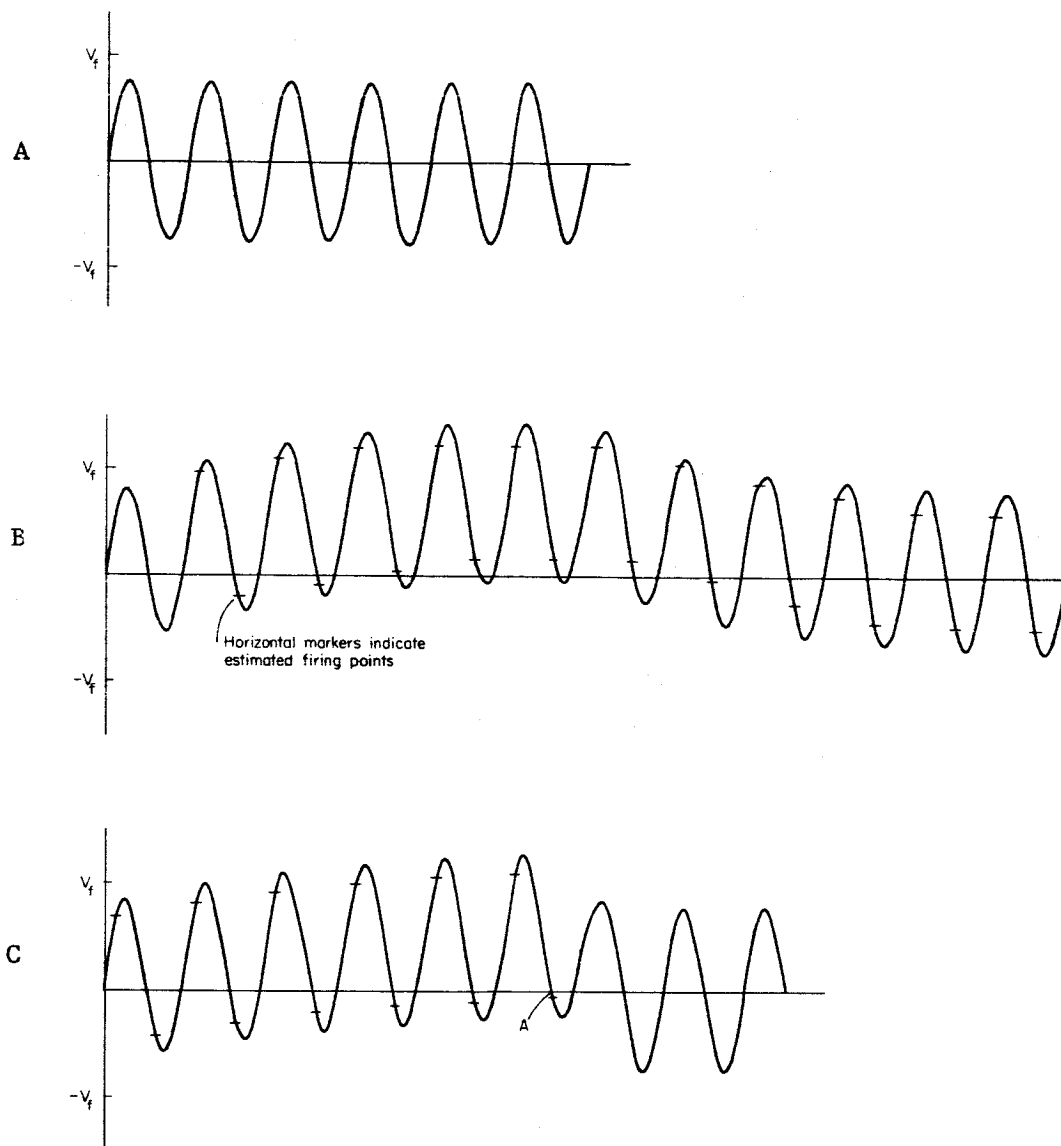


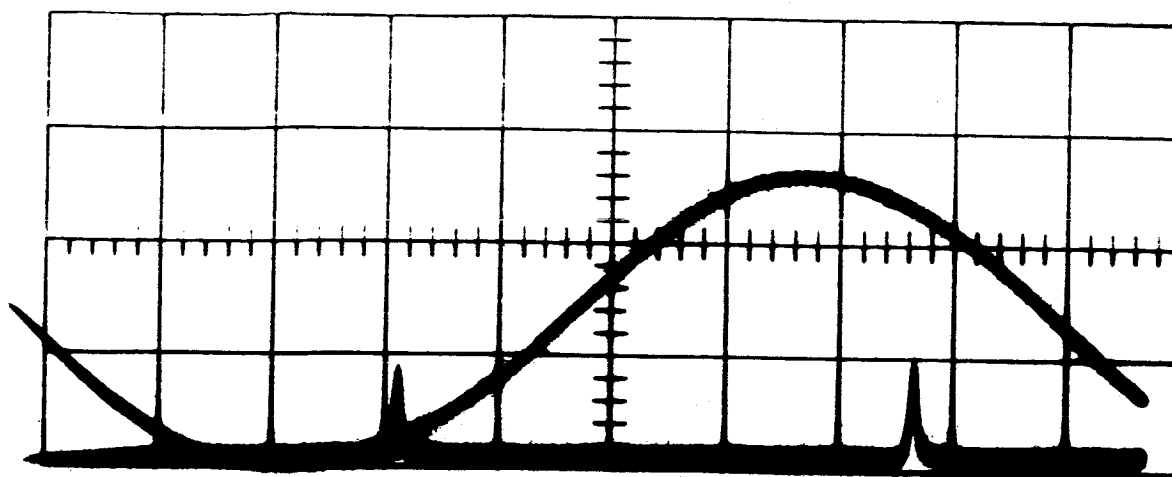
Fig. 5.1. Turn-on and Turn-off Signals for Plasma Display Tube.

compensates for the change in bias. When the bias voltage finally reaches a steady value, the only effect is a change in the steady voltages in the circuit. In fact, if the bias voltage is equal to half the charge transferred in the cell during normal firing, then, just after the firing at time A, the voltage due to the wall charge in the cell is zero. If the bias voltage is now removed within one-half cycle, the cell cannot refire, and it will be in the "0" or "off" state.

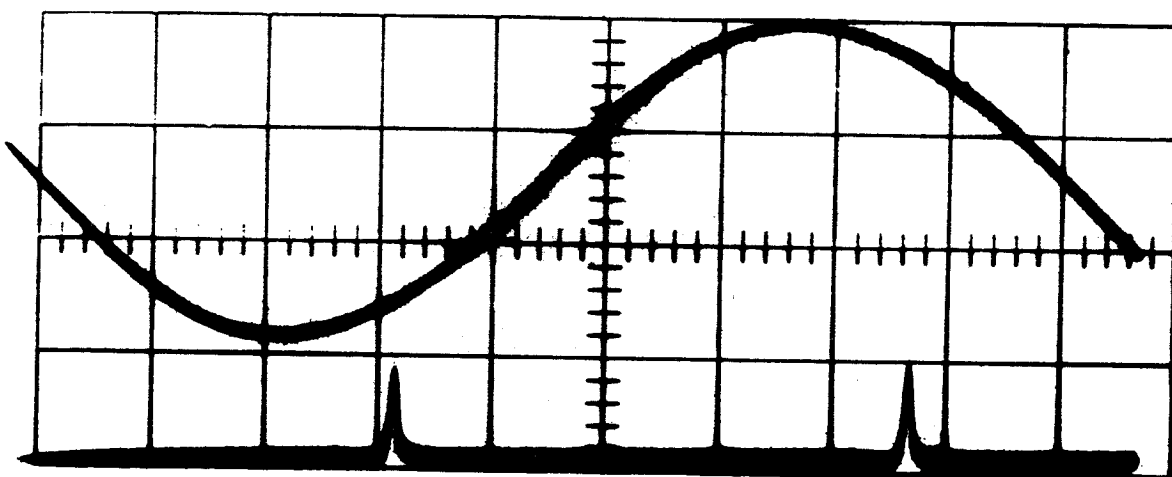
The slow voltage changes were produced by charging a 100 pF capacitor through 0.33×10^6 ohms, and the rapid changes were produced by discharging this capacitor through a 6BG6 vacuum tube. Figure 5.2 illustrates several stages in the "turn off" of a single cell. For the upper pair of traces, the bias voltage was zero. The pulses on the second trace are amplified photo-cell signals produced during the discharge. The middle pair of traces shows the voltage and the light signal after the bias is added to the cell, and the lower traces show that, after the bias has been removed (at a controlled time), the cell no longer fires.

The ability to turn selected cells on and off through high impedance circuits should simplify addressing problems, and in particular, should allow the use of gas switches in the selection circuits.

An experimental transistorized generator has been built which can drive the plasma display tube through a 50-to-1 step-up transformer. The signals consist of positive and negative pulses alternating with one another, and separated by a period in which the voltage is zero. The



Amplitude Scale (sine wave)
500 volts/division



Time Scale
0.5 microseconds/division

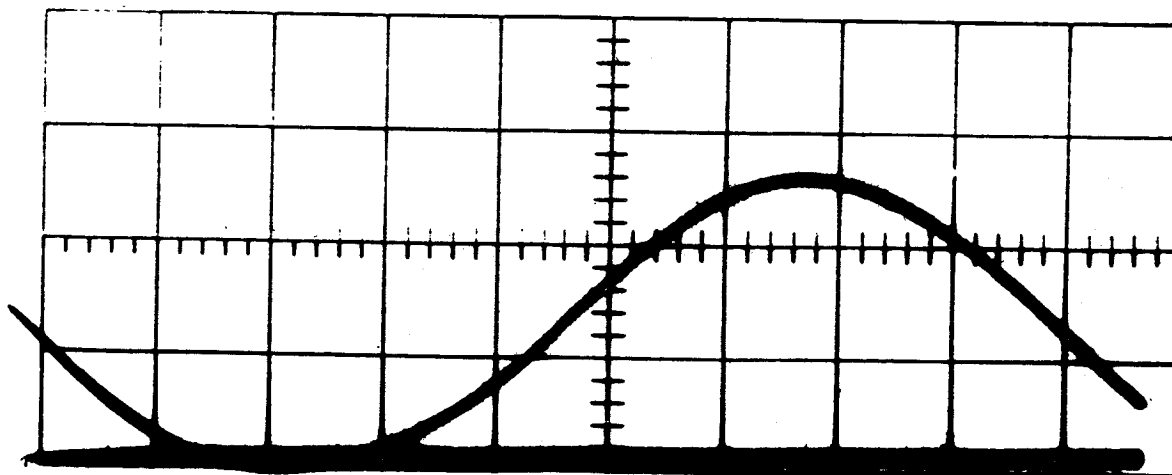


Fig. 5.2. Stages in Turn-off of Single Cell in Plasma Display Tube.

slopes of the wave forms are essentially uniform throughout the rise or fall time, and the time intervals between pulses are controllable.

The generator delivers 1500 volts; the rise time is about 1.0 microsecond, and the fall time about 1.5 microseconds. These figures hold for all ranges of repetition frequency up to about 200 kHz. An adjustable threshold detector provides a means of smoothly varying the output amplitude over its entire range.

A block diagram of the generator is shown in Fig. 5.3. The circuit is push-pull, and each half of the primary is driven alternately by means of a monostable multivibrator and a driver. When the voltage on the collector of transistor T_1 or T_2 reaches a preadjusted level, the monostable multivibrator flips and turns the driver off, thereby limiting the output to the desired value. The transistor T_3 or T_4 then drives the output voltage to zero. Furthermore they prevent oscillation in the time interval between pulses. The symmetry and the frequency of an external square wave generator determines the time delay between positive and negative pulses and the frequency of the generator output.

D. L. Bitzer
H. G. Slottow
B. M. Arora
R. Willson

5.4 PLATO Learning and Teaching Research

5.4.1 University Courses

5.4.1.1 Electrical Engineering 322--Circuit Analysis.

Two types of teaching logic are to be used during the spring semester to teach a three week session of EE 322; during this time the

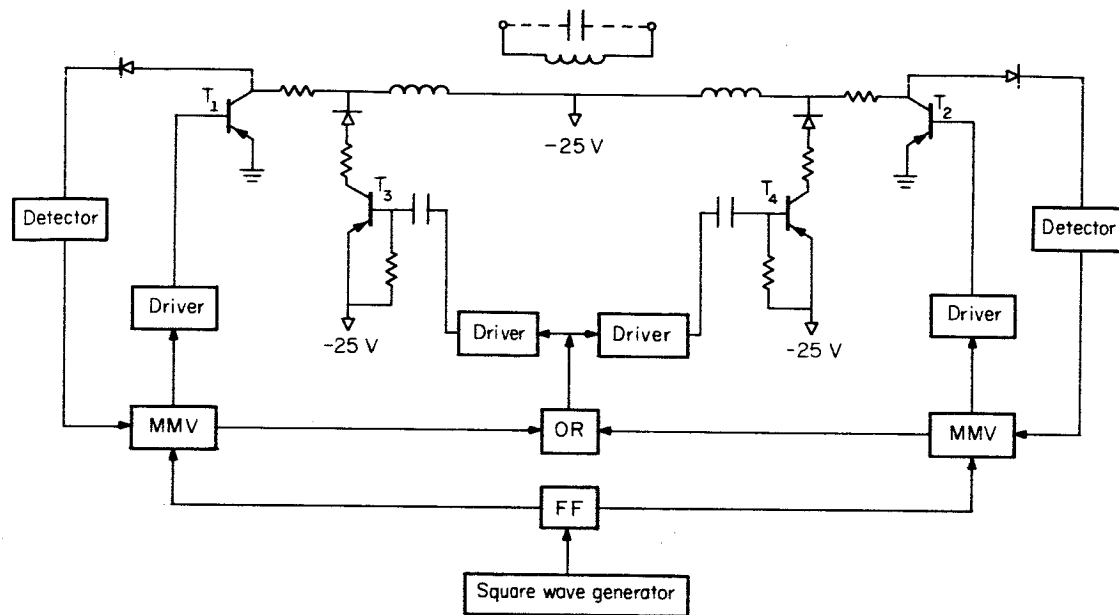


Fig. 5.3. Experimental Generator for Plasma Display Tube.

lesson material is to be presented only by PLATO (i.e., the PLATO sessions are not being supplemented with regular class sessions). One-half of the students involved will use the tutorial logic and the EE 322 lesson material described in previous reports. The remaining half will use a modified version of the tutorial logic which was designed to present the new inquiry-oriented type of lesson material. The new logic and lesson material were developed during this quarter. Although the logic is highly specialized at this time, there are plans to develop a generalized logic of this type which will be able to present both the tutorial and inquiry types of lesson material.

The students described above have been given a pre-test to obtain an indication of previous knowledge; a post-test will be given to determine the relative effectiveness of the two methods of teaching used. The results of this work and a description of the modified logic will be included in a later report.

R. L. Johnson

5.4.1.2 FORTRAN Programming for Business Students.

During the last quarter eight students completed the PLATO section of the course in FORTRAN computer language given for business and commerce students. Construction of a model for on-line compilation of programs was started. Plans are being completed for modifying the new PLATO tutorial logic to build in a capability for wash-back and wash-forward techniques.

M. Uretsky

5.4.1.3 Library Science 195. The twelve students who took the introductory course in library science during the fall semester using the PLATO system completed the course. From all evaluations these students did just as well as those students taught by the conventional lecture method. Comments received from the students show that they enjoyed learning on the PLATO system.

It was decided to allow another group of students to take the PLATO version of the course during the second semester. Thirteen students enrolled in the class. More detailed analyses of the students' work will be made at the end of the second semester. The computer program for examining the students' responses has been written.

M. Axeen

5.4.2 Mathematics Instructional Projects

5.4.2.1 ARITHDRILL. The teaching logic for ARITHDRILL has been completed and debugged. The logic includes several new parameters of practice and provision for assigning values to these parameters individually for each student from a master "teacher's" keyset. The most important capability provided by the new parameters is that of supplying prompting information to the student according to five different sets of contingencies.

An exploratory two-week trial has been completed which indicates that the basic program is effective, with most students, in maintaining learning behavior at the keyset for fifty-minute sessions. This would appear to be an important result, since the "attention span" of these low-achievers is usually considered to be fifteen minutes or less.

A program for reducing data from ARITHDRILL has been written and is being debugged. Student sessions on a regular basis will begin when time on the computer becomes available.

J. Gilpin

5.4.2.2 PROOF. Work is continuing on this teaching logic which permits students to compose proofs in algebra, geometry, and logic and check their work for logical validity. The basic logical checks have been programmed, but special features including the inversion of lemmas in the proof are yet to be made.

J. A. Easley, Jr.
W. Golden
T. Smith

5.4.3 Behavioral Science Projects

5.4.3.1 Retention of Conceptual Materials Research.

This project involves the utilization of PLATO for studies in the use of concepts and word-meaningfulness in verbal learning. During this last quarter, a general paired-associate learning computer program has been written, which allows great flexibility in experimental design with minimal program changes. Data from experiments carried out in the previous quarter have been analyzed and are currently being prepared for publication.

W. E. Montague
C. E. Webber
A. Wearing

5.4.3.2 Man-Computer Interface Study. Student communication with PLATO is achieved by a keyset. Data is being collected to assess the relative efficiency of different configurations of keys and to compare keyset input with input by a more useful method, namely, long hand writing. An annotated bibliography of the relevant literature on similar research is also in preparation.

W. E. Montague
A. Wearing

5.4.3.3 A Language-Free Test of Interpersonal Norms.

This project, directed by Dr. Charles Osgood, involves the use of the PLATO system in the production of short, animated films. Each film strip, or scenario, will portray an interpersonal intention composed of discrete sequences of visual events (which are, in turn, identified with abstract, theoretical components). For example, size differences will be used to indicate power differences, speed will represent levels of activity, etc. Subjects' reactions to the films will provide information on the relative importance of these components in the interpretation of interpersonal behavior. Since the research material is language-free, it will also have fruitful application to the study of cross-cultural differences in normative behavior.

An initial program has been compiled in which the size, movement, location, and speed of the characters is controlled. A fine resolution CRT is being adapted for use with the PLATO system. Direct filming of the displays from the CRT should begin in late March.

C. E. Osgood
M. Wilkins

5.4.3.4 Interaction Studies Group. A general PLATO

program has been written that will facilitate group-interaction studies. Its first use will be in the Inter-Nation Simulation (INS) studies of Guetzkow, et al., on the PLATO system. The program provides for the following activities with regard to messages: writing and editing, sending, reading and retrieving. The sending and retrieving are controlled by communication rules that in INS studies help define the roles of up to twenty decision-makers. The structure of the simulations and of the communications roles can be set in any way desired by the experimenter, or, if he so desires, by one or more of the players.

The program has been compiled and will be debugged in the next quarter. Decision forms and economic models can be inserted easily in the program as needed.

B. Hicks
S. Singer
M. Walker
D. Bitzer
M. Secrest
J. Walker

5.4.4 Project SIRA (System for Instructional Response Analysis)[†]

Work has begun on a program to interpret requests for information about student responses in the form of a multiple-stage sorting routine which will select and store information from PLATO dope tapes needed to answer requests. It is expected that this program will form the central element in the developing system.

[†]Portions of this work were supported by the U. S. Office of Education under Contract No. OE-6-10-184.

Work is nearly finished on the program called TEXT DOPE, which processes dope tapes and then, on request, plots graphs of time and errors against question number and lists student answers to questions in the lesson.

A new teaching logic has been designed and coding is nearly finished. This program, TEXT EDIT, plots questions for the student on the PLATO blackboard and has an author mode which permits on-line editing of these questions. This program also provides for auxiliary input devices, such as a Braille typewriter or apparatus (not yet available), on which a student can trace simple diagrams. It is expected that this logic will also form a part of the developing system.

J. A. Easley, Jr.
D. Bitzer
C. Bridges
W. Golden
T. Hastings
B. Hicks
J. Kraatz
R. Stake
J. Rubovits
P. Taylor
T. McGuire

5.5 The CATO Manual

The CATO manual for use with the PLATO system has undergone a major revision and augmentation. It is organized in four major parts with an appendix and is written as an aid to all users of the system from the non-technically-oriented to the experienced programmers. Part I contains a brief general description of the functions of the PLATO hardware (electronic equipment), its relationship to the PLATO software

(computer program), the operation of the system by student input, the relationship of the teacher and/or programmer to the system, and remarks on the preparation of material for the system. Part II describes the general operating procedures for the PLATO system. Part III is a section designed for the PLATO teacher or programmer who is writing his own PLATO program using the PLATO compiler (CATO). It is written in two parts, the first being detailed programming instructions, the second detailed compiling and editing instructions. Part IV discusses "doping" (student response records) procedures and analysis. The appendix, Part V, contains seven sections of more detailed information which might be desired by the experienced PLATO programmer. Preliminary copies have been distributed to present users of the system, and after revisions based on their reactions have been made, the CATO programming manual will be ready for general distribution.

L. Fillman

5.6 PLATO Seminars and Demonstrations

The PLATO group seminars reporting the research in progress with the PLATO system were concluded in this quarter with two in December:

"CIRCE--What is it and its relation to PLATO?" Professor Thomas Hastings, Director of CIRCE (Center for Instructional Research and Curriculum Evaluation), Professor of Education.

"The Use of PLATO in High Resolution Electron Spectrometry of Surfaces," Professor Frank Propst, Research Assistant Professor of Physics and Coordinated Science Laboratory.

The seminars will be resumed in the spring semester.

Nineteen demonstrations of the system were given this quarter introducing the system to approximately one hundred seventy-five persons (predominantly teachers).

6. VACUUM INSTRUMENTATION

D. Alpert
R. N. Peacock

F. M. Propst
W. C. Schuemann

F. Steinrisser

6.1 Pumping Speed of Getter-Ion Pumps

Measurements of the pumping speed of diode and triode ion pumps have recently been terminated, upon completion of the work. Measurements were made for H_2 , He, and N_2 , and over the pressure range of 10^{-11} to 10^{-6} Torr. Moderate saturation was found for all gases, and for pressures above 10^{-9} Torr, i.e., the pumping speed was found to decrease with pumping time to 70-90 per cent of the initial value after one day's time. Only for He at pressures above 10^{-7} Torr was severe saturation noted. Diode and triode pumps behaved similarly with respect to saturation and to pumping speed as a function of pressure.

In the diode pump, the discharge intensity I/P (where I is the pump current and P the pressure in the pump) was found to be proportional to the pumping speeds for short pumping times over the whole pressure range investigated. The number of molecules or atoms pumped per electric charge, PS/I , is therefore pressure independent. The values for H_2 , He, and N_2 are 0.5, 0.6, and 0.2, respectively. It was also found that the dependence of I/P on pressure for N_2 is practically the same as reported by Rutherford.¹

F. Steinrisser
F. Propst

¹S. L. Rutherford, Trans. AVS Vac. Symp. 10, 185 (1963).

6.2 CO Production under O₂ Admission

A number of experiments similar to those reported by Schuemann, de Segovia, and Alpert² were performed to study CO production under O₂ admission in the presence of a hot filament. Oxygen was admitted to a pressure of about 5×10^{-7} Torr, and the total and partial pressures were observed with different filaments operating. In the mass spectrometer a low-temperature cathode and regular tungsten filament were used, and, in the Bayard-Alpert gauge, normal tungsten and an ultra-pure (and carbon-free) tungsten filament were tested.

In Table I the observed CO pressures (given in percent of the O₂ pressure) are listed for several different conditions. In one case, the system processing was not done properly, and some oil was present in the system. The base pressure was still in the low 10^{-11} Torr range. In this case, the CO production rate was much greater. It was reported by Becker, Becker, and Brandes³ that carbon from oil cracking products diffuses into a tungsten filament. When O₂ is admitted with the filament hot, CO is produced, and carbon diffuses out. It is evident from Table I that conversion to CO can be quite moderate in a properly processed, clean system.

F. Steinrisser

²W. C. Schuemann, J. de Segovia, and D. Alpert, Trans. AVS Vacuum Symp. 10, 223 (1963).

³J. A. Becker, E. J. Becker, and R. G. Brandes, J. Appl. Phys. 32, 411 (1961).

TABLE I.

CO Production (in % of O₂, P_{O₂} $\approx 5 \times 10^{-7}$ Torr)

Emission Currents: Mass Spectrometer, 1 mA; B.A. Gauge, 10 mA

Conditions	% CO (T = 5 min)	% CO (T = 1 day)
Only mass spectrometer on, low temperature filament, no oil.	.75	.5
Only mass spectrometer on. W filament, no oil.	2.0	.9
B.A. gauge on, regular filament, no oil.	2.5	2.1
B.A. gauge on, ultra- pure filament, no oil.	1.8	.4
B.A. gauge on, regular filament, with oil.	3.0	25.0

6.3 Resumption of Work on the Suppressor Ionization Gauge

A type of ionization gauge called the photocurrent suppressor gauge was developed at the Coordinated Science Laboratory several years ago. This gauge is capable of effectively suppressing the photoelectric current (x-ray current) from the ion collector, thereby considerably extending the range of ionization-type gauges. Simple suppressor gauges have an x-ray limit of 1×10^{-13} Torr, about two or three orders less than that of the Bayard-Alpert gauge. These gauges have a higher sensitivity than typical inverted gauges, are only slightly more complicated, and can use the same power supplies and electrometers.

Readings of the Bayard-Alpert gauge,⁴ the most widely used instrument for measuring pressure in ultrahigh vacuum systems, are not linear with pressure in the vicinity of 1×10^{-10} Torr and lower because of a photoelectron current from the collector. This current is due to collector bombardment by soft x-ray photons released at the grid when it is struck by the ionizing electrons. Metson⁵ and Dalke-Schutze⁶ have designed gauges which suppress this photoelectron current by the utilization of a fourth electrode placed between the ionization region and collector at such a potential as to prevent photoelectrons from leaving the collector. Their gauges are limited in the measurement of

⁴R. T. Bayard and D. Alpert, Rev. Sci. Instr. 21, 571 (1950).

⁵G. H. Metson, Brit. J. Appl. Phys. 2, 46 (1951).

⁶W. E. Dalke and H. J. Schutze, 20th Annual Conference on Physical Electronics, M.I.T., Cambridge, Mass., 26 March 1960.

very low pressures by two factors: (1) low sensitivity and (2) a photoelectric current which flows from the suppressor electrode to the collector as the result of x-ray bombardment of the suppressor electrode.

Previous papers on the suppressor gauge being developed at CSL have described the first working model,⁷ a later version, the model 19 gauge,⁸ and the model 46 gauge,⁹ which has been used in our laboratory for several years. Redhead and Hobson¹⁰ have described their version of the suppressor gauge and developed methods for modulating the ion current in order to make pressure measurements in the low 10^{-15} Torr region possible.

6.4 Proposed Work on the Suppressor Gauge

Beginning this quarter, work is resuming on the development of the photocurrent suppressor gauge. The purpose of the work is two fold. First, we want to continue the development of a simple suppressor gauge capable of measuring linearly to the 10^{-12} to 10^{-13} Torr region; and second, we want to develop "super suppressor gauge" which hopefully

⁷W. C. Schuemann, Trans. of the Ninth National Vacuum Symp. (The Macmillan Company, New York, 1962), p. 428.

⁸W. C. Schuemann, Rev. Sci. Instr. 34, 700 (1963).

⁹W. C. Schuemann, Final Report on Photo Current Suppressor Gauge Development, Coordinated Science Laboratory Report R-249 (March, 1965).

¹⁰P. A. Redhead and J. P. Hobson, Fundamental Problems of Low Pressure Measurement Conf., Teddington (Middlesex) England (Sept. 1964).

will measure linearly to 10^{-15} to 10^{-16} Torr. The latter gauge would be limited by the ability to measure small ion currents.

The model 46 gauge developed several years ago has on occasion shown several limitations. These are (1) occasional negative collector currents apparently due to electron space charge oscillations; (2) outgassing of the shield electrode; and (3) occasional loss of electrical contact between the shield and the platinum bright coating on the glass walls of the tube. Work on a tube to eliminate these problems has proceeded to the point of assembly of the tube components and actual testing will soon begin.

The super suppressor gauge utilizes a more sophisticated shield, suppressor, and collector geometry to eliminate the "reflected x-ray effect." This gauge is being designed with liquid-cooled filament and grid leads to minimize outgassing at very low pressures. The parts for this gauge are being built and the system on which the gauge is to be tested may be operating by the end of the next quarter.

W. C. Schuemann

7. PLASMA PHYSICS

M. Raether
H. Böhmer
W. Carr
J. Chang

W. Bernhard
B. Hicks
R. Hosken
Y. Ichikawa
T. Lie

R. Huggins
C. Mendel
H. G. Slottow
M. A. Smith
S. M. Yen

7.1 Boltzmann Equation[†]

During the past quarter, the following modifications have been made in the computer program: (1) seven moments of the collision integral have been added to the two already in the program. (The nine calculated moments of the collision integral are equal to the rates of change of the corresponding moments of the distribution function that are calculated.) (2) the program to make a least-square adjustment of the Monte-Carlo estimates of the collision integral by keeping invariant the three conserved moments of the collision integral has been written.

Since Nordsieck's Monte-Carlo method can be used to evaluate the collision integral for any given distribution function, it is possible to make tests of the accuracy of the approximate solutions of the Boltzmann equation proposed for a shock wave. One direct test of proposed collision integrals was applied last year to a Mott-Smith shock, and a second test of the distribution functions has been applied in this quarter to both the Mott-Smith and Yen's 6-moment shocks. These results have been analyzed and summarized in an abstract submitted to England for presentation at the Fifth International Symposium on

[†]Portions of this work were supported by the Office of Naval Research under Contract No. ONR N00014-66-C0010-A01.

Rarefied Gas Dynamics in July, 1966. Two other abstracts submitted to the same symposium described Nordsieck's method of evaluating the collision integral and the (completed) work on the pseudo-shock.

The algebraic study of shock structure has been extended to diatomic gases. Also, the density distribution and shock thickness obtained by using negative powers of number density in the modifying polynomial proposed seem to show improvements over those from a polynomial of positive powers.

B. L. Hicks
S. M. Yen
M. A. Smith
K. R. Roth

7.2 Beam-Plasma Interaction

In the previous progress report (Sept., Oct., Nov., '65) we reported the observation of enhanced diffusion resulting from the beam-plasma instability.

During the last quarter, this effect has been investigated in some detail and its dependence on plasma and beam parameters has been measured. As described in the previous progress report, the enhanced diffusion is observed as a discontinuity in the fringe-shift pattern of a microwave interferometer (Figs. 7.1 and 7.2). It can be shown that the ratio of the slopes at the discontinuity is equal to the ratio of the diffusion coefficients at this point. This ratio has been measured as a function of beam current and plasma density. Figure 7.3 shows the dependence of the diffusion coefficient on the beam current.

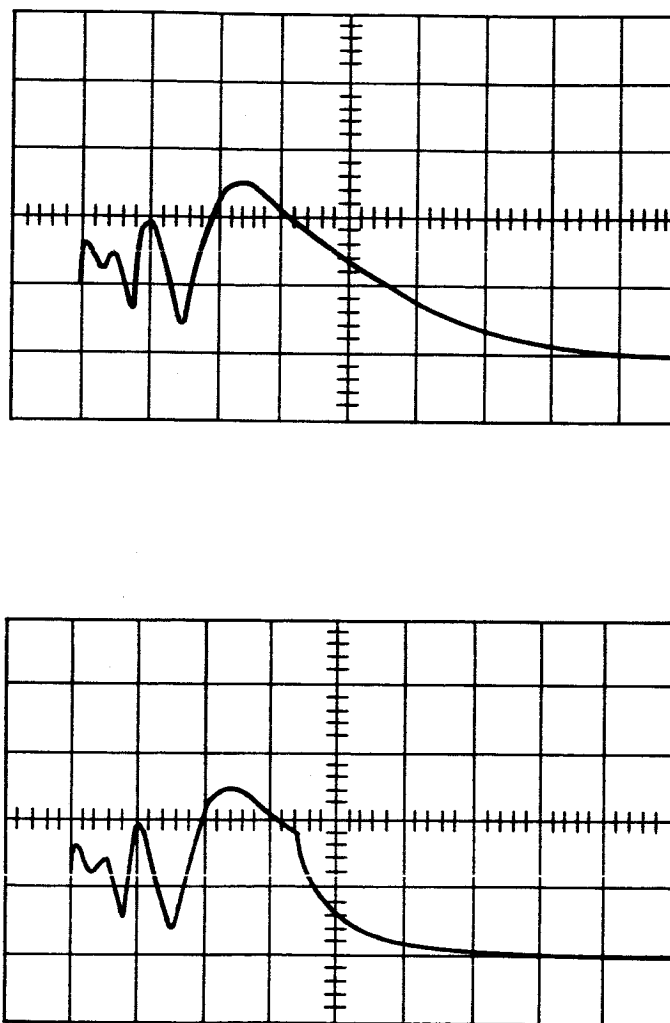


Fig. 7.1. Influence of the Electron Beam on the Interferometer Output. Timebase: 50 $\mu\text{sec/cm}$. Upper trace without beam, lower trace with beam.

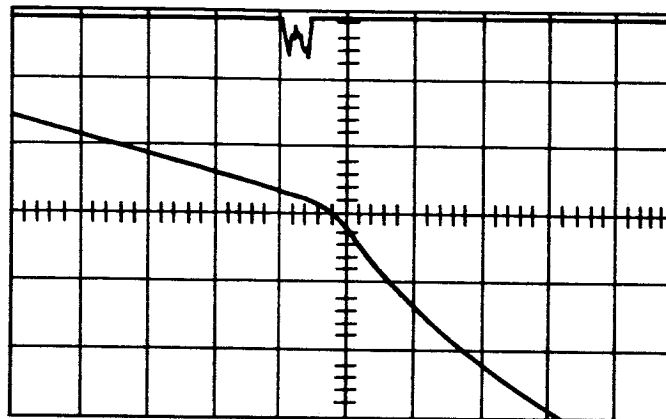


Fig. 7.2. Influence of the Electron Beam on the Interferometer Output.
Timebase: 5 μ sec/cm. Upper Trace: beam current.

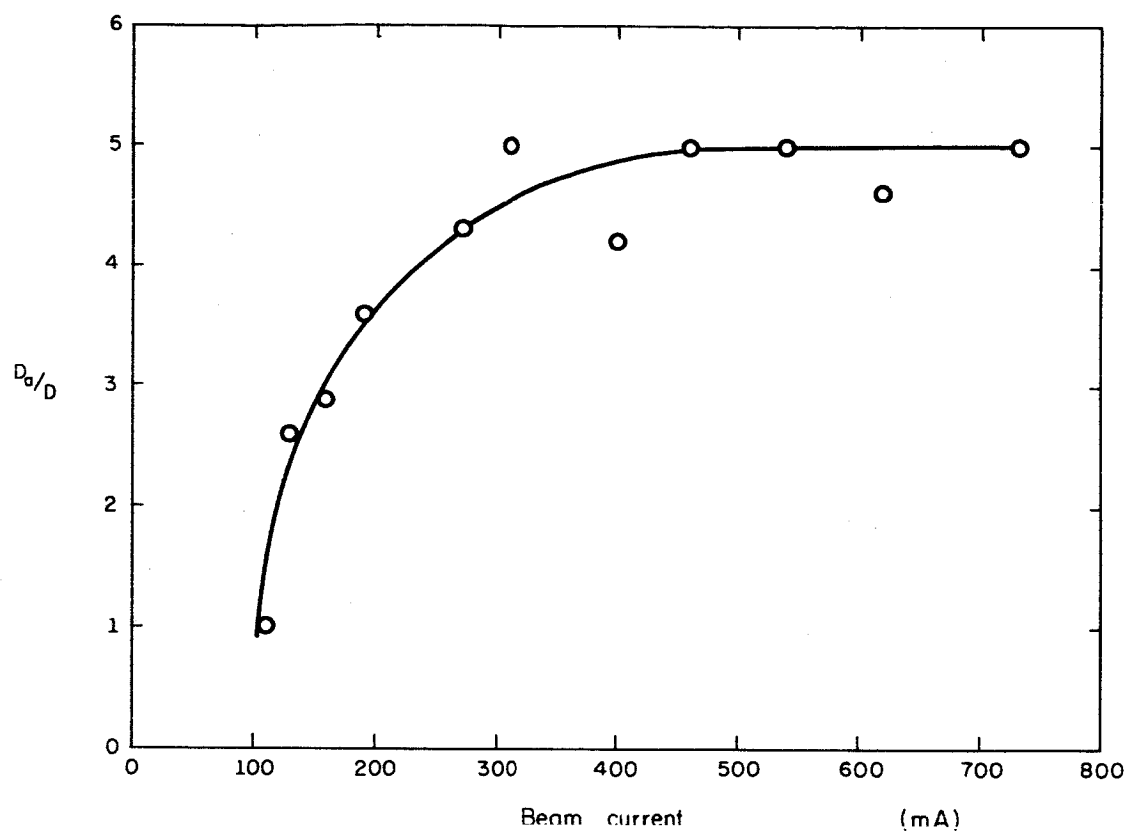


Fig. 7.3. Enhancement of the Diffusion Coefficient as a Function of Beam Current.

The interesting feature of Fig. 7.3 is that the ratio of D_a/D , where D_a is the enhanced diffusion coefficient and D the normal diffusion coefficient with no beam present, tend to a limiting value as the beam current increases. Simultaneous measurement of the noise emitted by the plasma oscillations does not exhibit this saturation effect. Instead, the noise power increases exponentially with beam current (see Fig. 7.4).

Figure 7.5 shows the dependence of D_a/D as a function of plasma density with the beam current as a parameter. We notice a pronounced maximum at a certain density. The location of this maximum depends slightly on the beam current, drifting to higher values as the beam current increases.

The enhancement of the diffusion coefficient is without doubt due to the beam-plasma instability, but the actual mechanism is not fully understood at the present time.

It is interesting to note that at the observed maximum (Fig. 7.5) the cold beam growth rate $\gamma \sim (\omega_B^2 \omega_p)^{1/3}$ is of the order of the coulomb collision frequency in the plasma. This would indicate that at higher plasma density a strong collisional damping of the instability occurs.

Work is in progress to investigate whether this maximum also occurs in the noise radiation emitted by the plasma oscillations.

H. Böhmer

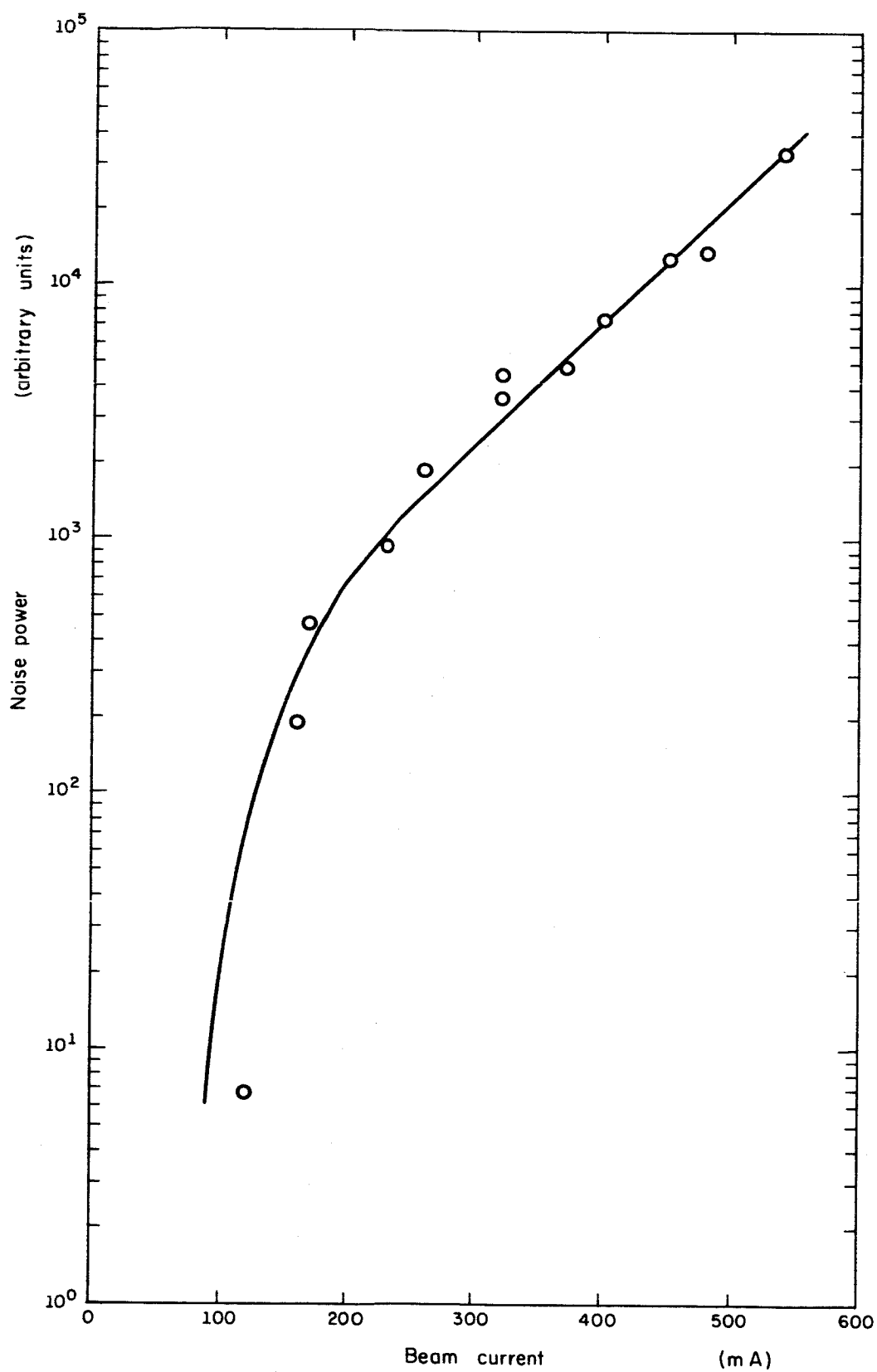


Fig. 7.4. Microwave Noise at the Plasma Frequency as a Function of Beam Current.

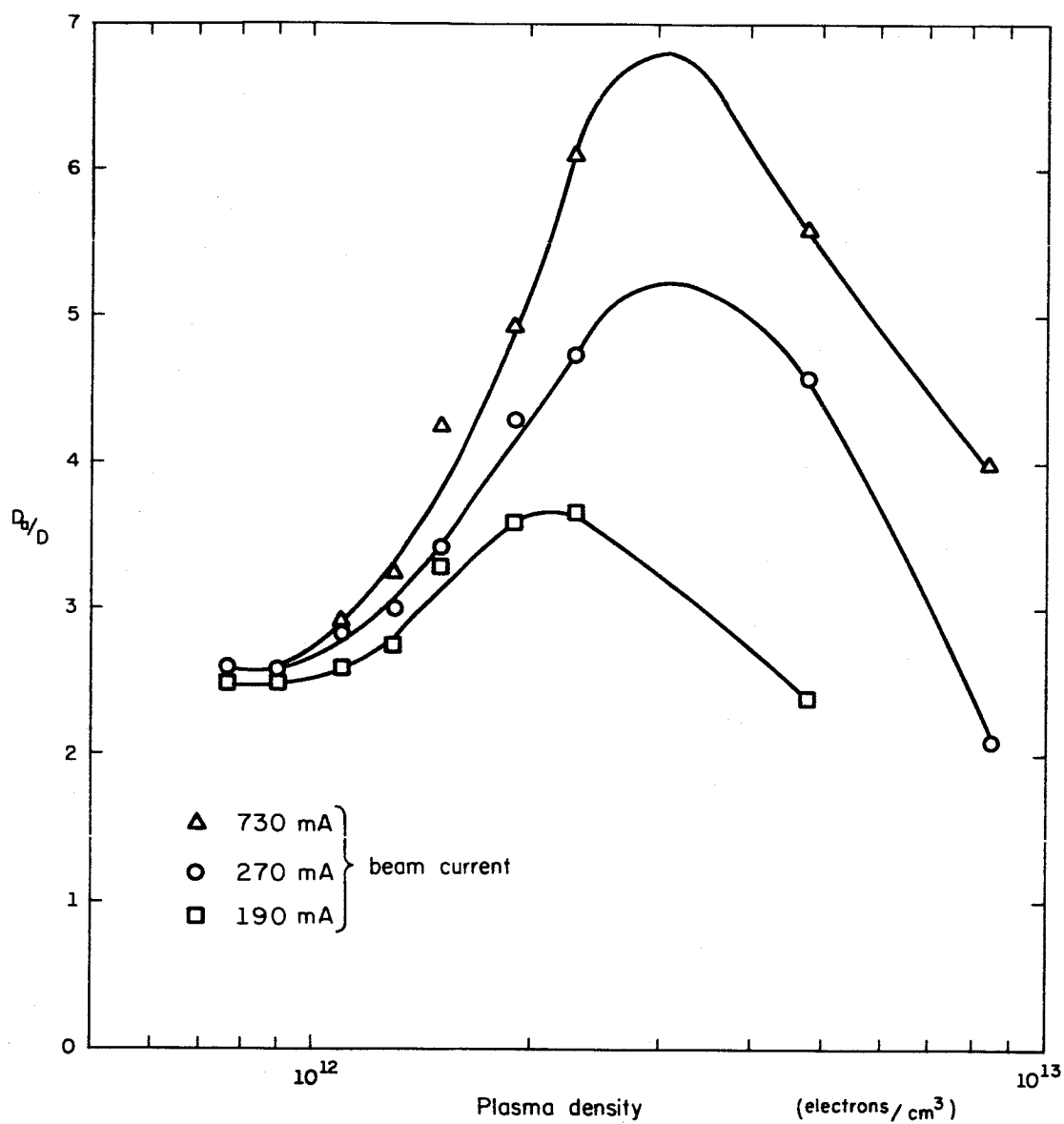


Fig. 7.5. Enhancement of the Diffusion Coefficient as a Function of Plasma Density.

7.3 Landau Damping in an Inhomogeneous Plasma

In the preceding report,¹ an experiment which was designed to correlate the linewidth of the Tonks-Dattner resonances with the ratio of tube diameter to the Debye length was described. This was somewhat of an exploratory experiment, and in several ways proved to be inadequate. Several modifications have therefore been made and results obtained which are in qualitative agreement with theoretical predictions, and are close enough to warrant further numerical calculations. Details of the modified experiment together with results obtained to date are given, and approximations in the theory are briefly discussed.

The main difficulty found in the experiment described in the previous report was that it was not possible to reach small enough values of L/λ_D , with a 22 mm. discharge tube. The smallest value reached was approximately 300 and Landau damping is significant only for values below 100. The diameter of the discharge tube was therefore reduced to 5 mm, but, because of the smaller discharge tube in the diagnostics waveguide (resulting in a smaller filling factor), the sensitivity of both the electron temperature and density measurements proved to be too small. The interferometer was therefore replaced by a microwave cavity² for the electron density measurement, and the temperature was inferred from the measured ambipolar diffusion coefficient.

¹Progress Report for Sept., Oct., Nov., 1965.

²M. A. Biondi and S. C. Brown, Phys. Rev. 75, 1700 (1949).

The present experimental arrangement is shown in Fig. 7.6.

The L-band waveguide is retained for the observation of the Tonks-Dattner resonances, but only a single discharge tube is used. An X-band TM_{010} transmission microwave cavity is mounted close to the L-band guide. The normal method of measuring the frequency shift of a microwave cavity³ is to vary the klystron frequency until the frequency equals that of the cavity at the desired time in the afterglow. This is observed by monitoring the transmitted signal with an oscilloscope with the timebase triggered by the dc pulse. The new klystron frequency is found with a wavemeter. As well as being inaccurate for small frequency shifts, this method of taking data is somewhat tedious.

A method by which the frequency shift can be recorded photographically together with the Tonks-Dattner resonances is shown in Fig. 7.7. By applying the klystron frequency f_0 across a crystal diode which also has a low frequency Δf applied across it, a spectrum of frequencies $f_0 \pm \Delta f$ will be generated. In practice four or five sidebands separated by Δf are found at the third port of the circulator. The frequency f_0 is fixed so that one of the lower sidebands coincides with the empty cavity resonance frequency, and, during the electron density decay, transmission occurs whenever the frequency shift equals $n \Delta f$. A typical photograph is shown in Fig. 7.8 with $\Delta f = 5 \text{ MHz}$, and, for the particular cavity used, the electron density is given by $\bar{n} = 1.29 \times 10^3 \times \Delta f$ where f is in MHz .

³Ibid.

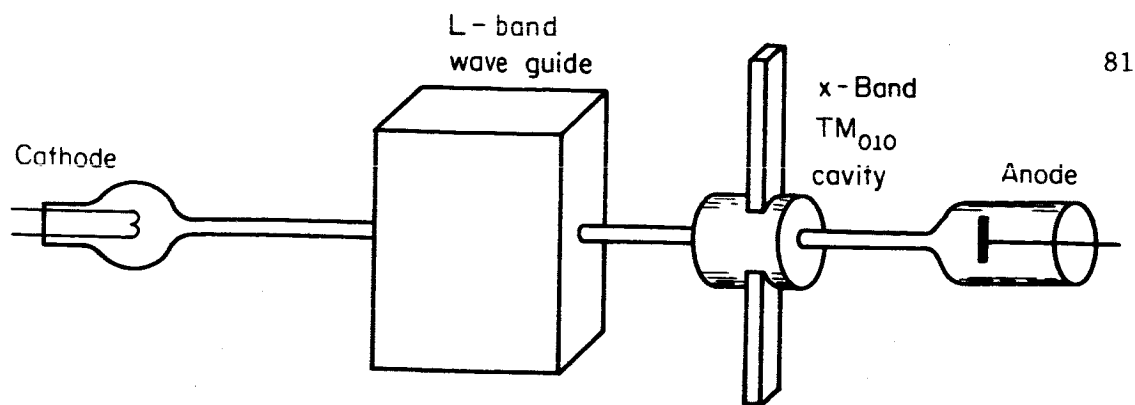


Fig. 7.6. Discharge Tube with L-band Waveguide and X-band Cavity.

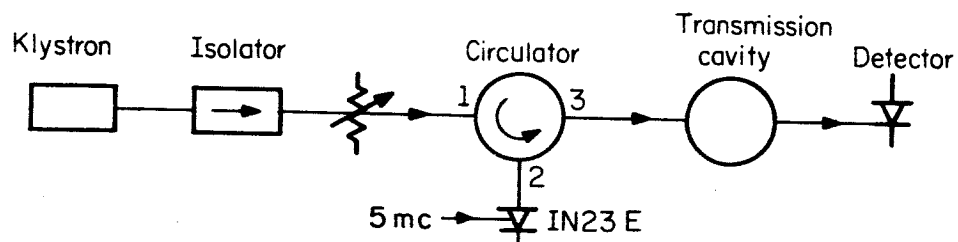


Fig. 7.7. Method of Measuring the Electron Density.

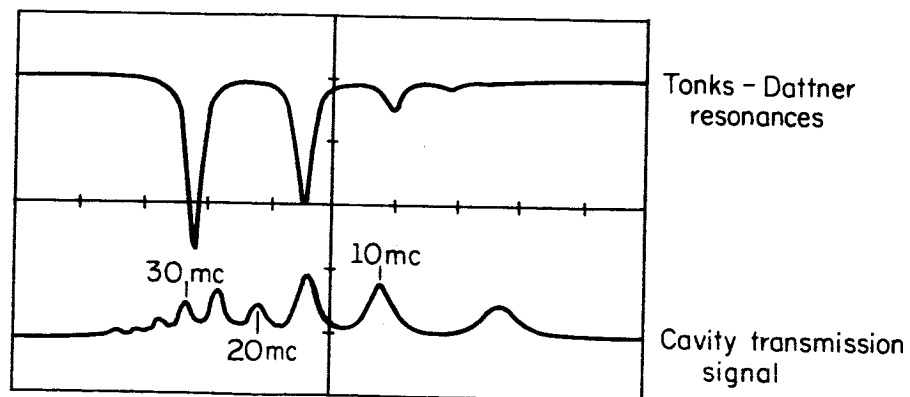


Fig. 7.8. Photograph of Resonances and Cavity Transmission Signal.

From the electron-density decay as found above, the temperature is estimated at any particular point in time by measuring the decay rate at that time. The ambipolar diffusion coefficient is found from the relation

$$D_a p_T = \Lambda^2 p / \tau$$

where Λ is the characteristic diffusion length of the tube, p is the pressure in Torr, and τ is the e-folding length of the decay. The temperature is found from

$$T = T_o [2D_a p_T / D_a p_o - 1]$$

where T_o is room temperature, and $D_a p_o$ is the ambipolar diffusion coefficient at room temperature. This method of measuring temperature is currently being checked against radiometer measurements.

A graph of the line width or "Q" of the first Tonks-Dattner resonance plotted against L/λ_D is shown in Fig. 7.9. The correction for collisional damping and the theoretical damping rate for an inhomogeneous plasma for which⁴ $\nu = 0.5$ are also shown. At the present time, only qualitative comparison between theory and experiment is possible for the following reasons:

1. Mathieu functions corresponding to values of $L/\lambda_D > 100$ are not available.

⁴E. A. Jackson and M. Raether, CSL Report R-239.

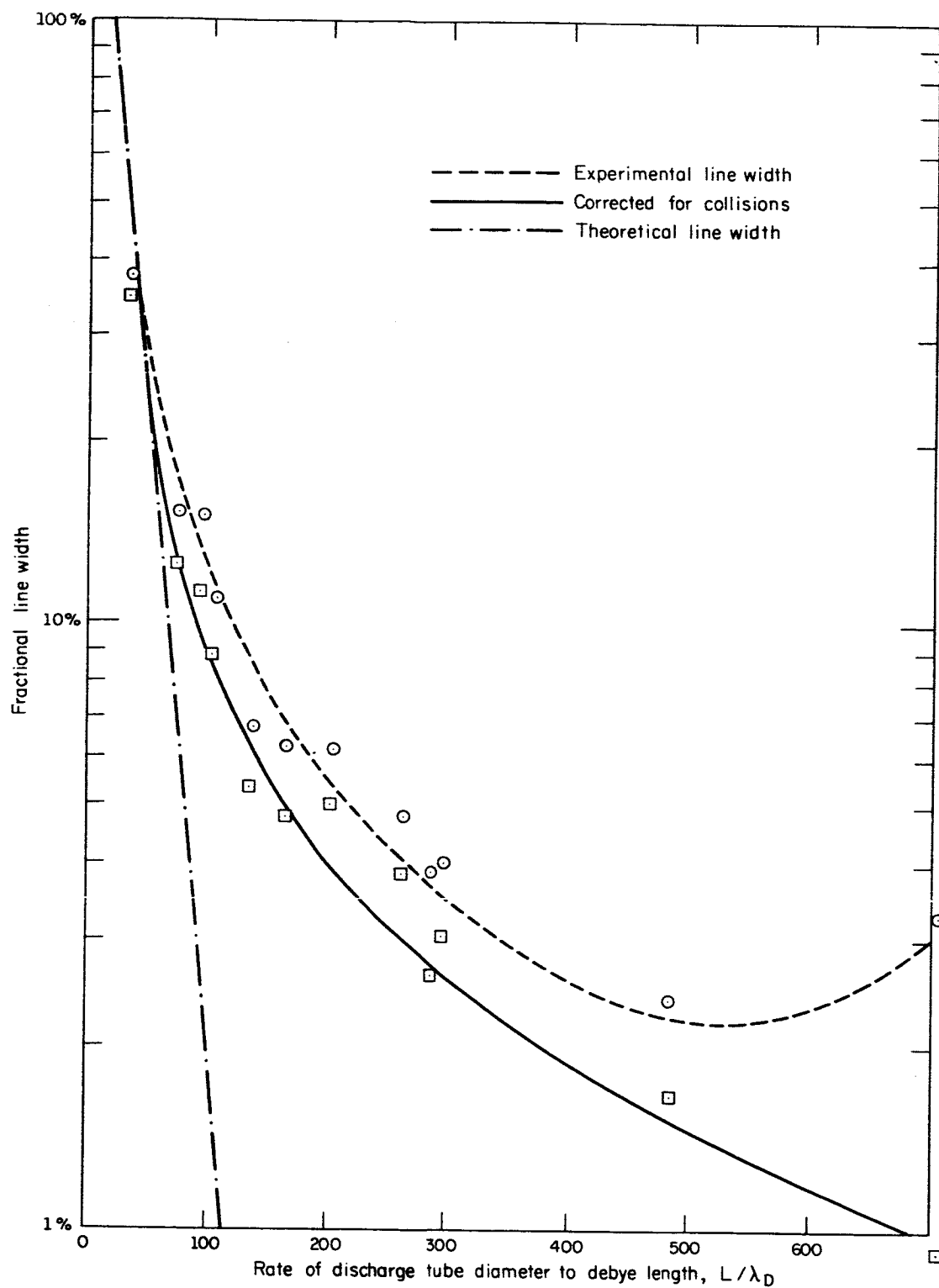


Fig. 7.9. Resonance Linewidth Plotted Against L/λ_D .

2. Coulomb collisions are the dominant collision mechanism, and thus the collision frequency varies with the radial position in the tube. This is not taken into account in the theory.
3. The theory applies to an infinite parallel-plate discharge, whereas the experiment was performed with a cylindrical discharge.

Numerical calculations are being carried out to evaluate Mathieu functions corresponding to high values of L/λ_D , and a more detailed analysis of the linewidth with Coulomb collisions integrated into the calculations is under consideration. A rectangular discharge tube is also being constructed.

R. Huggins

8. SUPERCONDUCTIVITY STUDIES

C. B. Satterthwaite
M. G. Craford

J. R. Carlson
B. K. Moore

I. Toepke
R. P. Ries
D. Gutman

8.1 Introduction

This group was originated in CSL and has been supported by CSL for the last four years. With the establishment of the Materials Research Laboratory (MRL) on the campus, it has appeared that the emphasis of this group on materials and low temperature physics coincides more closely with the mission of MRL than CSL. Support for much of the group has been transferred to MRL as of September 1, 1965, and the low temperature experimental effort will be moved in the near future. The two projects reported below will remain on CSL support until they are completed. Further collaborative work with the Thin Films Group is anticipated.

8.2 Superconducting Parametric Amplifier (Picovoltmeter)

The work of the present period has been aimed primarily at improving reproducibility and sensitivity of the picovoltmeter and at optimizing the input parameters. Some additional superconducting shielding has been added to reduce noise due to residual magnetic fields. The highest voltage sensitivity so far attained was 5×10^{-15} V with a signal-to-noise ratio of unity, with an input impedance of $2 \times 10^{-8} \Omega$, and with a time constant of approximately 60 sec. With a time constant of approximately 5 sec the best sensitivity was about 8×10^{-14} V.

R. P. Ries

8.3 Superconductive Tunneling in High-Purity Single-Crystal Niobium

The attempt to observe anisotropy of the superconducting energy gap in niobium is continuing.

Apparatus necessary for making ac measurements on the junctions has been completed. Preliminary measurements have indicated that anisotropy is not present in commercial crystals of the highest available purity. The anisotropy should be present if the crystal is of sufficient purity. Hence, a technique for further purification of the crystal by heating it in high vacuum with an electron beam is being developed. An attempt is being made to use the gettering action of the niobium, which has been evaporated from the surface of the hot crystal, to lower the pressure of active gases in the immediate vicinity of the crystal significantly below the 3×10^{-8} Torr pressure normally obtained in our vacuum system. This technique will be explained in more detail later.

At the present time, work is being delayed by a leak in the vacuum system. The Varian partial-pressure gauge which was recently obtained by the thin films group has been extremely useful for leak detection.

G. Craford

9. HIGH VOLTAGE BREAKDOWN

D. Alpert
E. M. Lyman

D. Lee
T. Casale

9.1 Review

During the last several years, the present group has been conducting experiments on electrical breakdown in vacuum. These investigations have led to the conclusion, at least for tungsten, that electrical breakdown is initiated by field-emission currents drawn from small sharp projections on the cathode surface. These sharp projections, of the order of a micron in length, greatly enhance the local electric field compared to the average electric field which would exist in their absence. For a particular set of electrodes, the relationship between the local electric field at the emission site and the applied voltage can be uniquely determined from a Fowler-Nordheim analysis of the voltage-current characteristics. A subsequent measurement of the breakdown voltage then gives directly the "breakdown field." This breakdown field has been measured for tungsten and has been found to be nearly constant independent of the electrode geometry or gap spacing for a range of breakdown voltages from 800 volts to 250 kV. The breakdown field for tungsten is $6.4 \pm 1.0 \times 10^7$ V/cm.

9.2 Calculations Concerning Electrical Breakdown

For the tungsten-point emitter, Dyke and his co-workers¹ have calculated that the field-emission currents at breakdown are sufficient to melt the projection. He then postulates that the material evaporated from the projection, when ionized by the field-emission currents, can greatly enhance the current by establishing a positive-ion space charge near the cathode surface. We agree with Dyke that the probable initiatory event is the melting of the projection. However, we advanced an alternative explanation for the transition mechanism. When the projection melts, it is mechanically unstable, with the melted portion drawn into the gap under the influence of the large mechanical forces associated with the electric field. This changing geometry further increases the electric fields and thus the current density. This is certainly a highly regenerative process with the resistance and total current rapidly increasing, and with the thermal coupling to the base decreasing. The conditions are similar to the exploding wire experiments in which current densities of the order of those found at breakdown, 10^8 A/cm², not only melt, but vaporize wires in a few nanoseconds.

At present there is no direct experimental evidence which identifies the transition mechanism. In any case, the criterion that electrical breakdown is initiated when the tungsten electrode melts

¹W. W. Dolan, W. P. Dyke, and J. K. Trolan, Phys. Rev. 91, 1054 (1953).

seems plausible. Using this criterion, calculations have been made to determine the current density, and therefore the electric field, necessary to melt a projection on the cathode surface. The shapes used for the calculations were necessarily idealized. Both cylinders and truncated cones were considered. The physical dimensions used, however, conformed roughly to those recently found on the surface of the electrodes.^{2,3} A report has been written detailing these calculations for tungsten (R-280). Figure 9.1 summarized some of the results of these calculations. The electric field necessary to induce melting is plotted against the half-cone angle. The lengths considered were between one and ten microns, and the areas were 10^{-12} , 10^{-10} , and 10^{-9} cm². At large cone angles, the radial symmetries dominate, and the breakdown fields are largely dependent on the area of the projection. However, at small cone angles, where the symmetry can be expected to be nearly cylindrical, the length of the projection is the dominating geometrical parameter.

Additional calculations have been made for other materials. Table I indicates the values of electric field necessary to melt a one-micron-long cylinder for various metals. It is seen that the breakdown fields are essentially the same. Recently Brodie has measured the breakdown fields for some of these materials. Table II indicates the measured breakdown fields for his experiments as well as the results of

²H. E. Tomaschke, "Study of the Projections on Electrodes and Their Effect on Electrical Breakdown in Vacuum," Ph.D. Thesis; University of Illinois, 1964.

³R. P. Little and S. T. Smith, J. Appl. Phys. 36, 1502 (1965); 34, 2430 (1963).

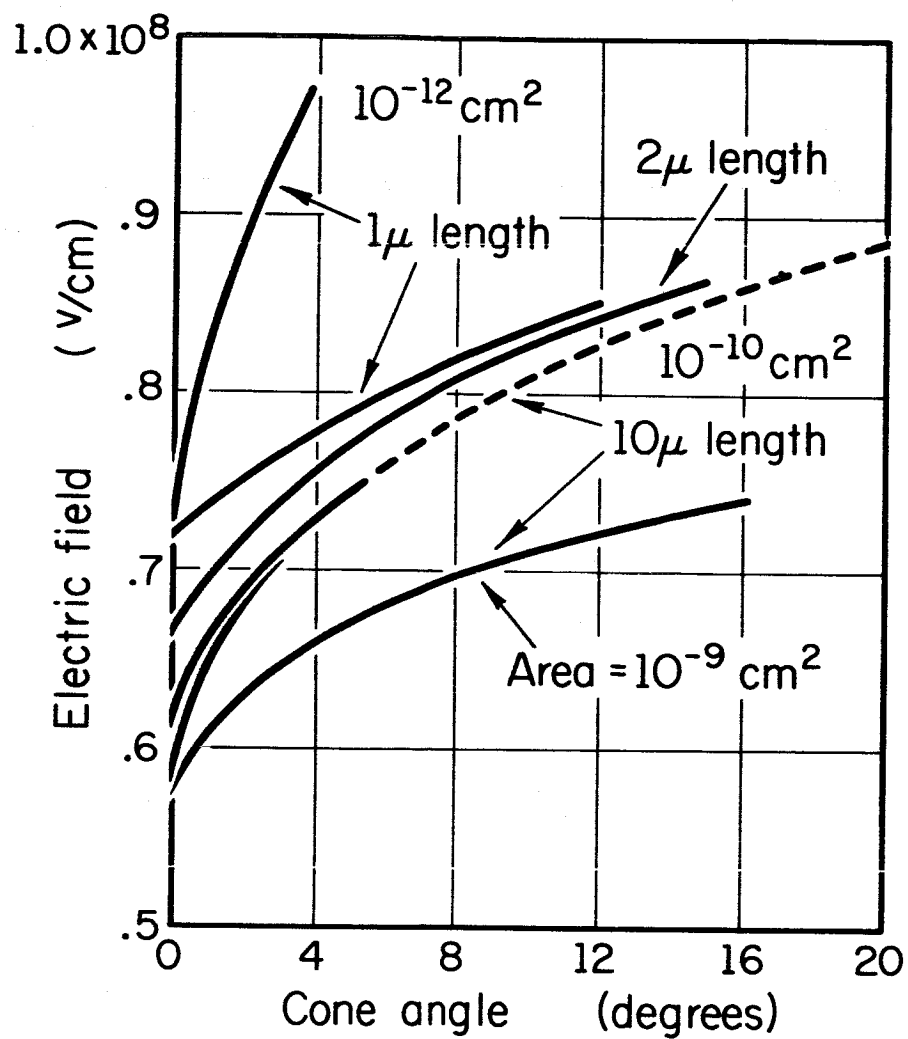


Fig. 9.1. The Critical Field as a Function of the Length and Cone Angle.

TABLE I.

Material	Critical Field
Au	8.9×10^7 V/cm.
Ag	8.6
Cu	8.2
Mo	8.0
Ni	7.6
W	7.5

TABLE II.

Metal	Investigator	No. of Tests	E_b (V/cm)	Beta
W	ALLT ^a	37	6.4×10^7	27 to 300
	Ahearn ^b	1	5.7	34
	Chambers ^c	4	7.8	not known
	BKG ^d	4	6.5	1 to 30
Mo	Pivovar and	3	6.6	98 to 311
	Gordienko ^e	3*	7.6	538 to 3069
	Brodie ^f	10	5.6	108 to 380
Ni	Brodie ^f	6	10.4	195 to 580
Cu	Brodie ^f	2	14.8	600, 640
Cr	Brodie ^f	4	5.3	166 to 300

*Outgassed at 2000°C.

^aD. Alpert, D. Lee, E. M. Lyman, H. Tomaschke, J. Vac. Sci. & Tech. 1, 35 (1964).

^bA. J. Ahearn, Phys. Rev. 50, 238 (1936).

^cC. Chambers, J. Franklin Inst. 218, 463 (1934).

^dW. Boyle, P. Kisliuk, and L. H. Germer, J. Appl. Phys. 26, 720 (1955).

^eL. I. Pivovar and V. I. Gordienko, Sov. Phys.--Tech. Phys. 7, 908 (1963).

^fI. Brodie, private communication; and J. Vac. Sci. & Tech. (to be pub.).

10. THIN FILMS

R. N. Peacock
M. G. Craford

J. T. Jacobs
W. P. Bleha

T. H. O'Meara
S. A. Smith
K. G. Aubuchon

10.1 Size Effects

The effects of the surface of a conductor on the conductivity of a sample do not depend on the geometry of the sample if the Fermi surface is spherical, and if the internal reflection of conduction electrons from the sample surface conserves momentum, i.e., if collisions with the surface are specular. Specular reflections should occur if the surface is smooth compared to the de Broglie wave length of the conduction electrons. The effects of nonspecular reflection in the electronic conductivity become important as the ratio of surface area to volume increases. Hence, such effects could be observed in thin conducting films. However, several authors report that, under special circumstances, they have observed specular reflections in gold films. This indicates the surfaces of these films may be extremely flat.

It is proposed that more careful experimental investigation of such size effects should reveal the circumstances, if any, under which specular reflection takes place. Such experiments would have to be done in an ultrahigh vacuum system in order to eliminate the effects of contaminants on the films. The required system must have high pumping speeds during the evaporation of the films. A cryopump has been designed to meet this need. It was constructed in our shop and delivered during the quarter.

J. T. Jacobs

10.2 Cryopump Tests

Efforts during the quarter were directed toward testing the cryopump in an uhv station. Measurements of system total pressure and partial pressures were made before and after bakeout and transfer of refrigerants.

It was initially thought that a Consolidated Electrodynamics Corporation mass spectrometer which was at hand might be used to analyze the residual gases in the vacuum system. However, failure of the mass-scan circuit and a collector breakage made this impossible. Efforts are still being made to return this instrument to useful service.

A new Varian Associates partial pressure gauge (PPG) was delivered in February, and has now been used in conjunction with the cryopumped uhv station. Although the resolution of this instrument is low, its sensitivity is much higher than the CEC mass spectrometer. This makes it suitable for measuring the limiting residual gases in the cryopump system.

The modified Swagelok on the cryopump helium dewar has leaked after every bakeout. Changing gold O-rings and seats has not eliminated the problem.

The best vacuum obtained during the last quarter was limited to 1×10^{-9} by a small leak in the helium dewar assembly. This leak was detected with the PPG. Since the leak was so small, it was decided that liquid helium should be put in the dewar to see if the leak could be further opened. The leak did open sufficiently so that it could be precisely located with a conventional leak detector.

One interesting feature of the above test is that the PPG indicated that, with liquid helium in the cryopump, the partial pressures of nitrogen and hydrogen was less than 7×10^{-11} Torr. This indicated that when the system is leak tight a total pressure of 2×10^{-10} Torr will be within reach.

J. T. Jacobs

10.3 Hall-Effect System

Previous reports have discussed a system to be used for in situ measurements of Hall mobilities in thin films. The electromagnet for the system has now arrived, and the apparatus is nearly ready to be put into operation. Preliminary tests have indicated that the motion feedthrough mechanism, a very critical part of the arrangement, does function as expected.

A water baffle, constructed by the shop, has been added between the cold trap and the diffusion pump. It is expected that this will help to reduce the amount of pump oil reaching the cold trap, and hence the amount in the working region. With the water baffle installed, but without a bakeout so far, a system pressure of 7×10^{-8} Torr was achieved.

K. G. Aubuchon

11. INFORMATION SCIENCE

R. T. Chien
R. B. Ash
T. Kasami

J. T. Barrows
L. Bahl
D. Chow

H. T. Hsu
V. Lum
R. J. Tracey

11.1 Introduction

The purpose of this research is to develop information-theoretic methods for the design and optimization of digital systems for data transmission and data processing. During the past quarter, a number of significant research results were obtained. These results are presented in the sections that follow.

11.2 Algebraic Theory of Bose-Chaudhuri-Hocquenghem Codes[†]

Investigation of the problem of determining whether a class of BCH codes has minimum weight larger than the BCH bound was started in the summer of 1965 and research in this direction continued throughout the past quarter. The technique used is that of Mattson-Solomon (SIAM, 1961). In the previous progress report, it was reported that the Golay (11,6) code over GF(3) can be shown to have minimum distance 5 while the BCH bound for this code is 4. Since then we have shown that the approach can be generalized to any BCH code over GF(q). This result is given as a main theorem below.

Let $x^n - 1$ be factored into irreducible polynomials over GF(q), i.e., $x^n - 1 = (x-1)f_1(x)f_2(x)\cdots f_t(x)$, with $f_i(x)$ irreducible for $i = 1, 2, \dots, t$. Let the recursive polynomial be given as $f(x) = (x-1)f_i(x)$,

[†]Portions of this work were supported by the National Science Foundation under Grant NSF GK-690.

$1 \leq i \leq t$. Previously in the August 1965 Progress Report, we have defined that for every $a \in A$, A being a BCH code, we have polynomials $g_a(x)$ and $p_a(x)$ given as

$$g_a(x) = c_0 + c_1 x^{e_2} + \dots + c_h x^{e_h},$$

and

$$p_a(x) = c_0 x^{e'_0} + c_1 x^{e'_1} + \dots + c_h x^{e'_h},$$

where

$$e_i \in E(\beta) = \{0 \leq e \leq n-1 \mid f(\beta^e) = 0\},$$

and

$$e'_i \in E'(\beta) = \{0 \leq e' \leq n-1 \mid f(\beta^{m+e'}) = 0\},$$

where β is a primitive n^{th} root of unity and m an arbitrary integer.

Let n be an odd prime and h the degree of $f_i(x)$. Assuming that there exist at least two unequal coefficients of the $(h-1)$ -degree term, and defining $m \equiv m_0 - (n-d_0+1) \pmod{n}$ ($\beta_0^m, \beta_0^{m+1}, \dots, \beta_0^{m+d_0-2}$ are roots of the generating polynomial) we have

Theorem - Let $a \in A$ over $\text{GF}(q)$ have $g_a(x)$ and $p_a(x)$ just as given. Let the leading coefficients of $p_a(x)$ be c_k and the constant term be $c_k^{q^i}$. If $(i, h) = 1$ and $d_0 < h$, then the code has minimum distance $\geq d_0 + 1$. If either the constant term or the leading coefficient of $p_a(x)$ is c_0 , and $d_0 < h$, then the code has minimum distance $\geq d_0 + 1$.

The theorem can be applied quite easily. To demonstrate its usefulness, examples in different fields are found by hand calculation. Among these examples we have in $\text{GF}(2)$, (17,9), (23,12), (43,15), (73,10) codes plus others, in $\text{GF}(3)$ we have the Golay (11,6) codes, in $\text{GF}(4)$ the

(11,6), (19,10), (23,12), (29,15) codes and in $GF(5)$ the (11,6) code. There are many others for which either the theorem or a slight modification of it applies.

An account of these research results has been summarized in technical report R-281.

V. Lum

11.3 Coding Methods for Information Retrieval[†]

Progress has been made in the construction of retrieval procedures by using the theory of group characters. The determination of the weight of the coset leaders from its syndrome can be accomplished by computing enough invariant functions on the orbits of a weight-preserving automorphisms of S . There is a set of invariant functions which forms an orthogonal basis of all real-valued functions which are constant on the orbits. The following lemmas have been proved and will show that the invariant functions ψ_i can only take certain values which is related to the number of one's in the cycle representatives of the dual code if the group of weight-preserving automorphisms contains a subgroup which corresponds to the cyclic permutation of the code. These lemmas will help choose the ψ_i functions.

Lemma 1: Let G_2 be a weight-preserving automorphism of S which corresponds to cyclic permutations of the code. Let G_2^T be a group whose elements are the transposes of the elements in G_2 . Let $m_1, m_2, \dots, m_\alpha$ be

[†]Portions of this work were supported by the National Science Foundation under Grant NSF GK-690.

the cycle representatives of the null space, i.e., all other elements in the null space are the cyclic shift of these representatives. The group G_2^T partitions S into α orbits. If we choose $H = [I_r R^T]$, then the elements in the i^{th} orbit consist of all possible r -consecutive digits in m_i .

Lemma 2: Let m_i be a cycle representative of the null space and $m_i = tH$ where t is a r -tuple, then the invariant function on i^{th} orbit $0_i''$ which contains t is

$$\sum_{t \in 0_i''} (-1)^{st^T} = \frac{e}{n} (n-2 \times \text{the number of ones in the polynomial } v_2(x)) ,$$

where $v_2(x) = s^*(x)m_i(x) \bmod x^n-1$, $s^*(x)$ is the reciprocal polynomial of $s(x)$, and e is the period of $m_i(x)$.

D. Chow

11.4 Coding for Compound Channels[†]

A class of shortened cyclic codes is developed for the compound channel. The generator polynomial, $g(x)$, of this class of code V may be written as

$$g(x) = (x^{b_0}-1)g'(x) .$$

The code V generated by $g(x)$ can correct, for a compound channel, all single bursts of maximum length b_0 and all t -tuple random errors, provided the minimum distance of the code V is $\geq 2t + 2$ and $b_0 \leq \text{Min}[b, b']$, where b' is the maximum length of all bursts correctable by V when considered as a burst-error-correcting code only.

[†]Portions of this work were supported by the National Science Foundation under Grant NSF GK-690.

In particular, we may consider $b = 2b' - 1$ and $g'(x)$ selected according to the BCH code, then

$$g(x) = (x^{2b'-1} - 1)g_{\text{BCH}}(x),$$

and all conditions are satisfied. This leads to a large class of codes all readily constructible.

It is also known that b' may be bounded from below by the expression

$$b' \geq \text{Max}(\lceil \frac{b}{2} \rceil, t + \lceil \frac{t-2}{2} \rceil),$$

where $[i]$ denotes the integer part of i .

T. Kasami

Gorog has shown that if

$$g(x) = p_1(x)p_2(x)\cdots p_n(x)$$

and $p_i(x)$ ($i = 1, 2, \dots, n$) are irreducible polynomials of the same cycle length, the burst correcting capability of $g(x)$ is easily determined. We are now investigating the use of this type of polynomials for the compound channel. The minimum distance of a large class of codes generated by these polynomials have been determined. The computation of F_t is in progress.

Another interesting result that is recently obtained concerning F_t is an accurate estimation of the complexity of computing F_t in general. It is found that if the number of computations are limited to about 10^3 t must be ≤ 5 .

H. T. Hsu

11.5 Linear Residue Codes[†]

A necessary and sufficient condition for a code to correct all t -tuple and smaller errors is that the minimum distance d of the code satisfy $d \geq 2t+1$. Given the number of code words B , and a code generator A , the minimum distance is given by $d = \min\{W(AN): N = 1, 2, \dots, B-1\}$, where $W(AN)$ is the arithmetic weight of the code word AN .

In this investigation, B is a given prime number. The total length of the code is then given by $e(2;B)$ or $e(2;B)/2$ where $e(2;B)$ is the exponent of 2 modulo B and the code generator is given by

$$A = (2^e - 1)/B$$

or

$$A' = (2^{e/2} + 1)/B.$$

It remains to find the minimum distance of such a linear residue code. The solution of this problem is divided into two parts. That is, letting the double bracket symbol $[[B/3]]$ denote the greatest odd integer $\leq B/3$, we find $d = \min\{W(AN): N \leq [[B/3]]\}$ and then make use of a general result which states that if $W(AN) \geq d$ for $N \leq [[B/3]]$ then $W(AN) \geq d$ for all $N < B$. Thus, if the first third of the multiples of A have weight $\geq d$, then so do all multiples, and d is the minimum distance of the code.

To ascertain the weight of the first third of the odd multiples, the following recursive relation is used:

[†]Portions of this work were supported by the National Science Foundation under Grant NSF GK-690.

$$x_{i-1} + \lambda_i B = x_i 2^{\alpha_i}, \quad (1)$$

with x_0 given odd; it is intended that $\lambda_i = \pm 1$ such that $\alpha_i \geq 2$, and that all x_i are odd and either positive or negative. After m steps we have $x_m = x_0$ and

$$x_0 (2^{\sigma_m} - 1) = B \left(\sum_{i=1}^m \lambda_i 2^{\sigma_{i-1}} \right) = BA_m, \quad (2)$$

where $\sigma_i = \sum_{k=1}^i \alpha_k$ and $\sigma_0 = 0$. Thus, since $\sigma_i \geq \sigma_{i-1} + 2$, A_m is in non-adjacent form (modified binary system) and $W(A_m) = m$. Also for $x_0 = 1$, the A_m constructed is taken as the generator of the code with $\sigma_m = e(2; B)$. Also for each x_0 taken, say $x_{0,j}$ with $x_{0,1} = 1$, we obtain a set of iterates

$$X_j = \{x_{i,j} : x_{0,j} \text{ given odd; } i = 1, 2, \dots, m_j\},$$

with $x_{m_j,j} = x_{0,j}$ and $\sigma_{m_j} = e(2; B)$ in Eq. (2).

There are as many sets (cycles) X_j as there are cosets associated with the cyclic subgroup generated by powers of 2 modulo B . That is, $j = 1, 2, \dots, v$, where $ve = \varphi(B) = B-1$. Also each $x_{i,j}$ satisfies $|x_{i,j}| \leq \lceil [B/3] \rceil$ if $|x_{0,j}| \leq \lceil [B/3] \rceil$. Thus each odd $N \leq \lceil [B/3] \rceil$ is an element of an X_j . Since A_{m_1} , constructed by using $x_{0,1} = 1$, is taken as the generator of the code, the minimum weight of NA_{m_1} for $N \leq \lceil [B/3] \rceil$ and odd, is m_j where $m_j = L(X_j)$ is the length, or rather, the number of elements in the cycle X_j , and $N \in X_j$. To see this, take any $x_{0,j} = N$ and iterate m_j times to get $x_{m_j,j} = x_{0,j}$ and A_{m_j} with $N(2^{e_j} - 1) = BA_{m_j}$. But $2^{e_j} - 1 = BA_{m_1}$, and therefore $NA_{m_1} = A_{m_j}$ with $W(NA_{m_1}) = W(A_{m_j}) = m_j$. Thus

the minimum weight of all (odd) code words is given by the length of the smallest cycle X_j . It is obvious that if the odd multiples have weight $\geq d$ then the even multiples also do, and the minimum distance of the code is taken as

$$d = \min\{m_j : j = 1, 2, \dots, v \text{ where } L(X_j) = m_j\}.$$

For prime B such that 2 is a primitive root of the finite field $G(B)$, there is only one cycle X_1 which contains all odd numbers (positive and negative) $\leq \lfloor B/3 \rfloor$. Thus half of this cycle is used to yield

$$A' = (2^{e/2} + 1)/B$$

with $d = W(A') = \frac{1}{2}(\lfloor B/3 \rfloor + 1)$. Similarly for -2 a primitive root, there are two cycles X_1, X_2 both of the same length ($X_1 = -X_2$) and we have

$$A = (2^e - 1)/B$$

with $d = W(A) = \frac{1}{2}(\lfloor B/3 \rfloor + 1)$. Thus for these two cases, the cycles do not have to be calculated. If B has more than two cycles associated with it ($v > 2$) then each cycle must be constructed and the length of the shortest cycle is taken as the minimum distance of the code.

Further investigations are being carried on with an eye toward ascertaining the length of the smallest cycle for an arbitrary B without having to actually construct the cycles. Current results have been summarized in a technical report (R-277).

J. T. Barrows

11.6 Coding for the Time-Discrete Gaussian Channel

Work is continuing on the problem of constructing explicit codes for the time-discrete Gaussian channel, as described in the previous progress report.

R. B. Ash
R. J. Tracey

11.7 Digital Addressing

A new investigation has been started in the area of digital methods for addressing. Selection schemes for conventional memory systems are being studied with potential generalizations to the organization and addressing of content-addressible memory systems.

Future area of investigations will include random-access digital communication systems and self-synchronizing sequences.

R. T. Chien
L. Bahi

12. SWITCHING SYSTEMS

S. Seshu
G. Metze
F. Preparata

S. J. Fenves
R. duPreez
R. Marlett

S. C. Chang
G. Martens
D. Crockett
W. J. Bouknight

12.1 Computer Compiler[†]

Work on the computer compiler was interrupted by the untimely death of Professor Sundaram Seshu (1926-1965) in an automobile accident on December 21. His career was cut short at a time of great productivity in which several long-term projects were beginning to bear fruit. He was actively engaged in research in network analysis and synthesis, the revision of his book on linear network analysis, the preparation of a book manuscript on the theory of sequential machines, and studies of fault diagnosis in digital and nondigital networks, in addition to the work on the computer compiler.

At the time of Dr. Seshu's death, large parts of the System Compiler had been written, with the exception of features such as MACRO and LIBRARY SUBROUTINE which had not progressed beyond the discussion stage. The Logic Compiler, which uses the micro-instruction string produced by the System Compiler to produce logic equations describing the system, had been outlined, and a preliminary investigation of logic-design schemes which reflect desired diagnosability criteria had been started. Both phases of the project will be continued.

G. Metze

[†] Portions of this work were supported by the National Science Foundation under Grant NSF GK-36.

12.2 Diagnosis of Computers[†]

An experiment has been conducted to test the computer design principles which allow diagnostic programs to be algorithmically derived without knowledge of the detailed logical design of the machine under test. The circuit tested was a portion of the CSX-1 computer, which was redesigned to conform to the necessary principles. The final circuit contained 275 logic blocks, including 24 flip-flops and 5 feedback lines and had 44 inputs and 6 outputs.

The manually derived checkout sequence was based on only a micro-order description of the circuit. The validity of this sequence was tested by means of the sequential analyzer program. This simulation experiment showed that all non-redundant failures were detected by the particular input sequence used, thus supporting the validity of the design principles and the test derivation procedure.

R. Marlett

12.3 Diagnosis of Combinational Logic Nets[†]

A new technique for the generation of test sequences for checkout and diagnosis of combinational logic nets is being investigated. For each input vector, the set of failed and good logic nets (machines) is partitioned on the basis of the output vector into equivalence classes of indistinguishable machines. The set of partitions obtained for all possible input vectors contains all the diagnostic information which

[†]Portions of this work were supported by the National Science Foundation under Grant NSF GK 36.

could be obtained by observing the terminal behavior of the combinational circuit. Hence, the set of equivalence classes for any sequence of inputs can be found by intersecting their corresponding partitions.

In the technique under investigation, a set of input vectors is selected to achieve a desired partitioning, according to some criterion. A program has been written to produce a "fixed" test schedule. The work will be extended to "serial" test schedules in which the outcome of the previous test determines the next test.

W. J. Bouknight

12.4 Synthesis of Sequential Networks[†]

The investigation of modular decompositions of (synchronous) sequential machines is being continued. Algorithms which give the parallel-series realization in terms of basic building blocks (such as shift registers and counters) as well as tests which determine the class of machines to which the algorithms apply are being developed.

E. D. Crockett

12.5 Analysis of Convolutional Transformations of Binary Sequences

The motivation for the present study is the consideration that sequence transformations represent an important necessity in several applications of information processing and transmission.

Non-feedback shift registers (finite-memory encoders) can be profitably adopted to perform transformations of binary sequences. The

[†]Portions of this work were supported by the National Science Foundation under Grant NSF GK-36.

output sequence is convolutionally obtained by "sliding" the encoding device along the input sequence and producing a symbol at each shift. Invertible transformations have been characterized, and decoding schemes analyzed. The crucial point in the decoding problem is that the simple finite-memory feedback decoder presents the undesirable well-known error propagation effect, while the non-feedback decoder contains, in general, an indefinite number of stages. Finite-memory non-feedback decoding is feasible, however, if some constraint is imposed on the input sequences, or, equivalently, if some decoding error is tolerated.

The analysis was conducted through the concepts of resynchronizing states of Boolean functions. The algebraic properties of resynchronizing states have been carefully analyzed and it was shown that they can be assigned only in special sets, termed clusters, which form a lattice. Moreover, each cluster of resynchronizing states belongs to a set of Boolean functions, which form a subspace of the vector space of all Boolean functions.

The work reported above is being published as a CSL report. Further investigation is in progress, in order to establish a formal relationship between the resynchronizing properties of the shift-register and the language constraint imposed on the input sequences for different lengths of the associated finite-memory decoder.

F. Preparata

12.6 Quasi-Linear Sequential Machines[†]

By assigning n -tuple vectors to nodes, one can represent a linear graph of 2^n nodes by an $n \times n$ matrix transformation of vectors. Crowell showed that nonsingular graphs of similar matrices are isomorphic but the converse is not true. We find that the matrix of a nonsingular graph is similar to one of the matrices in rational canonical form, and the number of the matrices in rational canonical form is determined by the number of irreducible polynomials for the elementary divisors. This idea is extendable to singular graphs.

Define $Y_{n \times 1} = A_{n \times n} y_{n \times 1} + u_{n \times 1}$ as a quasi-linear transformation of n -tuple vectors. We find that the quasi-linear transformation of a node-assignment yields isomorphic linear graphs. Hence, the permutation group of the 2^n n -tuple vectors can be partitioned into cosets by the quasi-linear transformation relationship. This implies that the linearity of a graph can be determined by testing only one node assignment in each coset, instead of having to test all possible node assignments.

S. C. Chang

12.7 Algebraic Network Synthesis[†]

An immittance matrix for a passive linear n -port may be obtained from the state equations by the algebraic elimination (node pulling) of state variables; conversely if state equations representing the given immittance matrix exist, they can be obtained from the

[†]Portions of this work were supported by the National Science Foundation under Grant NSF GK-36.

immittance matrix by node insertion. However, this process is not unique and hence is a synthesis problem.

A method has been developed for inserting nodes provided the numerator and denominator polynomials in the immittance matrix are relatively prime at each stage. The case in which the polynomials are not relatively prime is being investigated.

G. Martens

12.8 Computer System Evaluation[†]

The Console Timing Simulator System program was used in an initial investigation of blocking problems in time-sharing systems. Although the results obtained agreed closely with those obtained at other installations, work in this area has been suspended because the CTSS program proved too inflexible to permit much further investigation without considerable reprogramming effort.

W. J. Bouknight

[†]Portions of this work were supported by the National Science Foundation under Grant NSF GK-36.

13. NETWORK AND COMMUNICATION NETS

M. E. Van Valkenburg
W. Mayeda*
T. Kamae

T. Murata
J. A. Resh
G. H. Stumpff

S. Toida
T. N. Trick
N. Wax*

13.1 Some Periodic Solutions of the Lienard Equation[†]

Oscillations described by the generalized Lienard equation $\ddot{x} + f(x)\dot{x} + g(x) = 0$ have been investigated in the Lienard plane. When $f(x)$, $g(x)$, and $F(x) = \int_0^x f(\xi)d\xi$ are subject to certain restrictions, a number of analytic curves have been obtained in this plane which serve as bounds on solution trajectories. Piece-wise connection of such bounding curves provides explicit annular regions with the property that solution trajectories on the boundary of an annulus move to the interior with increasing time, t . The Poincare-Bendixson theorem then guarantees that at least one periodic orbit exists within such an annulus. Particular attention has been given to damping functions, $f(x)$, which are asymmetric.

N. Wax

13.2 Stability of Nonlinear Networks[†]

We are concerned with the stability of linear time-invariant networks which contain periodic sources and a nonlinear element whose first and second derivatives are defined over a certain allowable operating range of the device. By stability we mean that there exists a unique

*On leave.

[†]Portions of this work were supported by the Air Force Office of Scientific Research under Grant No. AFOSR 931.65.

steady-state periodic solution with the same period as the sources and all transients decay to this unique steady-state solution. The above problem has been studied by others and results obtained.¹ However, their sufficient condition for stability was proved to be highly conservative.² In the previous progress report a new criterion was reported which, hopefully, would not be quite so conservative.

In the past few months the example of Fig. 13.1 was considered in order to compare the two stability criteria. The quantity C_d is the varactor diode capacitance at the bias point and $R(q(t))$ is the nonlinear remainder. The circuit can go into subharmonic oscillations provided $|E|$, the amplitude of the pump voltage, is made large enough. From the above definition of stability we see that the subharmonic states are unstable.

Applying the conservative stability results,¹ it was determined that if $|E| \leq 0.088$ then the network would be stable in the above sense. However, our new stability criterion yielded the result that if $|E| \leq 0.103$ then the network would be stable. Thus, a 17% increase in the allowable pump voltage is tolerated. This result indicates that our new stability criterion is somewhat better; unfortunately, it is still too conservative and also very difficult to compute.

¹B. J. Leon and D. R. Anderson, "The Stability of Pumped Non-linear Reactance Circuits," IEEE Trans. on Circuit Theory, CT-10, 468, December, 1963. [Correction in CT-12, 143.]

²B. J. Leon, T. N. Trick, and T. C. Huang, "Prediction of Anomalous Behavior in Nonlinear Frequency Converters," Proc. NEC, Vol. XIX, pp. 456-460 (October, 1963).

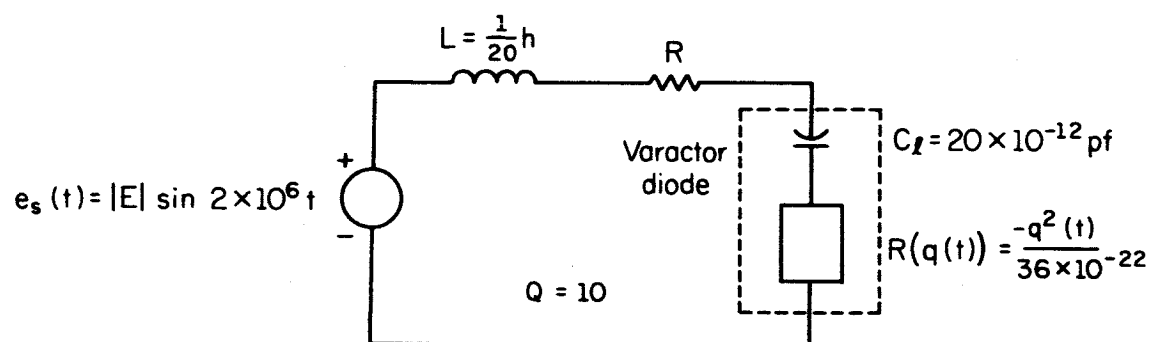


Fig. 13.1. Varactor Diode Circuit with dc Bias Terms Removed.

In view of the above results a perturbation approach was tried. It was assumed that the network was in the steady state and at some time t_0 the input was perturbed by some small amount. In order to be stable, the transients caused by the perturbation should decay such that the response, in the steady state, is periodic with the same period as the input. A sufficient condition has been determined such that the transients do indeed decay to the desired response. Applying this criterion to the above problem it was found that if $|E| \leq 1.0$ then the network is stable to "small" perturbations. Also, the computations involved were considerably less difficult. Note that the upper bound on $|E|$ has been increased by a factor of "ten."

Next, experimental results will be compared to our perturbational stability criterion before a complete report is written on the work.

T. N. Trick

13.3 On a Minimum Feedback Arc Set

The investigation of a minimum feedback arc set³ of a directed graph (in short, digraph) has been continued. New results obtained so far include the following.

13.3.1 Partition Not Affecting the Minimumness. A digraph in question may sometimes be too large to handle. We must, then, partition a digraph in some way. The best partition in this case is the one which

³D. H. Younger, "Minimum Feedback Arc Sets for a Directed Graph," IEEE Trans. on Circuit Theory, CT-10, pp. 238-245, June, 1963. See also Progress Report for September, October, November, 1965 (CSL, University of Illinois), pp. 98-99.

does not affect the minimumness of a feedback arc set. Two directed edges (diedges) $e(v_1, v_2)$ and $e(v_3, v_4)$ are strongly cyclic diedge connected if there exists a sequence P of directed circuits

$$P = C_1, C_2, \dots, C_k,$$

with $e(v_1, v_2) \in C_1$, $e(v_3, v_4) \in C_k$ such that each consecutive pair has at least one diedge in common. The totality of diedges which are strongly cyclic diedge connected to a diedge e_0 is called a lobe $M(e_0)$. Then a lobe $M(e_0)$ is an equivalence class containing diedge e_0 . By using this concept we have the next theorem.

Theorem: Let $M(e_1), M(e_2), \dots, M(e_n)$ be all distinct lobes of a given digraph G , and let F_1, F_2, \dots, F_n be minimum feedback arc sets of the corresponding lobes. Then the F_i 's are disjoint and their union is a minimum feedback arc set of G .

13.3.2. Topological Properties. A feedback arc set is said to be minimal if it is not a feedback arc set with the removal of a diedge from it. We can prove that a feedback arc set F is minimal if and only if, for any diedge $e(v_j, v_i)$ in F , there exists a directed path from vertices v_i to v_j which does not contain any element of F .

13.3.3 Bounds on the Order of a Minimum Feedback Arc Set. Let (C_1, C_2, \dots, C_r) be a maximum set of edge-disjoint directed circuits of G . Then, from 13.3.2 above, the order of a minimum feedback arc set F_m is greater than or equal to r . Let q be the number of vertices of G . Then the order of a minimum feedback arc set of the bi-complete graph

corresponding to G is $q(q-1)/2$. Therefore, we have the following theorem:

Theorem: $r \leq |F_m| \leq q(q-1)/2$.

T. Kamae

13.4 Linear Graphs in the Study of Reliability

The coefficient problem for terms of the reliability R_{ij} between two nodes of an arbitrary undirected R-net has been solved by introducing the concept of directed reliability. A directed \bar{R} -net, D , is defined in which two distinct component reliabilities are associated with each pair of nodes m, n of the original R-net, (r_{mn} from m to n and r_{nm} from n to m ($r_{nm} \neq r_{mn}$) both on $[0,1]$). The writer has shown that $\bar{R}_{ij}(r's)$ for this R-net, D , has the following interesting properties.

Assuming all cancellation within $\bar{R}_{ij}(r's)$ has been performed; then:

1. No term of \bar{R}_{ij} will contain a directed circuit or self loop.
2. Every term of \bar{R}_{ij} will have a coefficient of plus or minus one.
3. The sign of each term will be $(-1)^{e-n+1}$, where e is the number of edges (edge values) in the given term and $n(e)$ is the number of nodes on which these e edges terminate.

The transition from the directed net to the undirected net simply requires setting $r_{mn} = r_{nm}$ for each pair of nodes n , in D . If this procedure is performed for one pair of nodes at a time, then, for the first such transition, coefficients of plus or minus two will appear

in R_{ij} in addition to those of plus or minus one for the remaining edges (the sign still being determined as in (3) above). The second transition can produce coefficients of plus or minus 2, 3, or 4. In general, if there are n pairs, the largest coefficient (in magnitude) will be $2n$.

G. Stumpff

13.5 A Generating Function for R_{ij}

Given an R-net, R , either directed or undirected, and a corresponding R_{ij} (r 's) with nodes i and j in R , a generating function E for R_{ij} can be defined on the set P of all paths i to j as a recursion relation as follows:

Let the paths p_i of P be ordered arbitrarily ($i=1,2,\dots,n$). (Note each p_i is a product of the edge reliabilities of all edges in the i^{th} path.) Define the $*$ operation as ordinary multiplication but with the idempotent property (e.g., $abc*bcd=abcd$). Then for p_i in P

$$\begin{aligned} R_{ij} = E(P) &= \sum_{i=1}^n E(p_i) = p_n * (1 - \sum_{l=1}^{n-1} E(p_l)) + \sum_{l=1}^{n-1} E(p_l) = p_n * (E(p_1))' + \sum_{l=1}^{n-1} E(p_l) , \\ &= p_n + p_n' * \sum_{l=1}^{n-1} E(p_l) \end{aligned}$$

in which $(E)' = (1-E)$ and $p_n' = 1 - p_n$. The above equations simply give three alternate forms of expressing $\sum_{l=1}^n E$. Additional properties of E are:

$$\sum_{l=1}^1 E(p_i) = p_1; E(\emptyset) = 0; E(1) = 1; E(P_j) = 1 \text{ if for some } i, p_i = 1; p_i \in P_j \in P ,$$

$$E(P_j) * E(P_j) = E(P_j), \text{ and } (E(P_j))' * (E(P_j))' = (E(P_j))' ,$$

$$E(P_i * P_j) = E(P_i) + E(P_j) - E(P_i) * E(P_j) ,$$

$$E(P_j) * (E(P_j))' = 0 .$$

If we expand the domain of E to include the set S of all cutsets i to j , then the unreliability Q_{ij} (which is $1 - R_{ij}$) can be obtained as in the first equation above by replacing R_{ij} with Q_{ij} and P with S , etc. Further the "orthogonality" between cutsets and paths $i-j$ are reflected by the fact that $E(P_i) * E(S_j) = 0$, where P_i is a subset of P and S_j is any subset of S . Also $E(P) + E(S) = 1$.

G. Stumpff

13.6 Multistage Communication[†]

In an earlier report we described some communication net models for a class of two-stage communication systems, i.e., systems in which information transfer from one user to another is useless (or impossible or merely impractical) without the mediation of a processing stage ("censor"). One of those models, appropriate for systems characterized by noninteraction of the information flows preceding and following the processing stage, was seen not to require consideration of multicommodity flows. This allowed us, in the single-censor case, to obtain explicit expressions for the user-to-user terminal capacities in the model. This analysis result has now been extended to two-stage nets containing an arbitrary number of processing centers (censors). The work is the subject

[†]Portions of this work were supported by the Air Force Office of Scientific Research under Grant No. AFOSR 931.65.

of "Introduction and Analysis of a Model for Two-Stage Communication," a paper submitted for presentation at the Ninth Midwest Symposium on Circuit Theory.

J. Resh

13.7 The State Axioms in System Theory[†]

Both Zadeh⁴ and Kalman⁵ have formulated axiomatic definitions for the notion of state descriptions in the context of very general classes of systems. These definitions are presumably intended (and, in any event, should be required) to embody as much as possible of the substance of the ad hoc definitions for various special classes of systems. We have shown that, in addition to admitting system descriptions which would pass as state descriptions in the ordinary senses of the word, both of these definitions admit an extremely degenerate state description for any system. The existence of this degenerate description manifests a syndrome of flaws in Zadeh's and Kalman's definitions.

This problem and its resolution are the subject of CSL report R-282, now available for distribution.

J. Resh

[†]Portions of this work were supported by the Air Force Office of Scientific Research under Grant No. AFOSR 931.65.

⁴L. A. Zadeh, "The Concept of State in System Theory," Views on General System Theory (ed. M. D. Mesarovic), Ch. 3 (John Wiley & Sons, Inc., New York, 1964).

⁵R. E. Kalman, "Mathematical Description of Linear Dynamical Systems," J. SIAM Cont., Ser. A, 1, 152 (1963).

13.8 Topological Method for Stability Analysis of Linear Time-Varying Networks

In this work, the stability of linear time-varying networks is investigated in terms of the topology of the networks. It is shown that sufficient conditions for stability of general RLC time-varying networks can be formulated in terms of the summations of chord-set products of certain resistive n-ports derived from an original network. A similar approach makes it possible to express the coefficients of characteristic polynomials of the A-matrices of RC and RL time-varying networks in terms of topological quantities. Thus topological necessary and sufficient conditions for stability of periodically time-varying RC and RL networks are obtained by use of a time-dependent Hurwitz criterion.

T. Murata

13.9 Realizable Switching Conditions

A necessary and sufficient condition for given switching functions to be realizable is established. In the following only the theorems that lead to the final result together with one application are given. Further discussion is given in CSL report R-279.

Theorem 1: Given switching functions F_{ab} and F_{bc} between any two of three vertices a , b , and c in the contact network, the third switching function that is F_{ac} must satisfy the following equation:

$$F_{ac} + F_{ab} \cdot F_{bc} = F_{ac}$$

where "." and "+" are Boolean multiplication and addition, respectively.

Theorem 2: For three given switching functions F_{ab} , F_{bc} and F_{ca} , there exists a contact network containing vertices a , b and c such that switching functions between two of a , b and c are F_{ab} , F_{bc} and F_{ca} if and only if

$$F_{ab} + F_{bc} \cdot F_{ca} = F_{ab}$$

$$F_{bc} + F_{ca} \cdot F_{ab} = F_{bc}$$

$$F_{ca} + F_{ab} \cdot F_{bc} = F_{ca} .$$

Theorem 3: Let F_{ab} be a switching function between a and b . Also let $F_{ac}, F_{cd}, \dots, F_{ma}$ be switching functions between any two vertices in a path between a and b . Then

$$F_{ab} + F_{bc} \cdot F_{cd} \cdot \dots \cdot F_{ma} = F_{ab} .$$

Definition 1: Let $\{F_{ab}\}$ be a set of given switching functions. Then a corresponding network of $\{F_{ab}\}$ is a contact network formed by connecting an edge between vertex a and vertex b whose weight is F_{ab} for all F_{ab} .

Theorem 4: Switching functions are realizable if and only if for all possible paths between any two adjacent vertices in the corresponding graph the following relation holds:

$$F_{ab} + F_{ab}' = F_{ab}$$

where F_{ab} is a given switching function between vertex a and vertex b .

F_{ab}' is the Boolean sum of all possible path products between vertex a and vertex b less F_{ab} .

Theorem 5 (Application): If given switching functions are single-contact functions then for any three vertices a , b and c in the contact network the following equation holds:

$$F_{ab} \oplus F_{bc} = F_{ac}$$

where $X_i \otimes X_j = X_i \cdot X_j$ if $X_i \neq X_j$

$$X_i \otimes X_j = 1 \text{ if } X_i = X_j$$

and X_i 's are Boolean variables in F_{ab} , etc.

S. Toida

13.10 Flows in Communication Nets[†]

We are attempting to find conditions for simultaneous flows in a communication net. It is known that flow patterns are more important than a maximum terminal flow when simultaneous flows are involved. We have found a relationship between a set of cutsets and a relatively optimum flow which will be presented at the 3rd Colloquium on Microwave Communications in Budapest in April.

A condition for the absolutely optimum flow has not yet been found. However, the absolutely optimum flow is one of the relatively optimum flows. Hence it may not be necessary to find conditions and methods of obtaining absolutely optimum flow in order to find conditions for simultaneous flows. It is easily seen that there exists a relationship between cutsets and simultaneous flows. It is also clear that the

[†]Portions of this work were supported by the Air Force Office of Scientific Research under Grant No. AFOSR 931.65.

conditions for multi-flows are special cases of those for simultaneous flows. Thus such conditions must have something to do with cut sets. Several results have been found relating to this conclusion.

W. Mayeda

13.11 Computer Generation of Complete Trees[†]

One way of analyzing active networks by computers is to find all possible complete trees. Many networks whose voltage (or current) graph has a large number of trees have only a few complete trees. Hence it is very important to find a method of generating only complete trees without requiring excessive computer time. It has been found that when t_0 and t_1 are complete trees such that

$$t_0 - t_1 = \{a_1 a_2 \cdots a_n\},$$

and

$$t_1 - t_0 = \{e_1 e_2 \cdots e_n\},$$

then in order that there exist no complete tree t_1' such that

$$t_0 - t_1' = \{a_1' a_2' \cdots a_m'\},$$

and

$$t_1' - t_0 = \{e_1' e_2' \cdots e_m'\},$$

where $\{a_1' a_2' \cdots a_m'\}$ and $\{e_1' e_2' \cdots e_m'\}$ are proper subsets of $\{a_1 a_2 \cdots a_n\}$ and $\{e_1 e_2 \cdots e_n\}$, respectively, the following conditions must be satisfied:

[†]Portions of this work were supported by the Air Force Office of Scientific Research under Grant No. AFOSR 931.65.

$$e_i \in \{S_{a_i}(t_0) - \bigcup_{\substack{p=1 \dots n \\ p \neq i}} S_{a_p}(t_0)\} ,$$

for all $i = 1, 2, \dots, n$. When no such tree t_1' exists, the transformation from t_0 to t_1 by

$$t_1 = t_0 \oplus \{a_1 a_2 \dots a_n e_1 e_2 \dots e_n\}$$

is called an elementary complete tree transformation. It is believed that the generation of complete trees may be obtained by modifying this elementary complete-tree transformation.

W. Mayeda

Distribution list as of March 1, 1965

1 Dr. Chalmers Sherwin Deputy Director (Research & Technology) DD&RE Rm 3E1060 The Pentagon Washington, D. C. 20301	1 Commanding Officer U. S. Army Security Agency Arlington Hall Arlington, Virginia 22212	1 Director U. S. Army Electronics Laboratories Fort Monmouth, New Jersey 07703 Attn: ANSEL-RD-PE	1 Commanding Officer Office of Naval Research Branch Office 1000 Geary Street San Francisco, California 94109
1 Dr. Edward M. Reilly Asst. Director (Research) Off. of Defense Res & Eng Department of Defense Washington, D. C. 20301	1 Commanding Officer U. S. Army Limited War Laboratory Aberdeen Proving Ground Aberdeen, Maryland 21005 Attn: Technical Director	1 Director U. S. Army Electronics Laboratories Fort Monmouth, New Jersey 07703 Attn: ANSEL-RD-FF	1 Commanding Officer U. S. Naval Weapons Laboratory Asst. Director for Computation Dahlgren, Virginia 22448 Attn: G. H. Gleissner (Code K-4)
1 Dr. James A. Ward Office of Deputy Director (Research and Information Rm 3D1037) Department of Defense The Pentagon Washington, D. C. 20301	1 Commanding Officer Human Engineering Laboratories Aberdeen Proving Ground, Maryland 21005	1 Director U. S. Army Electronics Laboratories Fort Monmouth, New Jersey 07703 Attn: ANSEL-RD-PR	1 Inspector of Naval Material Bureau of Ships Technical Representative 1902 West Minnehaha Avenue St. Paul 4, Minnesota
1 Director Advanced Research Projects Agency Department of Defense Washington, D. C. 20301	1 Director U. S. Army Engineer/Geodesy, Intelligence and Mapping, Research & Devel. Agency Fort Belvoir, Virginia 22060	1 Director U. S. Army Electronics Laboratories Fort Monmouth, New Jersey 07703 Attn: ANSEL-RL-GF	5 Lt. Col. E. T. Gaines, SREE Chief, Electronics Division Directorate of Engineering Sciences Air Force Office of Scientific Research Washington, D. C. 20333
1 Mr. Charles Yost, Director for Materials Sciences Advanced Research Projects Agency Department of Defense Washington, D. C. 20301	1 Commandant U. S. Army Command and General Staff College Fort Leavenworth, Kansas 66207 Attn: Secretary	1 Director U. S. Army Electronics Laboratories Fort Monmouth, New Jersey 07703 Attn: ANSEL-RD-ADT	1 Director of Science & Technology Deputy Chief of Staff (R & D) USAF Washington, D. C. Attn: AFEST-EL/GU
20 Defense Documentation Center Cameron Station, Bldg. 5 Alexandria, Virginia 22314 Attn: TISIA	1 Dr. H. Rohl, Deputy Director U. S. Army Research Office (Durham) Box CM, Duke Station Durham, North Carolina 27706	1 Director U. S. Army Electronics Laboratories Fort Monmouth, New Jersey 07703 Attn: ANSEL-RD-FUM1	1 Director of Science & Technology Deputy Chief of Staff (R & D) USAF Washington, D. C. Attn: AFEST-SC
1 Director National Security Agency Fort George G. Meade, Maryland 20755 Attn: Librarian C-332	1 Commanding Officer U. S. Army Research Office (Durham) P. O. Box CM, Duke Station Durham, North Carolina 27706 Attn: CRD-AA-IP (Richard O. Uish)	1 Commanding Officer U. S. Army Electronics R&D Activity Fort Huachuca, Arizona 85163	1 Karl M. Fuechsel Electronics Division Director of Engineering Sciences Air Force Office of Scientific Research Washington, D. C. 20333
1 Chief of Research and Development Headquarters, Department of the Army Washington, D. C. 20310 Attn: Physical Sciences Division P & E	1 Commanding General U. S. Army Electronics Command Fort Monmouth, New Jersey 07703 Attn: ANSEL-SC	1 Commanding Officer U. S. Army Electronics Lab Activity White Sands Missile Range New Mexico 86002	1 Lt. Col. Edwin M. Myers Headquarters, USAF (AFRDR) Washington 25, D. C.
1 Chief of Research and Development Headquarters, Department of the Army Washington, D. C. 20310 Attn: Mr. L. H. Geiger, Rm 34442	1 Director U. S. Army Electronics Laboratories Fort Monmouth, New Jersey 07703 Attn: Dr. S. Benedict Levin, Director Institute for Exploratory Research	1 Director Human Resources Research Office The George Washington University 300 N. Washington Street Alexandria, Virginia	1 Director, Air University Library Maxwell Air Force Base Alabama 36112 Attn: CR-4803a
1 Research Plans Office U. S. Army Research Office 3045 Columbia Pike Arlington, Virginia 22204	1 Director U. S. Army Electronics Laboratories Fort Monmouth, New Jersey 07703 Attn: Mr. Bohart O. Barber, Executive Secretary, JSTAC (ANSEL-RD-X)	1 Commanding Officer U. S. Army Personnel Research Office Washington 25, D. C.	1 Commander Research & Technology Division AFSC (Mr. Robert L. Feik) Office of the Scientific Director Bolling AFB 25, D. C.
1 Commanding General U. S. Army Materiel Command Attn: AMCRD-RS-PE-E Washington, D. C. 20315	1 Superintendent U. S. Military Academy West Point, New York 10996	1 Commanding Officer U. S. Army Medical Research Laboratory Fort Knox, Kentucky	1 Commander Research & Technology Division Office of the Scientific Director Bolling AFB 25, D. C. Attn: RTHR
1 Commanding General U. S. Army Strategic Communications Command Washington, D. C. 20315	1 The Walter Reed Institute of Research Walter Reed Army Medical Center Washington, D. C. 20012	1 Commanding General U. S. Army Signal Center and School Attn: Chief, Office of Academic Operations Fort Monmouth, New Jersey 07703	1 Commander Air Force Cambridge Research Laboratories Attn: Research Library CROMEL-R L. G. Hanscom Field Bedford, Massachusetts 01731
1 Commanding Officer U. S. Army Materials Research Agency Watertown Arsenal Watertown, Massachusetts 02172	1 Director U. S. Army Electronics Laboratories Fort Monmouth, New Jersey 07703 Attn: ANSEL-RD-DR	2 Dr. Richard H. Wilcox, Code 437 Department of the Navy Washington, D. C. 20360	1 Dr. Lloyd Hollingsworth AFRL L. G. Hanscom Field Bedford, Massachusetts 01731
1 Commanding Officer U. S. Army Ballistics Research Lab. Aberdeen Proving Ground Aberdeen, Maryland 21005 Attn: V. W. Richards	1 Director U. S. Army Electronics Laboratories Fort Monmouth, New Jersey 07703 Attn: ANSEL-RD-X	1 Chief, Bureau of Weapons Attn: Technical Library, DL1-3 Department of the Navy Washington, D. C. 20360	1 Commander Air Force Cambridge Research Laboratories Attn: Data Sciences Lab (Lt. S. J. Kahne, CRB) L. G. Hanscom Field Bedford, Massachusetts 01731
1 Commanding Officer U. S. Army Ballistics Research Lab. Aberdeen Proving Ground Aberdeen, Maryland 21005 Attn: Kests A. Pullen, Jr.	1 Director U. S. Army Electronics Laboratories Fort Monmouth, New Jersey 07703 Attn: ANSEL-RD-XE	1 Chief, Bureau of Ships Department of the Navy Washington, D. C. 20360 Attn: Code 680	1 Commander Air Force Systems Command Office of the Chief Scientist (Mr. A. G. Wimer) Andrews AFB, Maryland 20331
1 Commanding Officer U. S. Army Ballistics Research Lab. Aberdeen Proving Ground Aberdeen, Maryland 21005 Attn: George C. Francis, Computing Lab.	1 Director U. S. Army Electronics Laboratories Fort Monmouth, New Jersey 07703 Attn: ANSEL-RD-KC	1 Chief, Bureau of Ships Department of the Navy Washington, D. C. 20360 Attn: Code 732	1 Commander Air Force Missile Development Center Attn: MDSGO/Major Harold Wheeler, Jr. Holloman Air Force Base, New Mexico
1 Commandant U. S. Army Air Defense School P. O. Box 9390 Fort Bliss, Texas 79916 Attn: Missile Sciences Div., C&S Dept.	1 Director U. S. Army Electronics Laboratories Fort Monmouth, New Jersey 07703 Attn: ANSEL-RD-NR	1 Commander Naval Electronics Laboratory San Diego, California 92052 Attn: Code 2222(Library)	1 Commander Research & Technology Division Attn: MAYT (Mr. Evans) Wright-Patterson Air Force Base Ohio 45433
1 Commanding General U. S. Army Missile Command Redstone Arsenal, Alabama 35809 Attn: Technical Library	1 Director U. S. Army Electronics Laboratories Fort Monmouth, New Jersey 07703 Attn: ANSEL-RD-NE	1 Commanding Officer Naval Electronics Laboratory San Diego, California 92052 Attn: Code 2800, C. S. Manning	1 Directorate of Systems Dynamics Analysis Aeronautical Systems Division Wright-Patterson AFB, Ohio 45433
1 Commanding General Frankford Arsenal Philadelphia, Pa. 19137 Attn: SMUFA-1310 (Dr. Sidney Ross)	1 Director U. S. Army Electronics Laboratories Fort Monmouth, New Jersey 07703 Attn: ANSEL-RD-NO	1 Director Naval Research Laboratory Washington, D. C. 20390 Attn: Technical Information Office (Code 2000)	1 Hqs. Aeronautical Systems Division AF Systems Command Attn: Navigation & Guidance Laboratory Wright-Patterson AFB, Ohio 45433
1 Commanding General Frankford Arsenal Philadelphia, Pa. 19137 Attn: SMUFA-1300	1 Director U. S. Army Electronics Laboratories Fort Monmouth, New Jersey 07703 Attn: ANSEL-RD-NP	6 Director Naval Research Laboratory Washington, D. C. 20390 Attn: Technical Information Office (Code 2000)	1 Commander Rome Air Development Center Attn: Documents Library, RAALD Griffiss Air Force Base Rome, New York 13442
1 U. S. Army Munitions Command Picatinny Arsenal Dover, New Jersey 07801 Attn: Technical Information Branch	1 Director U. S. Army Electronics Laboratories Fort Monmouth, New Jersey 07703 Attn: ANSEL-RD-SA	1 Commanding Officer Office of Naval Research Branch Office 219 S. Dearborn Street Chicago, Illinois 60604	1 Commander Rome Air Development Center Attn: RAWI-Major W. H. Hayris Griffiss Air Force Base Rome, New York 13442
1 Commanding Officer Harry Diamond Laboratories Connecticut Ave. & Van Ness St., N.W. Washington, D. C. 20438 Attn: Mr. Berthold Altman	1 Director U. S. Army Electronics Laboratories Fort Monmouth, New Jersey 07703 Attn: ANSEL-RD-SE	1 Chief of Naval Operations Department of the Navy Washington, D. C. 20350 Attn: OP-072	1 Lincoln Laboratory Massachusetts Institute of Technology P. O. Box 73 Lexington 73, Massachusetts Attn: Library A-082
1 Commanding Officer Harry Diamond Laboratories Attn: Library Connecticut Ave. & Van Ness St., N.W. Washington, D. C. 20438	1 Director U. S. Army Electronics Laboratories Fort Monmouth, New Jersey 07703 Attn: ANSEL-RD-SR	1 Chief of Naval Operations Department of the Navy Washington, D. C. 20350 Attn: OP-03EG	
	1 Director U. S. Army Electronics Laboratories Fort Monmouth, New Jersey 07703 Attn: ANSEL-RD-SS		

Continued next page

Distribution list as of March 1, 1965 (Cont'd.)

- 1 Lincoln Laboratory
Massachusetts Institute of Technology
P. O. Box 73
Lexington 73, Massachusetts
Attn: Dr. Robert Kingston
- 1 AFCC (PCART)
Eglin Air Force Base
Florida
- 1 Mr. Alan Barnum
Rome Air Development Center
Griffiss Air Force Base
Rome, New York 13442
- 1 Director
Research Laboratory of Electronics
Massachusetts Institute of Technology
Cambridge, Massachusetts 02139
- 1 Polytechnic Institute of Brooklyn
55 Johnson Street
Brooklyn, New York 11201
Attn: Mr. Jerome Fox
Research Coordinator
- 1 Director
Columbia Radiation Laboratory
Columbia University
538 West 120th Street
New York, New York 10027
- 1 Director
Coordinated Science Laboratory
University of Illinois
Urbana, Illinois 61803
- 1 Director
Stanford Electronics Laboratories
Stanford University
Stanford, California
- 1 Director
Electronics Research Laboratory
University of California
Berkeley 4, California
- 1 Professor A. A. Dougal, Director
Laboratories for Electronics and Related
Science Research
University of Texas
Austin, Texas 78712
- 1 Professor J. K. Aggarwal
Department of Electrical Engineering
University of Texas
Austin, Texas 78712
- 1 Director of Engineering & Applied Physics
210 Pierce Hall
Harvard University
Cambridge, Massachusetts 02138
- 1 Capt. Paul Johnson (USN Ret.)
National Aeronautics & Space Agency
1520 H. Street, N. W.
Washington 25, D. C.
- 1 NASA Headquarters
Office of Applications
400 Maryland Avenue, S.W.
Washington 25, D. C.
Attn: Code FC Mr. A. M. Greg Andrus
- 1 National Bureau of Standards
Research Information Center and Advisory
Serv. on Info. Processing
Data Processing Systems Division
Washington 25, D. C.
- 1 Dr. Wallace Sinaiko
Institute for Defense Analyses
Research & Eng. Support Div.
1666 Connecticut Avenue, N. W.
Washington 9, D. C.
- 1 Data Processing Systems Division
National Bureau of Standards
Conn. at Van Ness
Room 239, Bldg. 10
Washington 25, D. C.
Attn: A. K. Smailow
- 1 Exchange and Gift Division
The Library of Congress
Washington 25, D. C.
- 1 Dr. Alan T. Waterman, Director
National Science Foundation
Washington 25, D. C.
- 1 H. E. Cochran
Oak Ridge National Laboratory
P. O. Box X
Oak Ridge, Tennessee
- 1 U. S. Atomic Energy Commission
Office of Technical Information Extension
P. O. Box 62
Oak Ridge, Tennessee
- 1 Mr. C. D. Watson
Defense Research Member
Canadian Joint Staff
2450 Massachusetts Avenue, N. W.
Washington 8, D. C.
- 1 Martin Company
P. O. Box 5817
Orlando, Florida
Attn: Engineering Library MP-30
- 1 Laboratories for Applied Sciences
University of Chicago
6220 South Drexel
Chicago, Illinois 60637
- 1 Librarian
School of Electrical Engineering
Purdue University
Lafayette, Indiana
- 1 Donald L. Epley
Dept. of Electrical Engineering
State University of Iowa
Iowa City, Iowa
- 1 Instrumentation Laboratory
Massachusetts Institute of Technology
68 Albany Street
Cambridge 39, Massachusetts
Attn: Library WI-109
- 1 Sylvania Electric Products, Inc.
Electronics System
Waltham Labs. Library
100 First Avenue
Waltham 54, Massachusetts
- 2 Hughes Aircraft Company
Centinela and Teale Streets
Culver City, California
Attn: K. C. Rosenberg, Supervisor
Company Technical Document Center
- 3 Autonetics
9150 East Imperial Highway
Downey, California
Attn: Tech. Library, 3041-11
- 1 Dr. Arnold T. Nordsieck
General Motors Corporation
Defense Research Laboratories
6767 Hollister Avenue
Goleta, California
- 1 University of California
Lawrence Radiation Laboratory
P. O. Box 808
Livermore, California
- 1 Mr. Thomas L. Hartwick
Aerospace Corporation
P. O. Box 95085
Los Angeles 45, California
- 1 Lt. Col. Willard Levin
Aerospace Corporation
P. O. Box 95085
Los Angeles 45, California
- 1 Sylvania Electronic Systems-West
Electronic Defense Laboratories
P. O. Box 205
Mountain View, California
Attn: Documents Center
- 1 Varian Associates
611 Hansen Way
Palo Alto, California 94303
Attn: Tech. Library
- 1 Huston Denlow
Library Supervisor
Jet Propulsion Laboratory
California Institute of Technology
Pasadena, California
- 1 Professor Nicholas George
California Institute of Technology
Electrical Engineering Department
Pasadena, California
- 1 Space Technology Labs., Inc.
One Space Park
Redondo Beach, California
Attn: Acquisitions Group
STL Technical Library
- 1 The Rand Corporation
1700 Main Street
Santa Monica, California
Attn: Library
- 1 Miss F. Cloak
Radio Corp. of America
RCA Laboratories
David Sarnoff Research Center
Princeton, New Jersey
- 1 Mr. A. A. Lundstrom
Bell Telephone Laboratories
Room 2E-127
Whippany Road
Whippany, New Jersey
- 1 Cornell Aeronautical Laboratory, Inc.
4455 Genesee Street
Buffalo 21, New York
Attn: J. P. Desmond, Librarian
- 1 Sperry Gyroscope Company
Marine Division Library
155 Glenn Cove Road
Carle Place, L. I., New York
Attn: Miss Barbara Judd
- 1 Library
Light Military Electronics Dept.
General Electric Company
Armament & Control Products Section
Johnson City, New York
- 1 Dr. E. Howard Holt
Director
Plasma Research Laboratory
Rensselaer Polytechnic Institute
Troy, New York
- 1 Battelle-DEFENDER
Battelle Memorial Institute
505 King Avenue
Columbus 1, Ohio
- 1 Laboratory for Electroscience Research
New York University
University Heights
Bronx 53, New York
- 1 National Physical Laboratory
Teddington, Middlesex
England
Attn: Dr. A. M. Utley, Superintendent,
Autonomics Division
- 1 Dr. Lee Huff
Behavioral Sciences
Advanced Research Projects Agency
The Pentagon (Room 3E175)
Washington, D. C. 20301
- 1 Dr. Glenn L. Bryan
Head, Personnel and Training Branch
Office of Naval Research
Navy Department
Washington, D. C. 20360
- 1 Instituto de Fisica Aplicada
"L. Torres Quevedo"
High Vacuum Laboratory
Madrid, Spain
Attn: Jose L. de Segovia
- 1 Stanford Research Institute
Attn: G-037 External Reports
(for J. Goldberg)
Menlo Park, California 94025

REVISED U. S. ARMY DISTRIBUTION LIST

(As received at the Coordinated Science Laboratory 27 July 1965)

- | | | |
|--|--|---|
| 1 Dr. Chalmers Sherwin
Deputy Director (Research & Technology)
DD&RE Rm 3E1060
The Pentagon
Washington, D. C. 20301 | 1 Commanding General
Frankford Arsenal
Attn: SMUFA-1300
Philadelphia, Pennsylvania 19137 | 1 Director
Institute for Exploratory Research
U. S. Army Electronics Command
Attn: Mr. Robert O. Parker, Executive
Secretary, ISTAC (AMSEL-XL-D)
Fort Monmouth, New Jersey 07703 |
| 1 Dr. Edward M. Reilley
Asst. Director (Research)
Ofc. of Defense Res. & Eng.
Department of Defense
Washington, D. C. 20301 | 1 U. S. Army Munitions Command
Attn: Technical Information Branch
Picatinny Arsenal
Dover, New Jersey 07801 | 1 Commanding General
U. S. Army Electronics Command
Fort Monmouth, New Jersey 07703 |
| 1 Dr. James A. Ward
Office of Deputy Director (Research
and Information Rm 3D1037)
Department of Defense
The Pentagon
Washington, D. C. 20301 | 1 Commanding Officer
Harry Diamond Laboratories
Attn: Mr. Berthold Altman
Connecticut Avenue and Van Ness St., N.W.
Washington, D. C. 20438 | Attn: AMSEL-SC
RD-D
RD-G
RD-MAF-I
RD-MAT
RD-GF
RD-MN (Marine Corps Ln0)
XL-D
XL-E
XL-C
XL-S
HL-D
HL-L
HL-J
HL-P
HL-O
HL-R
NL-D
NL-A
NL-P
NL-R
NL-S
KL-D
KL-E
KL-S
KL-T
VL-D
WL-D |
| 1 Director
Advanced Research Projects Agency
Department of Defense
Washington, D. C. 20301 | 1 Commanding Officer
Harry Diamond Laboratories
Attn: Library
Connecticut Avenue and Van Ness St., N.W.
Washington, D. C. 20438 | |
| 1 Mr. E. I. Salkovitz, Director
for Materials Sciences
Advanced Research Projects Agency
Department of Defense
Washington, D. C. 20301 | 1 Commanding Officer
U. S. Army Security Agency
Arlington Hall
Arlington, Virginia 22212 | |
| 1 Colonel Charles C. Mack
Headquarters
Defense Communications Agency (333)
The Pentagon
Washington, D. C. 20305 | 1 Commanding Officer
U. S. Army Limited War Laboratory
Attn: Technical Director
Aberdeen Proving Ground
Aberdeen, Maryland 21005 | |
| 20 Defense Documentation Center
Attn: TISIA
Cameron Station, Building 5
Alexandria, Virginia 22314 | 1 Commanding Officer
Human Engineering Laboratories
Aberdeen Proving Ground, Maryland 21005 | |
| 1 Director
National Security Agency
Attn: Librarian C-332
Fort George G. Meade, Maryland 20755 | 1 Director
U. S. Army Engineer Geodesy,
Intelligence & Mapping
Research and Development Agency
Fort Belvoir, Virginia 22060 | 1 Mr. Charles F. Yost
Special Assistant to the Director
of Research
National Aeronautics & Space Admin.
Washington, D. C. 20546 |
| 1 U. S. Army Research Office
Attn: Physical Sciences Division
3045 Columbia Pike
Arlington, Virginia 22204 | 1 Commandant
U. S. Army Command and General Staff College
Attn: Secretary
Fort Leavenworth, Kansas 66207 | 1 Director
Research Laboratory of Electronics
Massachusetts Institute of Technology
Cambridge, Massachusetts 02139 |
| 1 Chief of Research and Development
Headquarters, Department of the Army
Attn: Mr. L. H. Gaiger, Rm 3D442
Washington, D. C. 20310 | 1 Dr. H. Robl, Deputy Chief Scientist
U. S. Army Research Office (Durham)
Box CM, Duke Station
Durham, North Carolina 27706 | 1 Polytechnic Institute of Brooklyn
55 Johnson Street
Brooklyn, New York 11201
Attn: Mr. Jerome Fox
Research Coordinator |
| 1 Research Plans Office
U. S. Army Research Office
3045 Columbia Pike
Arlington, Virginia 22204 | 1 Commanding Officer
U. S. Army Research Office (Durham)
Attn: CRD-AA-IP (Richard O. Uish)
Box CM, Duke Station
Durham, North Carolina 27706 | 1 Director
Columbia Radiation Laboratory
Columbia University
538 West 120th Street
New York, New York 10027 |
| 1 Commanding General
U. S. Army Materiel Command
Attn: AMCRD-RS-FE-E
Washington, D. C. 20315 | 1 Superintendent
U. S. Army Military Academy
West Point, New York 10996 | 1 Director
Stanford Electronics Laboratories
Stanford University
Stanford, California 94301 |
| 1 Commanding General
U. S. Army Strategic Communications Command
Washington, D. C. 20315 | 1 The Walter Reed Institute of Research
Walter Reed Army Medical Center
Washington, D. C. 20012 | 1 Director
Electronics Research Laboratory
University of California
Berkeley, California 94700 |
| 1 Commanding Officer
U. S. Army Materials Research Agency
Watertown Arsenal
Watertown, Massachusetts 02172 | 1 Commanding Officer
U. S. Army Electronics R&D Activity
Fort Huachuca, Arizona 85163 | 1 Director
Electronic Sciences Laboratory
University of Southern California
Los Angeles, California 90007 |
| 1 Commanding Officer
U. S. Army Ballistics Research Laboratory
Attn: V. W. Richards
Aberdeen Proving Ground
Aberdeen, Maryland 21005 | 1 Commanding Officer
U. S. Army Engineers R&D Laboratory
Attn: STINPO Branch
Fort Belvoir, Virginia 22060 | 1 Professor A. A. Dougal, Director
Laboratories for Electronics
and Related Science Research
University of Texas
Austin, Texas 78712 |
| 1 Commanding Officer
U. S. Army Ballistics Research Laboratory
Attn: Keats A. Pullen, Jr.
Aberdeen Proving Ground
Aberdeen, Maryland 21005 | 1 Commanding Officer
U. S. Army Electronics R&D Activity
White Sands Missile Range, New Mexico 88002 | 1 Professor J. K. Aggarwal
Department of Electrical Engineering
University of Texas
Austin, Texas 78712 |
| 1 Commanding Officer
U. S. Army Ballistics Research Laboratory
Attn: George C. Francis, Computing Lab.
Aberdeen Proving Ground, Maryland 21005 | 1 Director
Human Resources Research Office
The George Washington University
300 N. Washington Street
Alexandria, Virginia 22300 | 1 Division of Engineering and Applied Physics
210 Pierce Hall
Harvard University
Cambridge, Massachusetts 02138 |
| 1 Commandant
U. S. Army Air Defense School
Attn: Missile Sciences Division, C&S Dept.
P. O. Box 9390
Fort Bliss, Texas 79916 | 1 Commanding Officer
U. S. Army Personnel Research Office
Washington, D. C. | |
| 1 Commanding General
U. S. Army Missile Command
Attn: Technical Library
Redstone Arsenal, Alabama 35809 | 1 Commanding Officer
U. S. Army Medical Research Laboratory
Fort Knox, Kentucky 40120 | |
| 1 Commanding General
Frankford Arsenal
Attn: SMUFA-1310 (Dr. Sidney Ross)
Philadelphia, Pennsylvania 19137 | 1 Commanding General
U. S. Army Signal Center and School
Fort Monmouth, New Jersey 07703
Attn: Chief, Office of Academic Operations | |
| | 1 Dr. S. Benedict Levin, Director
Institute for Exploratory Research
U. S. Army Electronics Command
Fort Monmouth, New Jersey 07703 | |

Security Classification

DOCUMENT CONTROL DATA R&D

(Security classification of title, body of abstract and indexing annotation must be entered when the overall report is classified)

1. ORIGINATING ACTIVITY (Corporate author)		2a. REPORT SECURITY CLASSIFICATION	
University of Illinois Coordinated Science Laboratory Urbana, Illinois 61801		Unclassified	
3. REPORT TITLE		2b. GROUP	
PROGRESS REPORT FOR DECEMBER, 1965, JANUARY AND FEBRUARY, 1966			
4. DESCRIPTIVE NOTES (Type of report and inclusive dates)			
Quarterly progress report for period 1 Dec 1965 through 28 Feb 1966			
5. AUTHOR(S) (Last name, first name, initial)			
6. REPORT DATE		7a. TOTAL NO. OF PAGES	7b. NO. OF REFS.
April 1, 1966		125	
8a. CONTRACT OR GRANT NO.		9a. ORIGINATOR'S REPORT NUMBER(S)	
DA 28 043 AMC 00073(E) b. PROJECT NO. 20014501B31F			
c.		9b. OTHER REPORT NO(S) (Any other numbers that may be assigned this report)	
d.			
10. AVAILABILITY/ LIMITATION NOTICES			
Qualified requesters may obtain copies of this report from DDC. May be released to OTS.			
11. SUPPLEMENTARY NOTES		12. SPONSORING MILITARY ACTIVITY	
		Joint Services Electronics Program through U.S. Army Electronics Command Ft. Monmouth, New Jersey	
13. ABSTRACT			
<p>Studies of mechanical damping in possible gyro materials are reported along with studies of micrometeorite influence and the optimal choice of gyro diameter.</p> <p>Measurements of the scattering of electrons from the (100) surface of tungsten are reported. These measurements are interpreted in terms of the excitation of the vibrational states of surface atoms and in terms of the band structure. The experiments for the measurement of the angular distribution of particles scattered from surfaces and for the study of the adsorption-desorption kinetics of gases at surfaces are continuing. The status of these experiments is given.</p> <p>Operation statistics, new facilities for bubble-chamber processing, and new display equipment are reported.</p> <p>Several results were obtained in the continuing projects on the sensitivity problem, stability of nonlinear systems, optimization of systems with fixed control structure, and computer-oriented formulation of the optimal control problem. Bounds were obtained for sensitivity functions. Optimum regulator systems were found to be relatively insensitive. Some extensions of Popov's criterion were derived.</p>			

DD FORM 1473
1 JAN 64

Security Classification

13. ABSTRACT (continued)

Two "PLATO" university courses for credit are being given the second semester (LIB SCI 195 and EE 322). Three courses were completed by students during the fall term. Programming developments include an inquiry facility added to the new PLATO tutorial logic so that two different teaching methods for the electrical engineering course can be tried, a new logic for ARITHDRILL, a generalized program for the paired associate learning study, a program for a keyset design experiment, the first test program for the production of animated films for a language-free test of interpersonal norms, a general "messaging" program for use with group-interaction studies; and some initial SIRA routines for processing "dope" tapes (student response records). The twenty student-station circuitry-modernizing is nearing completion, a feasibility study of an audio feature for PLATO is being made, an investigation of the means for turning on and off the plasma display tube is underway as well as the construction of a new portable transistorized generator.

Final data for the pumping speeds of small diode and triode getter-ion pumps are given. Additional work on the conversion of O_2 to CO in vacuum systems has shown that the partial pressure of CO may be quite small in properly processed systems. The development of the Schuemann suppressor gauge is reviewed to the present, and a program of additional work intended to improve it still further is proposed.

Two methods of testing the accuracy of approximate solutions of the Boltzmann equation for a shock wave have been used to examine two different shock solutions. Enhanced diffusion resulting from the beam-plasma instability has been explored as a function of beam and plasma parameters. Experimental evidence has been obtained for the collisionless damping of Tonks-Dattner modes.

Progress is reported in studies of anisotropy of the energy gap in superconducting niobium and the superconducting parametric amplifier. The support of other activities of this group has been transferred to the Materials Research Laboratory.

Studies of the phenomenon of high-voltage breakdown are reviewed, and the theory of the melting of electrode projections is discussed. Predicted breakdown fields to produce melting are compared with experimental observations.

The state of the equipment to be used for size-effect measurements and for Hall mobility measurements in thin films is discussed.

Further progress has been made in all three areas of algebraic coding theory under investigation. A new investigation is initiated in digital addressing.

Further progress is reported on computer diagnosis studies, modular decompositions of sequential machines, the propagation of errors in finite-memory encoding/decoding schemes, and studies of quasi-linear machines. Progress is also reported on the problem of obtaining a realizable state model from an immittance matrix by node insertion. The study of time-shared computer systems has been suspended indefinitely. A new investigation on the generation of diagnostic tests for combinational logic nets has been started.

13. ABSTRACT (continued)

In the study of nonlinear systems, new bounds on the solution trajectories for the Lienard equation have been found, and a varactor diode circuit has been studied with respect to perturbational stability to obtain improved bounds. In graph-theoretic studies, new results are reported on the properties of feedback arc sets, system reliability, system stability for time-varying components, multistage communication nets, and the reliability of switching functions.